STUDIA

UNIVERSITATIS BABEŞ-BOLYAI

PHYSICA

1983

CLUJ-NAPOCA

ANUL XXVIII 1983

STUDIA

UNIVERSITATIS BABEŞ-BOLYAI

PHYSICA

Redacţia: 3400 CLUJ-NAPOCA str. M. Kogălniceanu, 1 ● Telefon 1 61 00

SUMAR — CONTENTS — SOMMAIRE

STUDIA UNIV BABEŞ-BOLYAI, PHYSICA, XXVIII, 1983

ELECTRON MAGNETIC RESONANCE STUDY OF RARE EARTH ZEOLITES*

LENNOX ITON**, ALEXANDRU NICULA and JOHN TURKEVICH**

As a continuation of studies of the EPR of metal ions in zeolites [1] we are investigating all the rare earth ions except Promethium, introduced in sodium Y zeolites and some into mordenite These have been examined both at X and Q band and at temperatures of 4 °K, 77 °K and 300 °K These were examined both in hydrated and calcined (820 K) forms, and γ — irradiated at 77 °K

As expected, only the S-state rare earth ions, Gd(III) and Eu(II), gave ESR spectra at room temperature All the non-S-state rare earth ions except Sm(III) gave spectra at 4 °K, the principal features being given by the g values, with corresponding line widths in parentheses given in gauss, for the hydrated and calcined forms

Rare earth elements	Hydrated zeolites	Calcined zeolites
Ce	1 98(2500G), 5 6(100)	1 64(1900), 5 6(100)
Pr	—	0 57(200)
Nd	2 73(1250)	disappears
Tb	22(700)	disappears
Dy	5 45(1270), 2 11(80), 2 26(80)	7 80(960)
Ho	17 5(350), 6 0(240)	disappears
Er	6 55(1240)	7 12(760)
Tm	17 7(600)	disappears
Yb	3 45(2550)	4 77(220), 2 98(640)

A detailed analysis of these spectra must await completion of further study Several points can be brought out Spectra are obtained not only for the ions with odd number of electrons (Kramers ions), but also for those with even number of electrons, Tb, Ho, Tm. No spectrum was observed for the Samarium ion This may be due to the EPR lying beyond the vailable X-band magnetic field of 12 KG ($g < 0{,}55$), perhaps due to the influence of a lowlying excited state The extreme width of the lines may be due either to short spin lattice relation times or to large spin-spin interaction of those rather heavily doped samples Changes engendered by calcining are quite marked as the preliminary data given above show No effect of gamma irradiation on the rare earth ion signals was noted in the above samples, indicating that valence changes in the rare earth, if they occur, were not extensive

* This work was performed in 1972 in the laboratories of the Princeton University An abstract of the paper concerning this work was published in Nucl Sci Abstr 28(9), 20764(1973) Taking into account the importance of these results we consider as necessary the publication of the whole paper, even of the work was performed several years ago We believe that paper can be a real help for the researches in magnetic resonance, as it contains a full study of the rare earth elements in zeolites, a study which to our knowledge, was never performed since In our laboratory at University of Cluj we have done some research in this field, mainly on Gd and Eu (see Al Nicula, *Rezonanța magnetică*, E D P , Bucuresti, 1980)

** Princeton University, Princeton, N J 08540 U S A

Extensive investigations were carried out on the $^8S_{7/2}$ state rare earth ions Gd(III) and Eu(II), since their relatively long relaxation time permitted observation of the EPR signals at 300°K and 77°K The following general observations can be made

The spectra of Gd(III) and Eu(II) are complex, quite different from the sharp lines of fine structure and hyperfine structure we have observed for Eu(II) in powders of KCl, ZnS cubic, ZnS hexagonal [2]. They are similar in appearance to Gd(III) found in glasses It must be concluded that the rare earth ions in calcined zeolites are in a very strong, asymmetric crystalline field, comparable to or stronger than the Zeeman field produced by the magnetic fields of the measurement (3,000 gauss) — (14,000 gauss).

The spectrum does not differ if the cubic Y zeolite is replaced by the orthorombic mordenite host crystal. Further, the hydrogen reduced Eu_2O_3, behaves in a similar manner to Gd(III) in zeolites.

The spectrum of calcined Gd(III) zeolite (Fig A) and that of Eu(II) zeolite produced by hydrogen reduction (Fig B) are different; this in spite of the

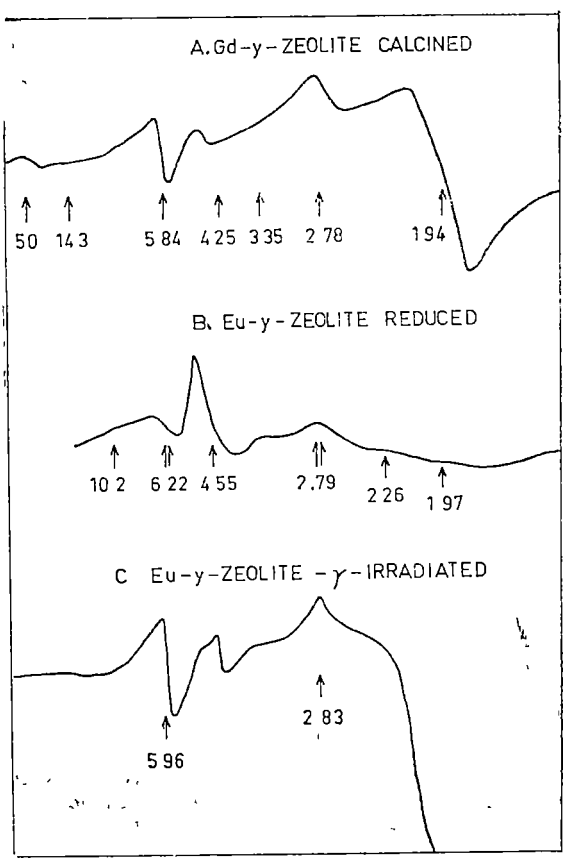

Fig 1.

fact that they are in the same state and should be subject to the same crystalline field. Furthermore, K a r a p e t y a n et al. [3] have found that Gd^{3+} and Eu^{2+} in zinc phosphate glass give identical spectra. This discrepancy was resolved when the Eu(II)-Y-zeolite was produced from Eu(III), not by hydrogen reduction at 720°K, but by gamma irradiation at 77°K Then a spectrum quite similar to that of Gd(III) was obtained (Fig. C). This would indicate that following high temperature reduction a substantial amount of Eu(II) occupies another site whose crystal field parameters are stonger, as we shall show below, than those experienced by the Gd(III) ion.

The behaviour of Eu(II) ion is different in another respect. On reoxidation of the Eu(II) zeolite, the characteristic features of the Eu(II) ion disappear However a broad line centered at $g = 2 \cdot 46$ (1400G) at 300°K, and at $2 \cdot 6$ (1550G) at 77°K, with temperature-independent intensity appears The same line appears following hydrogen reduction and reoxidation of Eu_2O_3 (7 ppm impurity of Fe), [4] and does not appear in similar treatment of Gd zeolite This apparently ferromagnetic type resonance may conceivably be due to Eu_3O_4, similar to Fe_3O_4 [5] The latter we might expect to find also in the Gd zeolite, but not in Eu_2O_3 with its small iron content Thus in the important phase of reoxidation of a cracking catalyst, such a species as Eu_3O_4 may play a role

Let us now examine in more detail the crystal field parameters of the S-state ions Gd(III) and Eu(II) It must be noted that action of the crystal field on S state ions occurs via high order mechanism, the theory of which is not well developed [6]. The $^8S_{7/2}$ state is split by a crystal field of sufficient symmetry into four different levels with values of m_j ranging from $\pm 7/2$ to $\pm 1/2$ These doublets are themselves split in varying degree, shifted with respect to each other and in an absolute sense, by the applied external field We wish to use the following spin Hamiltonian, orthorombic in the crystal field interaction, with D the axial parameter and E the orthorombic parameter, and truncated to the second order in spin operators

$$\mathcal{H} = g\mathbf{H} \quad \mathbf{S} + D(S_z^2 - 1/3S(S+1)) + E(S_\tau^2 - S_x^2).$$

The ratio E/D serves as a symmetry parameter with limit 0 corresponding to purely axial symmetry, and limit 0,33 to a large rhombic component Nicklin has computer calculated the g values obtained for such a system as a function of D, E and H for various wavelenghths of microwave radiation The experimental basis of our evaluation of the crystal fields in comparison of the spectra that we obtain for the calcined Gd and Eu zeolite at two frequencies, 9 3 and $34 \cdot 2$ GHz, with those calculated and observed by Nicklin The spectrum of calcined Gd zeolite at 77°K has a strong line at $g = 1$ 98 (245G), with a weak line at $g = 5 \cdot 90$ (140G), an asymmetric cluster at $g = 2 \cdot 79$, and a signal at $g = 50$. The spectrum at $34 \cdot 2$ GHz is markedly different consisting of one line at $g = 1 \cdot 98$ (700 gauss). We are thus dealing with a situation where the Zeeman energy in the X-band region is comparable to the splitting produced by the crystal field At Q band the Zeeman energy is substantially larger Since our spectrum is similar at both frequencies to those of Nicklin on Gd(III) in soda silicate glass, we adopt his parameter values: $|D| = 2 \cdot 06$ GHz, $|E| = 0 \cdot 62$ GHz and $|E/D| = 0 \cdot 30$. The last value indicates that the crystal field has a strong rhombic character

The spectrum of the Eu(II) Y zeolite produced by high temperature reducting, appears to be composite. It is characterized by a strong, fairly narrow line at $g = 4\,55$ (260G), as well as absorption at $g = 6.2$ and $2\,79$. Structure in the $g = 2$ region is markedly less intense than in the Gd zeolite The spectrum retains complex character at 34 GHz frequency, although its form is considerably changed This suggests that the Zeeman effect does not completely dominate, even at 34 HGz , i e the crystal field effect is substantially stronger in the site appropriate to the $g = 4.55$ signal than in the other site We estimate bounding ranges for the value of the crystal field parameters appropriate to this signal as·

$$9 \text{ GHz} < |D| < 34 \text{ GHz} \text{ and } |E/D| = 0{,}10.$$

Now, the appearance of such a signal would not be sensitive to the absolute value of D and E, but is determined completely by the ratio E/D Thus best concordance with the observed spectrum is given for $|E/D| = 0.10$, for which the zero-field energies of the four doublets are -5.33, $-2\,77$, $1\,07$, 7.02 in arbitrary units Then, the next to the lowest line (at $-2{,}77$) gives as almost isotopic g value with $g_x = 4.653$; $g_y = 4\,555$ and $g_z = 5.188$, while the other three doublets would give values that are either outside the range of the instrument or with such highly anisotropic g component values ($g_x g_y g_z$) that averaging over all orientations would at best give a very broad smear

In conclusion, we wish to report that the EPR on hydrated Gd(III)-Y-zeolite shows at room temperature a strong symmetric resonance at $g = 1\,99$ (350G) and very weak resonances at $g = 5\,90$ and $13\,0$, similar to an aqueous $GdCl_3$ (1%) solution which also exhibits a single line at $g = 1\,995$ (350G). On cooling to 77°K the hydrated Gd zeolite to 77°K, the spectrum becomes complex with new lines appearing at $g = 5.90$ (140G), an asymmetric cluster at $g = 2\,79$ and $2\,4$. This is to be contrasted to the behaviour of the aqueous $GdCl_3$ salt which at 77°K merely broadens (1080G) maintaining its symmetric shape. This must indicate that on lowering the temperature the Gd ion in the large cavity interacts with the ions of the zeolite framework The same behabiour was found in Cu(II) zeolite [1]

(Received September 20, 1982)

REFERENCES

1. Al Nicula, D Stamires, J Turkevich, J Chem Phys , **42**, 3684 (1965) , J Turkevich, Y Ono and J Soria, J Catalysis, **25**, 44 (1972)
2. Unpublished data from Princeton laboratory
3. G O Karapetyan, D M Yudin and D G Gallimov, Izv Akad Nauk SSSR, Ser Fig **31**, 809 (1967)
4 Data furnished by supplier, Alfa inorganics, Beverly, Mass
5 L S Singer and D N Stamires, J Chem Phys , **42**, 3299 (1965)
6 B. G Wybourne, Phys Rev , **148**, 317 (1966)
7 R C Nicklin, Ph D Thesis, Iowa State University, 1967 , published as Technical Report U S A E C **1967**, IS-T-203

CERCETĂRI DE REZONANȚĂ MAGNETICĂ ELECTRONICĂ ASUPRA ELEMENTELOR RARE ÎN ZEOLIȚI

(Rezumat)

Ca o continuare a studiilor de RPE ale ionilor metalici în zeoliți expuse în lucrările de la bibliografia [1], am investigat toți ionii din seria elementelor rare, cu excepția ionului Promethium, introduși în zeoliți Y de sodiu și unii în mordeniți. Ei au fost cercetați atît în banda X cît și în banda Q la temperaturile de 4°K, 77°K și 300°K, în stare hidratată și calcinată iar unele probe au fost radiate cu radiații γ la temperatura de 77°K. Interpretarea spectrelor a fost făcută folosind formalismul hamiltonianului din rezonanța magnetică, reținînd termenii de diferite simetrii și diferite tării în funcție de ionul în discuție.

STUDIA UNIV BABEŞ-BOLYAI, PHYSICA, XXVIII, 1983

UN STUDIU AL INFLUENŢEI CÎMPULUI MAGNETIC ASUPRA FLUIDULUI CONDUCTOR TURBULENT

STELIANA CODREANU

Modul în care mişcarea turbulentă a unui mediu conductor electric este influenţată de prezenţa unui cîmp magnetic, reprezintă una din problemele des întîlnite în fizica cosmică. Ea a fost pentru prima dată investigată de B. Lehnert [1], şi apoi de alţi cercetători printre care R. B. Deissler [2], H. K Moffat [3], K. H Rädler [4], L G. Ghenin, S P. Mangha, V G Svirıdov [5]

În prezentul studiul noı ne propunem să facem o analiză calitativă a problemei în cazul în care mediul turbulent conductor este incompresibıl şi omogen, iar cîmpul magnetic impus este uniform

Ecuaţiile fundamentale necesare studiului sînt ecuaţiile magnetohidrodinamicii şi anume

— ecuaţia Navier-Stokes

$$\frac{\partial \vec{u}}{\partial t} + (\vec{u}\,\nabla)\vec{u} = -\frac{1}{\rho}\nabla p + \nu\Delta\vec{u} + \frac{1}{\rho}\vec{j}\times\vec{B} \tag{1}$$

— ecuaţia de continuitate

$$\nabla\vec{u} = 0 \tag{2}$$

— ecuaţiile lui Maxwell

$$\nabla\times\vec{B} = \mu\vec{j} \tag{3}$$

$$\nabla\times\vec{E} = -\frac{\partial\vec{B}}{\partial t} \tag{4}$$

$$\nabla\vec{B} = 0 \tag{5}$$

— legea lui Ohm generalizată

$$\vec{j} = \sigma\left(\vec{E} + \vec{u}\times\vec{B} - \frac{1}{en}\vec{j}\times\vec{B}\right) \tag{6}$$

în care

$\vec{u}$ — viteza mediului, ρ — densitatea masică, p — presiunea hidrodinamică, ν — coeficientul de vîscozitate cinematic, σ — conductivitatea electrică, e — sarcina electronului, n — numărul de electroni, μ — permeabilitatea magnetică, $\vec{E}$ — cîmpul electric, $\vec{B}$ — inducţia magnetică. În relaţia (6), ultimul termen ţine seama de existenţa curentului Hall.

Ţinînd cont de (3), relaţia (6) devine

$$\frac{1}{\mu}(\nabla\times\vec{B}) = \sigma\vec{E} + \sigma(\vec{u}\times\vec{B}) - \frac{\sigma}{en\mu}(\nabla\times\vec{B})\times\vec{B} \tag{7}$$

Aplicînd rotorul ecuației (7) și ținînd cont de (2), (4) și (5), precum și de faptul că

$$(\nabla \times \vec{B}) \times \vec{B} = (\vec{B}\,\nabla)\vec{B} - \frac{1}{2}\,\Delta B^2 \tag{8}$$

obținem

$$\frac{\partial \vec{B}}{\partial t} = (\vec{B}\,\nabla)\vec{u} - (\vec{u}\nabla)\vec{B} + \frac{1}{\mu\sigma}\,\Delta\vec{B} - \frac{1}{en\mu}\,\nabla\times(\vec{B}\,\nabla)\vec{B} \tag{9}$$

De asemenea ținînd cont de (3) și (8), ecuația (1) devine

$$\frac{\partial \vec{u}}{\partial t} + (\vec{u}\nabla)\vec{u} = -\frac{1}{\rho}\,\nabla p + \nu\Delta\vec{u} + \frac{1}{\rho\mu}\left[(\vec{B}\,\nabla)\vec{B} - \frac{1}{2}\,\nabla B^2\right] \tag{10}$$

Ecuațiile (9) și (10) pot fi scrise pe componente astfel

$$\frac{\partial B_i}{\partial t} = \frac{\partial}{\partial x_k}\,(B_k u_i - u_k B_i) + \frac{1}{\mu\sigma}\,\frac{\partial^2 B_i}{\partial x_k^2} - \frac{1}{en\mu}\,\varepsilon_{ijk}\,\frac{\partial^2 (B_i B_k)}{\partial x_j^2} \tag{11}$$

$$\frac{\partial u_i}{\partial t} + \frac{\partial}{\partial x_k}\,(u_k u_i) = -\frac{1}{\rho}\,\frac{\partial p}{\partial x_i} + \nu\,\frac{\partial^2 u_i}{\partial x_k^2} + \frac{1}{\rho\mu}\,\frac{\partial (B_k B_i)}{\partial x_k} - \frac{1}{2\rho\mu}\,\frac{\partial (B_k^2)}{\partial x_i} \tag{12}$$

în care

$$\varepsilon_{ijk} = \begin{cases} 0 & \text{dacă există o coincidență de indici} \\ +1 & \text{dacă indicii sînt în ordine ciclică} \\ -1 & \text{dacă indicii sînt în ordine neciclică} \end{cases}$$

$(i,\ j,\ k,\ l = 1,\ 2,\ 3)$

În ecuațiile (11) și (12) nu se face însumarea după indicele i

Admitînd că viteza mediului într-un punct se compune din viteza medie și viteza pulsatorie, mediul considerat fiind omogen, viteza medie va fi nulă și astfel ecuația (12) descrie tocmai evoluția în timp a componentei i a vitezei pulsatorii dintr-un punct

Cîmpul magnetic, în orice punct al mediului, este dat de cîmpul magnetic impus $\vec{B}^\circ$ și de cîmpul magnetic pulsatoriu $\vec{b}$, adică

$$\vec{B} = \vec{B}^\circ + \vec{b} \tag{13}$$

Ținînd cont de (13) și de faptul că $\vec{B}^\circ$ este constant, ecuațiile (11) și (12) se pot scrie:

$$\frac{\partial u_i}{\partial t} + \frac{\partial}{\partial x_k}\,(u_k u_i) = -\frac{1}{\rho}\,\frac{\partial p}{\partial x_i} + \nu\,\frac{\partial^2 u_i}{\partial x_k^2} + \frac{1}{\rho\mu}\,(B_k^0 + b_k)\left(\frac{\partial b_i}{\partial x_k} - \frac{\partial b_k}{\partial x_i}\right) \tag{14}$$

$$\frac{\partial b_i}{\partial t} = (B_k^0 + b_k)\,\frac{\partial u_i}{\partial x_k} - u_k\,\frac{\partial b_i}{\partial x_k} + \frac{1}{\mu\sigma}\,\frac{\partial^2 b_i}{\partial x_k^2} - \frac{\varepsilon_{ijk}}{en\mu}\left[(B_e^0 + b_e)\,\frac{\partial^2 b}{\partial x_j \partial x_e} + \frac{\partial b_e}{\partial x_j}\,\frac{\partial b_k}{\partial x_e}\right] \tag{15}$$

Să admitem că cîmpul magnetic exterior impus este mult mai mare decît cîmpul magnetic pulsatoriu. În acest caz, în expresiile în care apare $(B_k^0 + b_k)$

îl vom neglija pe b_k. Înmulţind apoi (14) cu u_i, (15) cu b_i şi efectuînd medierea, vom avea:

$$\frac{\partial}{\partial t}\left\langle \frac{u_i^2}{2} \right\rangle + \left\langle u_i u_k \frac{\partial u_i}{\partial x_k} \right\rangle = -\frac{1}{\rho}\left\langle u_i \frac{\partial p}{\partial x_i} \right\rangle + \nu \left\langle u_i \frac{\partial^2 u_i}{\partial x_k^2} \right\rangle + \\ + \frac{1}{\rho\mu} B_k^0 \left[\left\langle u_i \frac{\partial b_i}{\partial x_k} \right\rangle - \left\langle u_i \frac{\partial b_k}{\partial x_i} \right\rangle \right] \tag{16}$$

$$\frac{\partial}{\partial t}\left\langle \frac{b_i^2}{2} \right\rangle + B_k^0 \left\langle b_i \frac{\partial u_i}{\partial x_k} \right\rangle - \left\langle b_i u_k \frac{\partial b_i}{\partial x_k} \right\rangle + \frac{1}{\mu\sigma}\left\langle b_i \frac{\partial^2 b_i}{\partial x_k^2} \right\rangle - \\ - \frac{\varepsilon_{ijk}}{e n \mu}\left[B_l^0 \left\langle b_i \frac{\partial^2 b_k}{\partial x_j \partial x_l} \right\rangle + \left\langle b_i \frac{\partial b_l}{\partial x_j} \frac{\partial b_k}{\partial x_i} \right\rangle \right] \tag{17}$$

Remarcînd că în cazul turbulenţei omogene, mărimile mediate nu variază în funcţie de coordonate, în ecuaţia (16) putem face următoarele modificări:

$$\left\langle u_i u_k \frac{\partial u_i}{\partial x_k} \right\rangle = \frac{\partial}{\partial x_k}\langle u_i u_k u_i \rangle - \left\langle u_i \frac{\partial}{\partial x_k}(u_i u_k) \right\rangle = -\left\langle u_i u_k \frac{\partial u_i}{\partial x_k} \right\rangle = 0$$

$\left(\frac{\partial u_k}{\partial x_k} = 0,\ \text{mediul fiind incompresibil}\right)$

$$\left\langle u_i \frac{\partial p}{\partial x_i} \right\rangle = \frac{\partial}{\partial x_i}\langle u_i p \rangle - \left\langle p \frac{\partial u_i}{\partial x_i} \right\rangle = -\left\langle p \frac{\partial u_i}{\partial x_i} \right\rangle \text{ (nu se însumează după i)}$$

$$\left\langle u_i \frac{\partial^2 u_i}{\partial x_k^2} \right\rangle = \frac{\partial}{\partial x_k}\left\langle u_i \frac{\partial u_i}{\partial x_k} \right\rangle - \left\langle \frac{\partial u_i}{\partial x_k} \frac{\partial u_i}{\partial x_k} \right\rangle = -\left\langle \frac{\partial u_i}{\partial x_k} \frac{\partial u_i}{\partial x_k} \right\rangle$$

$$\left\langle u_i \frac{\partial b_i}{\partial x_k} \right\rangle = \frac{\partial}{\partial x_k}\langle u_i b_i \rangle - \left\langle b_i \frac{\partial u_i}{\partial x_k} \right\rangle = -\left\langle b_i \frac{\partial u_i}{\partial x_k} \right\rangle$$

şi analog $\left\langle u_i \frac{\partial b_k}{\partial x_i} \right\rangle = -\left\langle b_k \frac{\partial u_i}{\partial x_i} \right\rangle$

Astfel ecuaţia (16) se simplifică devenind:

$$\frac{\partial}{\partial t}\left\langle \frac{u_i^2}{2} \right\rangle = \frac{1}{\rho}\left\langle p \frac{\partial u_i}{\partial x_i} \right\rangle - \nu \left\langle \frac{\partial u_i}{\partial x_k} \frac{\partial u_i}{\partial x_k} \right\rangle + \frac{1}{\rho\mu} B_k^0 \left[\left\langle b_k \frac{\partial u_i}{\partial x_i} \right\rangle - \left\langle b_i \frac{\partial u_i}{\partial x_k} \right\rangle \right] \tag{18}$$

Efectuînd transformări similare în ecuaţia (17), şi anume:

$$\left\langle b_i u_k \frac{\partial b_i}{\partial x_k} \right\rangle = 0, \quad \left\langle b_i \frac{\partial^2 b_i}{\partial x_k^2} \right\rangle = -\left\langle \frac{\partial b_i}{\partial x_k} \frac{\partial b_i}{\partial x_k} \right\rangle,$$

$$\left\langle b_i \frac{\partial^2 b_k}{\partial x_j \partial x_i} \right\rangle = -\left\langle \frac{\partial b_i}{\partial x_i} \frac{\partial b_k}{\partial x_j} \right\rangle$$

obţinem

$$\frac{\partial}{\partial t}\left\langle \frac{b_i^2}{2} \right\rangle = B_k^0 \left\langle b_i \frac{\partial u_i}{\partial x_k} \right\rangle - \frac{1}{\mu\sigma}\left\langle \frac{\partial b_i}{\partial x_k} \frac{\partial b_i}{\partial x_k} \right\rangle + \\ + \frac{\varepsilon_{ijk}}{e n \mu}\left[B_e^0 \left\langle \frac{\partial b_i}{\partial x_l} \frac{\partial b_k}{\partial x_j} \right\rangle - \left\langle b_i \frac{\partial b_e}{\partial x_i} \frac{\partial b_k}{\partial x_l} \right\rangle \right] \tag{19}$$

Dacă înmulțim ecuația (18) cu ρ și împărțim ecuația (19) cu μ, vom avea:

$$\underset{\text{I}}{\frac{\partial}{\partial t}\left\langle \rho \frac{u_i^2}{2} \right\rangle} = \underset{\text{II}}{\left\langle p \frac{\partial u_i}{\partial x_i} \right\rangle} - \underset{\text{III}}{\eta \left\langle \frac{\partial u_i}{\partial x_k} \frac{\partial u_i}{\partial x_k} \right\rangle} + \frac{1}{\mu} B_k^0 \left[\underset{\text{IV}}{\left\langle b_k \frac{\partial u_i}{\partial x_i} \right\rangle} - \underset{\text{V}}{\left\langle b_i \frac{\partial u_i}{\partial x_k} \right\rangle} \right] \tag{20}$$

$$\underset{\text{I}}{\frac{\partial}{\partial t}\left\langle \frac{b_i^2}{2\mu} \right\rangle} = \frac{1}{\mu} B_k^0 \underset{\text{II}}{\left\langle b_i \frac{\partial u_i}{\partial x_k} \right\rangle} - \frac{\nu_m}{\mu} \underset{\text{III}}{\left\langle \frac{\partial b_i}{\partial x_k} \frac{\partial b_i}{\partial x_k} \right\rangle} + \frac{\varepsilon_{ijk}}{en\mu^2} \left[\underset{\text{IV}}{B_l^0 \left\langle \frac{\partial b_i}{\partial x_i} \frac{\partial b_k}{\partial x_j} \right\rangle} - \right. \tag{21}$$

$$\left. - \underset{\text{V}}{\left\langle b_i \frac{\partial b_l}{\partial x_j} \frac{\partial b_k}{\partial x_l} \right\rangle} \right]$$

în care $\eta = \nu\rho$, iar $\nu_m = \frac{1}{\mu\sigma}$ este coeficientul de vîscozitate magnetică.

Semnificația fizică a termenilor ce apar în ultimele două ecuații este următoarea:

— în ecuația (20)

I — Variația în timp a energiei cinetice corespunzătoare componentei i a cîmpului vitezei într-un punct al mediului.

II — Redistribuirea energiei pe cele trei componente ale cîmpului vitezei ca urmare a pulsațiilor presiunii. Această redistribuire nu modifică valoarea energiei cinetice totale. Dacă se face însumarea după i, acest termen se anulează

III — Disiparea energiei cinetice ca urmare a existenței vîscozității.

IV — Redistribuirea energiei cîmpului vitezei pe cele trei componente, ca urmare a influenței cîmpului magnetic pulsatoriu. Această redistribuire de asemenea nu modifică energia cinetică totală, însumînd după i termenul se va anula

V — Schimbul de energie între componentele cîmpului vitezei și ale cîmpului magnetic.

— în ecuația (21)

I — Variația în timp a energiei magnetice corespunzătoare componentei i a cîmpului magnetic.

II — Schimbul de energie între componentele cîmpului magnetic și ale cîmpului vitezei

III — Disiparea energiei magnetice ca urmare a vîscozității magnetice

IV și V — Variația energiei cîmpului magnetic ca urmare a efectului Hall.

Din analiza semnificației fizice a termenilor celor două ecuații, putem face următoarele observații

Observația 1 Adunînd ecuațiile (20) și (21) vom avea

$$\frac{\partial}{\partial t}\left(\left\langle \rho \frac{u_i^2}{2} \right\rangle + \left\langle \frac{b_i^2}{2\mu} \right\rangle \right) = \left\langle p \frac{\partial u_i}{\partial x_i} \right\rangle - \eta \left\langle \frac{\partial u_i}{\partial x_k} \frac{\partial u_i}{\partial x_k} \right\rangle + \frac{1}{\mu} B_k^0 \left\langle b_k \frac{\partial u_i}{\partial x_i} \right\rangle - \tag{22}$$

$$- \frac{\nu_m}{\mu} \left\langle \frac{\partial b_i}{\partial x_k} \frac{\partial b_i}{\partial x_k} \right\rangle + \frac{\varepsilon_{ijk}}{en\mu} \left[B_l^0 \left\langle \frac{\partial b_i}{\partial x_i} \frac{\partial b_k}{\partial x_j} \right\rangle - \left\langle b_i \frac{\partial b_l}{\partial x_j} \frac{\partial b_k}{\partial x_l} \right\rangle \right]$$

Din această ecuație se poate obține o condiție de staționaritate a turbulenței considerate, și anume

$$\left\langle p\frac{\partial u_i}{\partial x_i}\right\rangle - \eta\left\langle \frac{\partial u_i}{\partial x_k}\frac{\partial u_i}{\partial x_k}\right\rangle + \frac{1}{\mu}B_k^0\left\langle b_k\frac{\partial u_i}{\partial x_k}\right\rangle - \frac{\nu_m}{\mu}\left\langle \frac{\partial b_i}{\partial x_k}\frac{\partial b_i}{\partial x_k}\right\rangle = \frac{\varepsilon_{ijk}}{en\mu}\left[\left\langle b_i\frac{\partial b_i}{\partial x_j}\frac{\partial b_k}{\partial x_i}\right\rangle - B_l^0\left\langle \frac{\partial b_i}{\partial x_i}\frac{\partial b_k}{\partial x_j}\right\rangle\right] \tag{23}$$

remarcîndu-se că energia disipată a turbulenței este compensată pe seama prezenței efectului Hall.

Observația 2. Să considerăm, în particular, cîmpul magnetic impus orientat după axa Oz a unui sistem cartezian de axe, adică

$$B_k^0 \to B_3^0$$

Ecuațiile (20) și (21) se vor transcrie în acest caz astfel

$$\frac{\partial}{\partial t}\left\langle \frac{\rho u_1^2}{2}\right\rangle = \left\langle p\frac{\partial u_1}{\partial x_1}\right\rangle - \eta\left\langle \frac{\partial u_1}{\partial x_k}\frac{\partial u_1}{\partial x_k}\right\rangle + \frac{1}{\mu}B_3^0\left[\left\langle b_3\frac{\partial u_1}{\partial x_1}\right\rangle - \left\langle b_1\frac{\partial u_1}{\partial x_3}\right\rangle\right] \tag{24}$$

$$\frac{\partial}{\partial t}\left\langle \frac{b_4^2}{2\mu}\right\rangle = \frac{1}{\mu}B_3^0\left\langle b_1\frac{\partial u_1}{\partial x_3}\right\rangle - \frac{\nu_m}{\mu}\left\langle \frac{\partial b_1}{\partial x_k}\frac{\partial b_1}{\partial x_k}\right\rangle + \frac{1}{en\mu}\left[B_3^0\left\langle \frac{\partial b_1}{\partial x_3}\frac{\partial b_3}{\partial x_2}\right\rangle - \right.$$

$$\left. - \left\langle b_1\frac{\partial b_1}{\partial x_2}\frac{\partial b_3}{\partial x_1}\right\rangle - \left\langle b_1\frac{\partial b_2}{\partial x_2}\frac{\partial b_1}{\partial x_2}\right\rangle - \left\langle b_1\frac{\partial b_3}{\partial x_2}\frac{\partial x_3}{\partial x_3}\right\rangle\right] \tag{25}$$

$$\frac{\partial}{\partial t}\left\langle \frac{\rho u_2^2}{2}\right\rangle = \left\langle p\frac{\partial u_2}{\partial x_2}\right\rangle - \eta\left\langle \frac{\partial u_2}{\partial x_k}\frac{\partial u_2}{\partial x}\right\rangle + \frac{1}{\mu}B_3^0\left[\left\langle b_3\frac{\partial u_2}{\partial x_2}\right\rangle - \left\langle b_2\frac{\partial u_2}{\partial x_3}\right\rangle\right] \tag{26}$$

$$\frac{\partial}{\partial t}\left\langle \frac{b_2^2}{2\mu}\right\rangle = \frac{1}{\mu}B_3^0\left\langle b_2\frac{\partial u_2}{\partial x_3}\right\rangle - \frac{\nu_m}{\mu}\left\langle \frac{\partial b_2}{\partial x_k}\frac{\partial b_2}{\partial x_k}\right\rangle - \frac{1}{en\mu}\left[B_3^0\left\langle \frac{\partial b_2}{\partial x_3}\frac{\partial b_3}{\partial x_1}\right\rangle - \right. \tag{27}$$

$$\left. - \left\langle b_2\frac{\partial b_1}{\partial x_1}\frac{\partial b_3}{\partial x_1}\right\rangle - \left\langle b_2\frac{\partial b_2}{\partial x_1}\frac{\partial b_3}{\partial x_2}\right\rangle - \left\langle b_2\frac{\partial b_3}{\partial x_1}\frac{\partial b_3}{\partial x_3}\right\rangle\right]$$

$$\frac{\partial}{\partial t}\left\langle \frac{\rho u_3^2}{2}\right\rangle = \left\langle p\frac{\partial u_3}{\partial x_3}\right\rangle - \eta\left\langle \frac{\partial u_3}{\partial x_k}\frac{\partial u_3}{\partial x_k}\right\rangle \tag{28}$$

$$\frac{\partial}{\partial t}\left\langle \frac{b_3^2}{2\mu}\right\rangle = \frac{1}{\mu}B_3^0\left\langle b_3\frac{\partial u_3}{\partial x_3}\right\rangle - \frac{\nu_m}{\mu}\left\langle \frac{\partial b_3}{\partial x_k}\frac{\partial b_3}{\partial x_k}\right\rangle \tag{29}$$

Legăturile energetice existente între termenii ecuațiilor (24)—(29) pot fi reprezentate în mod schematic astfel.

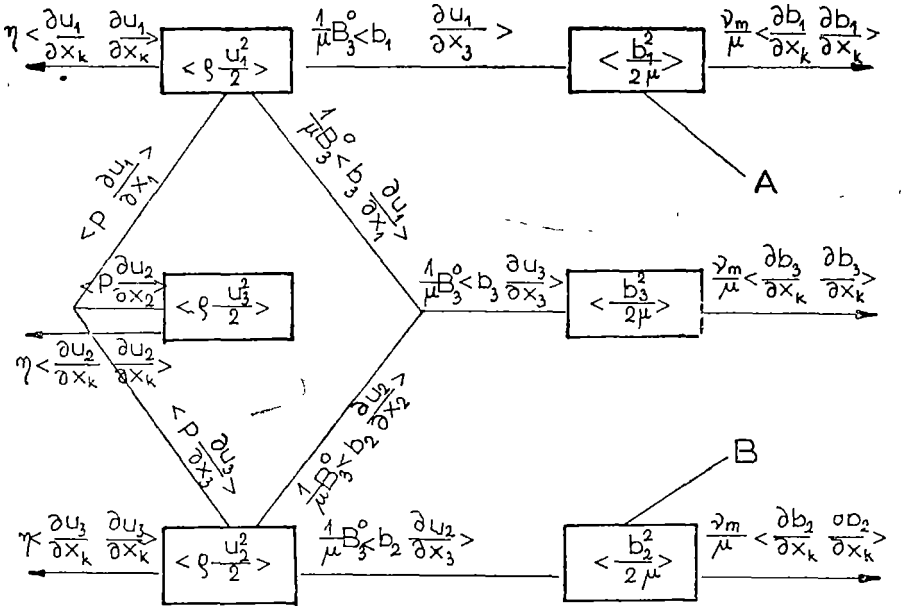

Fig 1

O asemenea reprezentare permite o analiză calitativă a influenței cîmpului magnetic asupra turbulenței considerate Astfel, cîmpul magnetic nu interacționează nemijlocit cu componenta vitezei din direcția cîmpului magnetic. Într-adevăr pe diagramă nu apare o legătură directă între $\left\langle \rho \frac{u_3^2}{2} \right\rangle$ și $\left\langle \frac{b_3^2}{2\mu} \right\rangle$

Dacă legăturile cu A și B se echilibrează (termenii au semn opus), și procesul de disipare vîscoasă a energiei cîmpului de vitezei devine egal cu procesul de disipare a energiei cîmpului magnetic, legăturile dintre $\left\langle \rho \frac{u_1^2}{2} \right\rangle$ și $\left\langle \frac{b_1^2}{2\mu} \right\rangle$, precum și dintre $\left\langle \rho \frac{u_2^2}{2} \right\rangle$ și $\left\langle \frac{b_2^2}{2\mu} \right\rangle$, trebuie să slăbească. Această situație nu se poate realiza decît prin diminuarea și apoi anularea gradienților după axa Oz (după direcția cîmpului magnetic) a tuturor mărimilor pulsatorii Se creează astfel turbulența bidimensională, turbulență obținută experimental [6] din una tridimensională prin aplicarea unui cîmp magnetic intens.

(Intrat în redacție la 11 februarie 1982)

BIBLIOGRAFIE

1. B. Lehnert, Quart. Appl Math, **12**, 321 (1955)
2. R B Deissler, Phys. Fluids, **6**, 1250 (1963)
3. H. K. Moffat, J Fluid Mech, **28**, 571 (1967)

4 K H Rad' Astron Nachr, Bd **295**, H 6, 265 (1974).
5 L G Ghe r, V G Sviridov, S P Mangha, Magn Ghidr, **2**, 87 (1974)
6 A B Tsinober, Magn Ghidr, **1**, 7 (1975)

UNE ÉTUDE DE L'INFLUENCE DU CHAMP MAGNÉTIQUE SUR UN FLUIDE TURBULENT CONDUCTEUR

(Résumé)

On fait une étude qualitative de l'influence d'un champ magnétique uniforme sur une turbulence magnétohydrodynamique homogène en présence de l'éffet Hall

STUDIA UNIV. BABEŞ-BOLYAI, PHYSICA, XXVIII, 1983

HEAT OR MASS TRANSFER IN SOME COUNTERCURRENT SYSTEMS AND THE CORRESPONDING STURM-LIOUVILLE BOUNDARY PROBLEM

ILIE HODOR

1 **Introduction.** Some years ago a detailed analytical study of heat or mass transfer in some countercurrent systems were performed [1—10] The obtained partial differential equations are similar to classical equations of some well studied transfer fenomena Starting from this similarity, the separation-of-variables technique used to classical problems has been also applied to the new problems. In both cases a Sturm-Liouville boundary problem is obtained The so obtained solutions of the new problems do not meet any contradiction Nunge and Gill [1] solved such a problem both by separation-of-variables method and by a finite difference technique An excellent agreement between the two methods was obtained According to the opinion of Blanco and Gill [4], Mason's papers [11, 12] and those of Picone [13] and Bôcher [14] represent a complete mathematical base for the analysis of countercurrent systems In our opinion, although the separation-of-variables technique, very probably, leads to correct solutions for countercurrent transfer problems, there is not a complete mathematical theory to justify this procedure. The purpose of this paper is just to show that if such obtained solutions are supposed to be correct then some theorems which have not been mentioned so far in the mathematical literature must be true The theorems consist of a special completeness of the eigenfunctions of a kind of Sturm-Liouville problem

Mathematical difficulties have been encountered in solving the very particular case of equal heat capacity flow rates of the heat exchanging fluids because, in this case, the Sturm-Liouville problem leads to a double eigenvalue $\lambda = 0$ Stein [9] has studied this case for double pipe heat exchanger by solving the problem in the vicinity of this very particular case It is also the purpose of this paper to show that in the case of equal heat capacity flow rates there exists a particular solution of the heat equation which cannot be found by usual method of separation-of-variables.

2. **The Model and the Sturm-Liouville Boundary Problem.** The mathematical problem which we are studying is common to a class of systems concerning with the heat or mass transfer in countercurrent flow The double pipe heat exchanger is an example [2] For our purpose, it is sufficient to consider the heat transfer on a simple flat plate geometry presented schematically in Fig. 1. A fluid substance moves countercurrently between two thermo-insulating plan-parallel walls The movement is parallel to Oz-axis, the velocity $v(x)$ is a function of x alone which changes its sign in the plane $x = x_0$,

$$v(x) \qquad x_1 < x < x_0\,,$$
$$v(x) < 0. \qquad x_0 < x < x_2$$

Institute of Isotopic and Molecular Technology, Cluj-Napoca, P O Box 700, Romania

The substance may be inhomogeneous in such a way that thermal conductivity p, density ρ and specific heat C_s may be functions of x alone In the interval $x_1 < x < x_2$, the functions p, ρ and C_s are everywhere positive. The function

$$r = r(x) = \rho C_s v$$

has the same sign as $v = v(x)$

By neglecting longitudinal heat conduction, the equation of heat transfer is

$$\frac{\partial}{\partial x}\left(p\,\frac{\partial \theta}{x}\right) = r\,\frac{\partial \theta}{\partial z}, \quad x_1 < x < x_2, \qquad -l < z < l, \tag{1}$$

where $\theta = \theta(x, z)$ is the temperature field. The insulating property of the walls is expressed mathematically as follows

$$\frac{\partial \theta}{\partial x}(x_1, z) = 0, \qquad -l < z < l; \tag{2}$$

$$\frac{\partial \theta}{\partial x}(x_2, z) = 0, \qquad -l < z < l. \tag{3}$$

It is necessary to be given the substance temperature at the entrance of the considered domain Because of the countercurrent movement there are two entrances of the substance thus the folowing two conditions have to be taken into consideration

$$\theta(x, -l) = g^+(x), \qquad x_1 < x < x_0; \tag{4}$$

$$\theta(x, l) = g^-(x), \qquad x_0 < x < x_2; \tag{5}$$

$g^-(x)$, $g^+(x)$ are given functions and $dg^+/dx = 0$ for $x = x_1$, $dg^-/dx = 0$ for $x = x_2$

For simplicity we suppose that $p' = dp/dx$ exists and that p, p', ρ, C_s, v, g^- and g^+ are continuous finite functions in the interval $x_1 < x < x_2$

The model defined in this way is physically completely determined which means that the system (1—5) has a unique solution. The separation-of-variables method applied to the equations (1—3) leads to such particular solutions as

$$\theta_i = f_i(x) e^{-\lambda_i z} \tag{6}$$

where λ_i and $f_i(x)$ are eigenvalues and eigenfuctions of the Sturm-Liouville boundary problem

$$\frac{d}{dx}\left(p\,\frac{df}{dx}\right) + \lambda r f = 0, \qquad x_1 < x < x_2, \tag{7}$$

$$f'(x_1) = f'(x_2) = 0. \tag{8}$$

It is known [15] that if r changes sign in $x_1 < x < x_2$, there exist an infinite set of real eigenvalues which have the limit points $-\infty$ and $+\infty$ If the positive and negative eigenvalues are arranged each in order of increasing numerical value and are denoted by

$$\left.\begin{aligned} &\lambda_0^+, \ \lambda_1^+, \ \lambda_2^+, \ \ldots, \ \lambda_m^+, \quad \ldots \\ &\lambda_0^-, \ \lambda_1^-, \ \lambda_2^-, \ \ldots, \ \lambda_m, \quad \ldots \end{aligned}\right\} \tag{9}$$

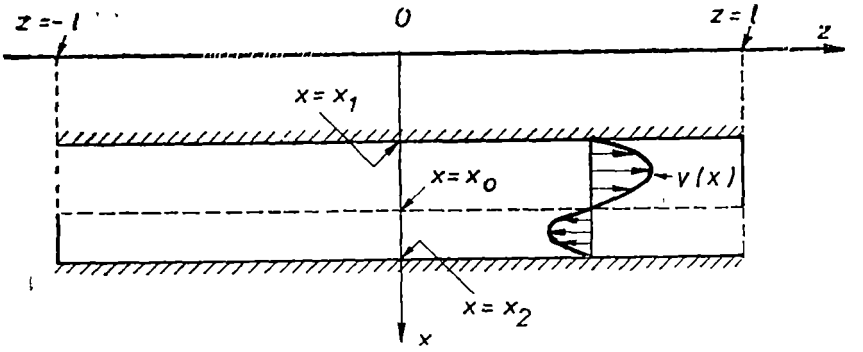

Fig 1 Schematic diagram of the model

and the corresponding eigenfunctions by

$$\begin{aligned} &f_0^+,\ f_1^+,\ f_2^+,\ \ldots,\ f_m^+,\ \ldots,\\ &f_0^-,\ f_1^-,\ f_2^-,\ \ldots,\ f_m^-,\ \ldots, \end{aligned} \tag{10}$$

then f_m^+ and f_m^- have exactly m zeros in the interval $x_1 < x < x_2$. Using a classical technique [15] one can show that f_m^+ is oscillatory and has its zeros on the subinterval $x_1 < x < x_0$, similarly, f_m^- is oscillatory and has m zeros on the subinterval $x_0 < x < x_2$.

The integral

$$F = \int_{x_1}^{x_2} r(x)dx \tag{11}$$

represents the difference between the heat capacity flow rates of the two parts of the substance which flows countercurrently. As it is known [9, 14], depending on F value the following situations can occur

$$F > 0, \quad \lambda_0^+ = 0, \quad \lambda_0^- < 0; \tag{12}$$

$$F < 0, \quad \lambda_0^+ > 0, \quad \lambda_0^- = 0; \tag{13}$$

$$F = 0, \quad \lambda_0^+ = 0, \quad \lambda_0^- = 0. \tag{14}$$

The first two cases are equivalent so that only the first and the last cases will be analysed.

For the eingenvalue $\lambda = 0$, (7) and (8) lead to eigenfunction

$$f_0 = \text{const}. \tag{15}$$

The eigenfunctions satisfy the orthogonality relations

$$\int_{x_1}^{x_2} f_m^+ f_m^- r dx = 0; \tag{16}$$

$$\int_{x_1}^{x_2} f_m^+ f_n^+ r dx = 0, \qquad \int_{x_1}^{x_2} f_m^- f_n^- r dx = 0, \qquad m \neq n. \tag{17}$$

When $F = 0$, the function f_0 cannot be normed because

$$\int_{x_1}^{x_2} f_0^2 r dx = f_0^2 \int_{x_1}^{x_2} r dx = 0 \tag{18}$$

For this reason instead of eigenfunction normalisation, the conditions

$$f_m^+(x_1) = 1, \qquad f_m^-(x_2) = 1 \tag{19}$$

can be considered as satisfied

3. **Comparison with a Classical Problem.** Equation (1) is parabolic and has the particularity that $r(x)$ changes sign. As far as we know such an equation appears in a practical application for the first time in [1—10] which are of relative recent date. The corresponding Sturm-Liouville problem has been largely applied in physics, chemistry and technics, still the case in which $r(x)$ changes sign has not occurred but recently in the same papers [1—10] It is useful to present, for comparison, a problem of a classical type in which $r(x)$ does not change sign

A thin inhomogeneous bar, termically insulated from surroundings, is plased on Ox-axis, x_1 and x_2 being the abscissae of the two ends Initially, the bar temperature is a given function $\theta_0^*(x)$ with the property $d\theta_0^*/dx = 0$ in the points $x = x_1$ and $x = x_2$. The problem is to find the evolution of temperature field $\theta^*(x, t)$ in cours of time Mathematical formulation of this problem is ·

$$\frac{\partial}{\partial x}\left(p^* \frac{\partial \theta^*}{\partial x}\right) = r^* \frac{\partial \theta^*}{\partial t}, \quad x_1 < x < x_2, \quad t < 0, \tag{20}$$

$$\frac{\partial \theta^*}{\partial x}(x_1, t) = 0, \qquad t > 0, \tag{21}$$

$$\frac{\partial \theta^*}{\partial x}(x_2, t) = 0, \qquad t > 0, \tag{22}$$

$$\theta^*(x, 0) = \theta_0^*(x), \qquad x_1 < x < x_2 \tag{23}$$

Here $p^* = p^*(x) < 0$ is the thermal conductivity of the bar, $r^* = r^*(x) < 0$ is a caloric capacity, p^* and r^* are continuous functions in the interval $x_1 < x < x_2$ and $p^{*\prime}$ exists. The similarity with the previous problem is evident. Coordonate z in (1—5) coresponds to time t in (20—23) But in one case the phenomenon develops in the infinite interval $0 < t < \infty$, in the other, the interval is finite, $-l < z < l$. This difference is closely connected with the fact $r^*(x) > 0$ while $r(x)$ changes sign.

The separation-of-variables technique applied to (20—23) leads to

$$\theta^*(x, t) = \sum_{n=0}^{\infty} C_n^* f_{n1}^*(x) e^{-\lambda_n t} \tag{24}$$

where $f^*(x)$ and λ^* are eigenfunctions and eigenvalues of Sturm-Liouville problem

$$\left(\frac{d}{dx} p^* \frac{df^*}{dx}\right) + \lambda^* r^* f^* = 0, \quad x_1 < x < x_2, \tag{25}$$

$$f^{*\prime}(x_1) = f^{*\prime}(x_2) = 0 \tag{26}$$

Eigenvalues λ_n^* are not negative Initial condition (23) permits to determine constants C_n^*,

$$C_n^* = \int_{x_1}^{x_2} 0^*(x) r^*(x) f^*(x) dx. \tag{27}$$

To obtain (27) the property of orthonormality

$$\int_{x_1}^{x_2} r^* f_n^* f_m^* dx = \begin{cases} 0, & n \neq m, \\ 1, & n = m \end{cases}$$

was used

4 **The Case** $F > 0$, $\lambda_0^+ = 0$, $\lambda_0^- < 0$

Following the model of solving classical problem (20—23), the general solution of equation (1) with limit conditions (2) and (3) is

$$\theta(x, z) = \sum_{n=0}^{\infty} [C_n^+ f_n^+(x) e^{-\lambda_n^+(z+l)} + C_n^- f_n^-(x) e^{-\lambda_n^-(z-l)}], \quad -l < z < l \tag{29}$$

Similarly, the constants C_n^+ and C_n^- have to be determined from conditions (4) and (5) and it leads to

$$\sum_{n=0}^{\infty} [C_n^+ f_n^+(x) + C_n^- f_n^-(x) e^{2l\lambda_n^+}] = g^+(x), \quad x_1 < x < x_0, \tag{30}$$

$$\sum_{n=0}^{\infty} [C_n^+ f_n^+(x) e^{-2l\lambda_n^+} + C_n^- f_n^-(x)] = g^-(x), \quad x_0 < x < x_2 \tag{31}$$

Although functions f_n^+ and f_n^- satisfy orthogonality conditions (16) and (17), constants C_n^+ and C_n^- cannot be determined with simple relations like (27) because conditions (4) and (5) are bilocal

This solving procedure was applied to a series of countercurrent transfer problems [1—10] and methods to determine constants C_n have been proposed The obtained results do not contradict the experimental facts Moreover, in some cases these results were compared with the solutions obtained by a finite difference technique and an excellent agreement was obtained [1]

The following reasonings are based on the hypothesis that the solution of the problem is really given by (29—31)

The heat transfer phenomenon tends to uniform the temperature field so that the maximum and the minimum temperature values are attained at the entrance of the substance in the considered domain But entrance temperatures $g^+(x)$ and $g^-(x)$ are supposed to be finite which means that the temperature field is also finite in the whole domain.

Suppose now that the model lengthens unlimited in both senses, $l \to \infty$. The eigenfunctions do not change because they do not depend on l C_n^+ and C_0^+ do generally depend on l and since the temperature field is bounded, the limits

$$\lim_{l \to \infty} C_n^+ = a_n^+, \qquad \lim_{l \to \infty} C_n^- = a_n^- \tag{32}$$

exist

If $l \to \infty$, it is clear, physically, that the temperature field in central zone becomes uniform, tending to a constant, θ_∞ This constant mast be a solution of the mathematical problem and it cannot be other than

$$\theta_\infty = a_0^+ f_0^+(x) e^{-\lambda_n^+(z+l)} = a_0^+ \tag{33}$$

Making the limit of (29) and taking into account (32) and (33), one obtains

$$\lim_{l \to \infty} \theta(x, z) = \begin{cases} \sum_{n=0}^{\infty} a_n^+ f_n^+(x) e^{-\lambda_n^+(z+l)}, & 0 \leqslant z + l < \infty, \\ a_0^+, & -\infty < z < \infty, \\ a_0^+ + \sum_{n=0}^{\infty} a_n^- f_n^-(x) e^{-\lambda_n^-(z-)}, & -\infty < z - l \leqslant 0 \end{cases} \tag{34}$$

As one observes, in the vicinity of the ends of the infinite heat exchanger the temperature field is, generally, variable but it tends to constant a_0^+ for a point which moves away to the central zone of the exchanger

For the infinite heat exchanger, equations (30) and (31) reduce to

$$\sum_{n=0}^{\infty} a_n^+ f_n^+(x) = g^+(x), \qquad x_1 < x < x_0, \tag{35}$$

$$\sum_{n=0}^{\infty} a_n^- f_n^-(x) = g^-(x) - a_0^+, \qquad x_0 < x < x_2. \tag{36}$$

These equations are interconnected only with constant a_0^+ It is a known fact that if in a very long countercurrent heat exchanger the fluids have at the entrance constant temperatures, that is to say, if $g^+(x) = g_0^+ = \text{const}$ and $g^-(x) = g_0^- = \text{const}$, then the temperature in the central zone is equal to the entrance temperature of that fluid which has the greatest caloric capacity In our case $F > 0$, that is the fluid which flows in the sense of Oz-axis has the greatest caloric capacity Thus, the temperature in the central zone will be

$$\theta = a_0^+ = g_0^+$$

independent of the temperature g_0^- with wich the other fluid enters the other end of the exchanger Even if instead of a constant temperature g_0^- the fluid would enter with a variable temperature $g_0^-(x)$, the temperature in the central zone would be the same, g_0^+ It follows that (35) is independent and yields all constance a_n^+ including a_0^+ a^+ determined from (35) is then introduced in (36) which yield constants a_n^-

Since $g^-(x)$ is an arbitrary continuous function, the difference $g^-(x) - a_0^+$ is also an arbitrary function Consequently, every continuous function $G^+(x) = g^+(x)$ defined on the interval $x_1 < x < x_0$ can be expanded into a series of the form (35) Similarly, every continuous function $G^-(x) = g^-(x) - a_n^+$ can be expanded into a series of the form (30). This result can be expressed as follows

THEOREM I The subset of eigenfunctions $f_n(x)$ $(n = 0, 1, 2, \ldots)$ defined on the whole interval $x_1 < x < x_2$ is a complete system with respect to the class of continuous functions defined on the subinterval $x_1 < x < x_0$ and having a null derivative in the point $x = x_1$ The subset of eigenfunctions f_n^- $(n = 0, 1, 2, \ldots)$ defined on the whole interval $x_1 < x < x_2$ is a complete system with respect to the class of continuous functions defined on the subinterval $x_0 < x < x_2$ an having a null derivative in the point $x = x_2$

5 **The Case** $F = 0$, $\lambda_0^+ = \lambda_0^- = 0$

If $F \to 0$ then $\lambda_0^+ \to 0$ and $\lambda^- \to 0$ If $F \neq 0$, there exist two eigenfunctions f_0^+ and f_0^- Still, if $F = 0$ the Sturm-Liouville boundary problem (7,8) yields only one eigenfunction for $\lambda = 0$

Apparently nobody has observed, so far, that if and, only if, $F = 0$, the equation (1) with boundary conditions (2) and (3) has a very particular solution of the form

$$\bar{\theta} = \varphi(z) + f^*(x)$$

where both $\varphi(z)$ and $f^*(x)$ are not simple constants Substituting this particular solution into (1—3), we obtain

$$\bar{\theta} = \frac{1}{l}\,[z + f(x)] \tag{37}$$

where

$$f(x) = \int_{x_1}^{x} \frac{ds}{p(s)} \int_{x_1}^{s} r(t)\,dt \tag{38}$$

The factor $1/l$ in (37) is necessary because the temperature has to be bounded if $l \to \infty$ for every point in the interval $-l < z < l$. The solution (37) is independent, it cannot be expanded in series by the particular solutions of the form (6). Consequently, the most general solution of the system (1—3) will be a linear combination of all particular solutions both those of the type (6) and the solution (37),

$$\theta = \frac{C}{l}\,[z + f(x)] + C_0 f_0 + \sum_{n=1}^{\infty} [C_n^+ f_n^+(x) e^{-\lambda_n^+(z+l)} + C_n^- f_n^-(x) e^{-\lambda_n^-(z-l)}] \tag{39}$$

where

$$f_0 = f_0^+ = f_0^- = 1 \tag{40}$$

and C, C_0 are arbitrary constants.

Constants C, C_n^+, C_n^- and C_0 must be determined from conditions (4) and (5) which leads to

$$\frac{C}{l}\,[-l + f(x)] + C_0 + \sum_{n=1}^{\infty} [C_n^+ f_n^+(x) + C_n^- f_n^-(x) e^{2l\lambda_n^-}] = g^+(x),$$

$$x_1 < x < x_0, \tag{41}$$

$$\frac{C}{l}[l + f(x)] + C_0 + \sum_{n=1}^{\infty} [C_n^+ f_n^+(x) e^{-2l\lambda_n^+} + C_n^- f_n^-(x)] = g^-(x),$$

$$x_0 < x < x_2 \tag{42}$$

We suppose now, as in previous case, that the exchanger lengthens unlimited Similar to (32), it must exist the limits

$$\lim_{l\to\infty} C = a, \quad \lim_{l\to\infty} C_0 = a_0, \quad \lim_{l\to\infty} C_n^+ = a, \quad \lim_{l\to\infty} C_n^- = a_n^- \tag{43}$$

the first term in (39) reduces to az/l and represents a temperature field which is independent of x, but changes extremely slightly with z so that on the infinite length of the exchanger it changes from $-a$ to $+a$

At the limit, equations (41) and (42) reduce to

$$a_0 - a + \sum_{n=1}^{\infty} a_n^+ f_n^+(x) = g^+(x), \quad x_1 < x < x_0, \quad l \to \infty, \tag{44}$$

$$a_0 + a + \sum_{n=1}^{\infty} a_n^- f_n^-(x) = g^-(x), \quad x_0 < x < x_2, \quad l \to \infty \tag{45}$$

It is to observe that instead of a_0 and a, other two constants can be introduced,

$$a_0 + a = a_0^-, \quad a_0 - a = a_0^+ \tag{46}$$

Taking into account (40), equations (44) and (45) can be written

$$\sum_{n=0}^{\infty} a_n^+ f_n^+(x) = f^+(x), \quad x_1 < x < x_0, \quad l \to \infty, \tag{47}$$

$$\sum_{n=0}^{\infty} a_n^- f_n^-(x) = g^-(x), \quad x_0 < x < x_2, \quad l \to \infty. \tag{48}$$

This result can be expressed as follows

THEOREM II The subset of eigenfunctions $f_n^+(x)$ $(n = 0, 1, 2, \ldots)$ defined on the whole interval $x_1 < x < x_2$ is a complete system with respect to the class of continuous functions defined on the subinterval $x_1 < x < x_0$ and having a null derivative in the point $x = x_1$ The subset of eigenfunctions $f_n^-(x)$ $(n = 0, 1, 2, \quad)$ defined on the whole interval $x_1 < x < x_2$ is a complete system with respect to the class of continuous functions defined on the subinterval $x_0 < x < x_2$ and having a null derivative in the point $x = x_2$.

It is to be noted that unlike of theorem I where f_n^+ and f_n^- are disjunct subsets, in theorem II, the two subsets have a common element, namely $f_0^+ \equiv f_0^-$.

As a rule, equations (47) and (48) will yield constants a_n^+ and a_n^- respectively The constants a and a will be then determined using (46).

6. **Conclusions.** The above reasonings are based on the hypothesis that separation-of-variables method applied to countercurrent transfer problems leads to the correct solution This hypothesis is based in its turn, on the fact

that the obtained solutions do not contradict the experimental facts. Also, in the course of reasonings a series of physical arguments are used. In conclusion, this paper presents a series of arguments which indicate the existence of two theorems of completeness which have not been known so far, but it does not offer a rigorous mathematical demonstration.

It may seem curious that the two theorems have not been descovered up to the present although the Sturm-Liouville problem is old and much work was spent to study it. In our opinion the explanation consists just in the fact that problems in which $r(x)$ changes sign have not appeared in practice but recently.

In the very particular case when the caloric capacities of the two fluids which flow countercurrently are equal, the Sturm-Liouville boundary problem leads, for the double eigenvalue $\lambda = 0$, to only one eigenfunction. This paper shows that in this, and only in this case, the transfer equations admit a particular solution, liniar in z, which cannot be expressed by the eigenfunctions of the Sturm-Liouville boundary problem

Acknowledgement The author wishes to thank Prof Ioan A Rus of the Babeş-Bolyai University at Cluj-Napoca, Romania, for his helpful suggestions and comments

(Received February 13, 1982)

REFERENCES

1 R J Nunge, W N Gill, Int J, Int J Heat Mass Transfer, **8**, 873 (1865)
2 R J Nunge, W N Gill, AIChE J, **12**, 297 (1966)
3 R J Nunge, E W Porta, W N Gill, Chem Eng Progr Symposium Ser No **77**, **63**, 80 (1967)
4 J A Blanco, W N Gill, Chem Eng Progr Symposium Ser No 77, **63**, 66 (1967).
5 J A Blanco, W N Gill, R J Nunge, AIChE J, **14**, 505 (1968)
6 R P Stein, Chem Eng Progr Symposium Ser No 59, **61**, 64 (1965)
7 R P Stein, Chem Eng Progr Symposium Ser No 59, **61**, 76 (1965)
8 R P Stein, AIChE J, **12**, 1217 (1966)
9 R P Stein, Chem Eng Progr Symposium Ser No 82, **64**, 219 (1968)
10 I Hodor, *Thesis*, Univ „Babeş-Bolyai", Cluj-Napoca (Romania), 1971
11 M Mason, Trans Am Math Soc, **7**, 337 (1906)
12 M Mason, Trans Am Math Soc, **8**, 427 (1907)
13 M Picone, Math Z, **28**, 519 (1928)
14 M Bocher, Bull Am Math Soc, **21**, 6 (1914)
15 E L Ince, *Ordinary Differential Equations*, Dover Publications, Inc, London, 1956

TRANSFER DE CĂLDURĂ SAU MASĂ ÎN UNELE SISTEME ÎN CONTRACURENT ŞI PROBLEMA LA LIMITĂ STURM-LIOUVILLE CORESPUNZĂTOARE

(Rezumat)

Se studiază problema matematică a transferului de căldură sau masă în unele sisteme în care are loc o mişcare în contracurent Aplicarea metodei separării variabilelor conduce la un tip de problemă la limită Sturm-Liouville care are caracteristici deosebite ce n-au mai fost întîlnite în aplicaţii Pe baza unor raţionamente fizice se ajunge la concluzia că funcţiile proprii ale problemei trebuie să satisfacă niste teoreme (conjecturi) care, se pare, n-au fost semnalate pînă în prezent

STUDIA UNIV BABEŞ-BOLYAI, PHYSICA, XXVIII, 1983

STUDY OF THE MICROPHASE SEPARATION PROCESS IN 90% (16%Na_2O—84%B_2O_3)—10%V_2O_5 GLASS

E. CULEA, AL. NICULA, I. BRATU, I. BIRIŞ

1. **Introduction.** The microphase separation is a very important process which occurs in the vitreous materials and can generate essential modifications on their structure and properties In the last 30 years were obtained vitreous materials with very interesting properties, due to a controled microphase separation and today they are used currently in many top technologies (Vycor glass, thermoresistant glasses, photochromic glasses, etc)

For these reasons the study of the microphase separation of the vitreous materials is of special importance They were performed investigations in order to clear up the connections exist wich between structural modifications induced by the microphase separation and the modifications wich occur in their macroscopic properties

The majority of these studies use optical or electron microscopy, but in the last years were reported some attempts to utilise new investigation techniques. Thus K a w a z o e et al [1—4] have evidenced the possibility to utilise EPR of Cu^{2+} ions in order to detect microphase separation in the oxide glasses of K_2O—RO—B_2O_3 vitreous system, where R=Ca, Ba or Mg

The aim of this paper was to study the microphase separation in 90% (16%Na_2O—84%B_2O_3)—10%V_2O_5 vitreous system (the composition is expressed in molar %), using EPR, IR spectroscopy and electron microscopy

2. **Experimental results.** The samples were prepared by mixing H_3BO_3, borax and V_2O_5 in the suitable proportion This mixtures was melted in sinter-

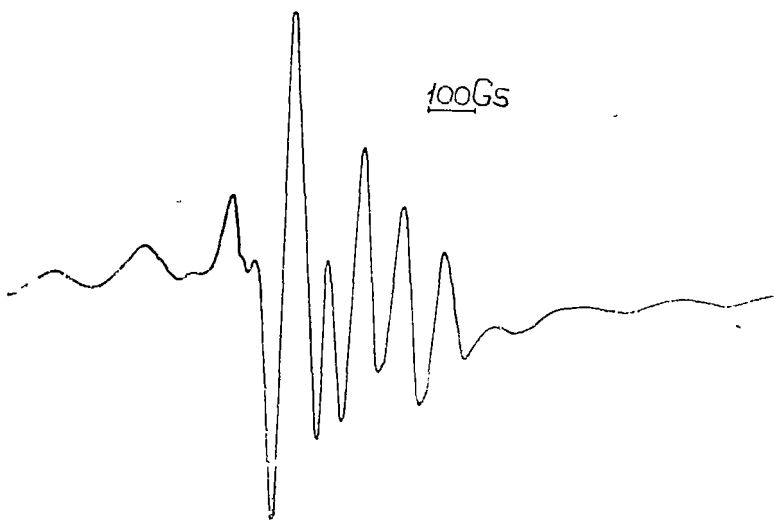

Fig 1 EPR spectrum of 90% (16% Na_2O—84% B_2O_3)—10% V_2O_5 glasses

corundum crucibles at 1200 °C. After being kept at this temperature for 1h the melts were cooled onto a rust-proof steel plate. Then the samples were heated to 550 °C and maintained at this temperature 0 5 to 12h for thermal treatment.

Chemical analysis reveals no sensible deviations from the nominal composition

The EPR study was performed at 9.4GHz (X band), using a standard JEOL equipment, at room temperature A representative EPR spectrum of our glasses is presented in fig 1.

The calculated EPR parameters are presented in Table 1

Table 1

EPR parameters of 90% ($16\%Na_2O-84\%B_2O_3$)$-10\%V_2O_5$ glasses, heat treated for t = 0.5 to 12h

nr	Sample	Thermal treatment duration (h)	$A_{\parallel}$ 10^4cm^{-1}	$A_{\perp}$ 10^4cm^{-1}	$g_{\parallel}$	$g_{\perp}$
1	S_1	0	176 7	60 5	1 935	1 979
2	S_2	0 5	175 6	60 5	1 936	1 980
3	S_3	1	177 2	60 9	1 936	1 979
4	S_4	2	176 5	60 5	1 935	1 978
5	S_5	3	178 1	61 2	1 936	1 979
6	S_6	6	177 5	61 0	1 935	1 979
7	S_7	9	178 8	60 8	1 936	1 980
8	S_8	12	177 9	61 2	1 936	1.979

The infrared absorption spectra were obtained with a UR—20 spectros meter The technique of the powder tablet in KBr was used Fig. 2 presents the infrared absorption spectra for samples S_1(a), S_7(b), for the host glas- $16\%Na_2O-84\%B_2O_3$ (c) and for V_2O_5 (d)

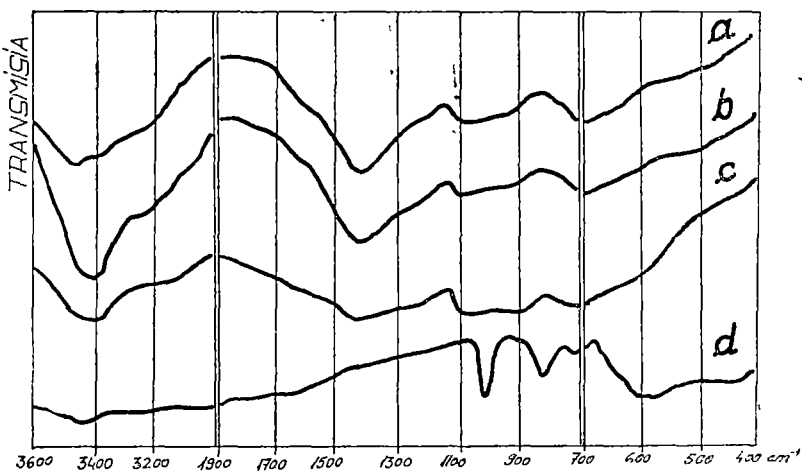

Fig 2 Infrared absorption spectra of a) sample S_1 (t = Oh), b) sample S_8 (t = 9h), c) host gl , d) V_2O_5

The electron microscopic investigation was performed with a TESLA BS—613 equipment, using carbon replica on glass fractures. Fig. 3 shows electron microscopic images for samples S_1(a), S_2(b) and S_5(c).

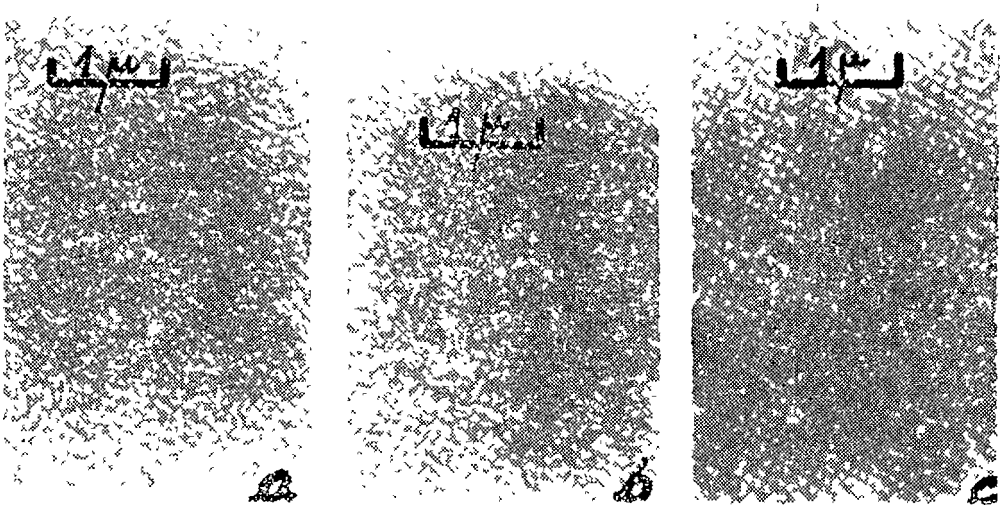

Fig. 3. Electron microscopic images of a) sample S_1 (t = 0h), b) sample S_2 (t = 0.5h), c) sample S_5 (t = 3h)

3 **Discussion of results.** The electron microscopic investigation indicates the development of a microphase separation, similar with that described by [5] for the host glass. The addition of 10% mol V_2O_5 seems to not influence the phase separation. For this reason we suppose that the two phase wich were evidenced in our glasses are essentially the same like in the host glass: a droplet-phase, rich in Na^+ ions and a matrix-phase, consisting mainly of the vitreous boron oxide network.

It was proved that in sodium borate glasses the phase separation tendency presents a maximum for about 16% mol Na_2O. This tendency remaines very important after the addition of V_2O_5. Thus even for the sample S_1 wich was not heat-treated, a phase separation was observed. The sample S_5 evidences a more advanced phase separation than that described by [5] for the host glass, due probably to different preparation techniques.

Application of SAXS and MAXS techniques to alkali borate glasses [6] permitted to find even in samples wich don't exhibit a phase separation, a special kind of submicroheterogeneous structure due to the non-uniform distribution of alkali ions in the glass matrix. It was shown that about 25% of alkali oxide ions are grouped in these submicroheterogeneous regions and the remaining part of alkali ions are statistically randomly distributed within the glass matrix.

The infrared absorption characterizes the vibration state of the lattice. By comparing the infrared absorption spectra of the host glass with that of 90% ($16\%Na_2O-84\%B_2O_3$)—$10\%V_2O_5$ samples, information on the nature of vitreous state of our glasses can be obtained.

In order to make a comparative analysis and at same time to check the accuracy of measurements, we obtained spectra of 16% Na_2O—84% B_2O_3 glass matrix and of V_2O_5 (fig 2). These are in good agreement with the previous data [7, 8].

The spectrum of the 16%Na_2O—84%B_2O_3 glass shows a wide band between 1200—1500 cm^{-1} characteristic for the drawing vibration of B—O bands (wich also includes the characteristic vibration of BO_3 configuration located at about 1250 cm^{-1}) and another important band at 900—1100 cm^{-1} due to BO_4 configuration

The infrared spectrum of V_2O_5 shows a wide absorption band at 830 cm^{-1} due to the vibrations of V—O bonds (1 77Å, 1 88Å and 2 02Å) and a narrow band at 1019 cm characteristic for the vibration of V=O bonds [8]

The infrared spectra of 90% (16%Na_2O—84%B_2O_3)—10%V_2O_5 glass have the same bands as the host glass No bands characteristic to V_2O_5 or to any new structural groupings are observed This proves that V_2O_5 is perfectly solved in the host glass and don't modify the constitutive structural groupings of this glass (tetraborate groupings [7, 9]) These data are consistent with NMR data on sodium borate glasses with 10% mol V_2O_5 [10]

It is possible that V_2O_5 addition produces weak infrared absorption bands wich are masked by the wide bands of the host glass

The heat-treatment don't produces important modifications on the infrared spectra of our glasses Only a narrowing of the wide band located at 3200—3500 cm^{-1}, due to the vibration of O—H bonds, was observed This indicates the decrease of the number of O—H . . O—H bonds when the heat-treatment duration increases and it was to be expected

The infrared spectra of our glasses suggest that the constitutive structural groupings show a considerable stability to heat-treatment Consequently it is expected that the alkali ion content of the microphases don't change during the heat-treatment

The EPR spectra obtained on our glasses are characteristic for the V^{4+} ion wich in oxidic glasses appears as vanadyl ion VO^{2+} and forms molecular complexes of symmetry C_{v4} [11—13] These spectra can be analysed by means of the spin hamiltonian of axial symmetry

$$H = \beta(g_{||}H_zS_z + g_{\perp}H_xS_x + g_{\perp}H_yS_y) + A_{\perp}S_xI_z + A_{\perp}S_xI_x + A_{\perp}S_yI_y \qquad (1)$$

wich leads to the following resonance condition

$$h\nu = g\beta H(m) + K(\theta)m \qquad (2)$$

where

$$g = \sqrt{g_{||}^2\cos_{||}\theta + g_{\perp}^2\sin^2\theta} \qquad (3)$$

$$K(\theta) = \sqrt{A_{||}^2g_{||}^2\cos^2\theta + A_{\perp}^2g_{\perp}\sin^2\theta}$$

with the usual notation [13].

The EPR parameters are not affected by the heat-treatment The hiperfine structure constant $A_{||}$, the most sensible EPR parameter, increases weakly with heat-treatment duration It seems that the heat-treatment don't influence practically the microvicinity of V^{4+} ions

In barium borosilicate glasses it was proved that cobalt ions are preferencially distributed, having an important tendency to occupy sites in modifier oxide rich phase [14] It is possible that in the same manner V^{4+} ions have a non-uniform distribution in 90% ($16\%Na_2O-84\%B_2O_3$)$-10\%V_2O_5$ glass, with preference for the phase rich in Na^+ ions These regions or phases with a higher content of Na^+ ions have more stable structural elements and this could explain the remarcable stability of the microvicinity of V^{4+} ions, expressed in a relative constancy of the EPR parameters during the heat-treatment

4 **Conclusion.** The phase separation process in 90% ($16\%Na_2O-84\%B_2O_3$) $-10\%V_2O_5$ glass is similar with the phase separation in $16\%Na_2O-84\%B_2O_3$ The constitutive structural groupings of our glasses are the same like in the host glass and are not affected by the heat-treatment

The microvicinity of V^{4+} ions in these glasses are not affected by the heat-treatment

Our glasses show a classical phase separation process The structural elements and the compozition of phases are very well defined even in the early stages of the separation process and are not affected by the heat- treatment. The heat-treatment affects only the dimensions of droplets of sodium rich microphase

(Received February 22, 1982)

REFERENCES

1 H Kawazoe, H Hosono, T Kanazawa, J Non-Cryst Solids, **29,** 173 (1978)
2 H Kawazoe, H Hosono, T Kanazawa, J Non-Cryst Solids, **29,** 249 (1978)
3 H Kawazoe, H Hosono, T Kanazawa, Yogyo-Kyokai-Shi, **87,** 23 (1979)
4 H Kawazoe, H Hokumai, H Hosono, T Kanazawa, J Non-Cryst Solids, **38—39,** 717 (1980)
5 W Vogel, *Struktur und Kristalisation der Glasser,* VEB Deutscher Verlag fur Grundstoffindustrie, Leipzig, 1965
6 V V Golubkov, A P Titov, T N Vasilevskaya, E A Porai-Koshits, Fizika i Khim Stekla, **4,** 633 (1978)
7 J Krogh-Moe, Phys Chem Glasses, **6,** 2, 46 (1965)
8 M Sayer A Mansingh, Phys Rev B, **6,** 12, 4629 (1972)
9 G E Jellinson, P J Bray, J Non-Cryst Solids, **29,** 187 (1978)
10 S Simon, V Simon, Al Nicula, Studia Univ Babeş-Bolyai, Phys, **26** (1), 11 (1981)
11 H G Hecht, T Johnston, J Chem Phys, **46,** 1, 23 (1967)
12 L D Bogomolova, V A Iachkin, V N Lazukin, *Proceeding of* **19***th Congress Ampere,* Heidelberg, 235 (1976)
13 Al Nicula, E Culea, L Stănescu, Studia Univ Babeş-Bolyai, Phys, **23** (1), **55** (1978)
14 W Vogel, J Non-Cryst Solids, **25,** 1—3, 170 (1977)

STUDIUL PROCESULUI DE SEPARARE ÎN MICROFAZE ÎN SISTEMUL VITROS 90% ($16\%Na_2O-84\%B_2O_3$)$-10\%V_2O_5$

(Rezumat)

Se studiază procesul de separare în microfaze a sistemului vitros 90% ($16Na_2-84\%B_2O_3$)$-10\%V_2O_5$ prin RPE, absorbţie în IR şi microscopie electronică Se constată că tratamentul termic produce dezvoltarea microfazei picătură, dar nu modifică grupurile structurale de bază şi nici microvecinătăţile ionilor V^{4+}

STUDIA UNIV BABEŞ-BOLYAI, PHYSICA, XXVIII, 1983

A PROCEDURE OF GRADUAL GENERATING TREES IN A LINEAR GRAPH

V. MILITARU

1 **Introduction.** A useful instrument for the application of the topological methods of solving the problems of analysis and synthesis of the electrical networks is the algebra of structural numbers, proposed by Bellert [1] and extended in more complex systems by Gandhi and collaborators [2]. In particular, the theorems demonstrated in [1] give simple algorithms for the determination of all the possible trees or co-trees of a graph or multigraph

Starting from a tree of the graph and using the properties of the fundamental cut-sets, a generalizing theorem is demonstrated, which permit the gradual forming of the trees by a process of substitution of the twigs of the initial tree Any set of trees which maintains unchanged a desired part of the starting tree is obtainable, because of the possibility to control the order of generation The process can go on till all the trees are obtained

Avoiding the matrix algebra, this method offers advantages in programming.

2 **The Generation of New Trees Using F-Cut-Sets.** The structural and interconnectional characteristics, determining to a great extent the dynamic behaviour of an electrical network, are revealed by the linear graph associated with it [5, 6] In such a linear graph, supposed to be connected, with $n + 1$ nodes and b branches, each of its trees will have n branches, referred as twigs, the rest $b - n$ being considered links Each link closes a fundamental loop (f—loop), having thus a set of $b - n$ f-loops with respect to the chosen tree. Each twig defines a fundamental cut-set (f-cut-set), obtaining n such f-cut-sets, i.e., a fundamental set of cut-sets with respect to the same tree

The graph obtained out of the tree together with any link contains only one closed path, given by the f-loop of the respective link. Any twig of this path can become a link and so new trees are obtained In order to turn to account this idea we must take into consideration the structural interdependence between the set of the fundamental loops and the fundamental set of cut-sets having — as it is demonstrated in [3] — the following properties

— Any f-cut-set with respect to a chosen tree of a connected graph is formed by a twig together with the links of those f-loops which contain that twig

— The same link belongs to the f-cut-sets of all the twigs which form the path through the tree of the f-loop of this link and only to those.

Combining the aforesaid idea with the first property we can see that, starting from a tree of a connected graph, we can generate new trees by replacing a twig with any of the links of the f-cut-set of the respective twig. The second property underlines that these are the only links able to achieve the replacement, the f-loops of others links remaining intact at the elimination of a branch that does not belong to them

The elaboration of a systematic procedure of the gradual substitution of the twigs of the initial tree can be obtained by using the algebra of structural numbers.

3 **Structural Numbers. Product.** Starting from the custom of numbering the branches of a graph, B e l l e r t, turning to account an older idea of Wang's, defines [1] the structural number as a rectangular array of natural numbers Its primary element is the column, which describes the composition of a tree of the graph The graph with all the trees described by the columns of a structural number is its geometrical image Bellert also elaborates an algebra of the structural numbers, from which we shall take the product

Each f-cut-set may have a correspondent structural number fo one row:

$$P_i = (t_i, l_{i1}, l_{i2}, \quad), \qquad i = 1, 2, \quad , n \tag{1}$$

in which t_i is the twig and (l_{ij}) is the set of the links, taken in any order

Using this notation we can now formulate the following

THEOREM Let $(t_1, t_2, \quad ., t_n)$ be the set of twigs of a tree in a linear graph, taken in any order The columns of the structural number

$$N_i = P_1 \quad P_2 \qquad P_i, \qquad k \leqslant n$$

represent all the possible combinations of k branches, each ot them, together with the set $(t_{k+1}, t_{k+2}, \quad , t_j)$, making up a tree of the same graph

Demonstration Using the method of complete induction, for the step $k = 1$ we obtain

$$N_1 = P_1 \tag{2}$$

The validity of the theorem in this case is assured by the observation at the end of section 1

Supposing the theorem valid for a step $i < k$, we shall pass to the step $i + 1$

$$N_{i+1} = N_i \quad P_{i+1} \tag{3}$$

In order to work out the product (3) we shall add each element of P_{i+1} to each column in N_i So, starting from each tree generated in phase i we shall search for all the possibilities of replacing the twig t_{i+1} As $t_{i+1} \in P_{i+1}$ we shall obtain, besides new trees, all the trees of the anterior phase As to replacing the twig by links of its cut-set, fundamental with respect to the initial tree, there will be the following situations

1 The column in N_i contains no element of P_{i+1}, then the cut-set represented by P_{i+1} is fundamental with respect to the tree corresponding to the aforesaid column. There is the same situation as for $k = 1$, the elements of P_{i+1} being all and at the same time the only ones acceptable for the replacement of t_{i+1}

2. Let a column of N_i in which there is an element $l \in P_{i+1}$. There is, by hypothesis, a corresponding tree to this column, in which l and t_{i+1} appear as twigs Let T_1, T_2, T_3 be the parts of the tree interconnected by these twigs.

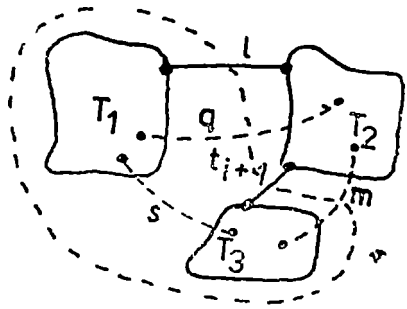

Fig 1

We, generaly, obtain the topological situation in the figure. Eliminating the twigs l and t_{i+1}, we can easily render evident the partition of nodes operated by the cut-set P_{i+1} On the figure one of the groups of nodes is delimited by dotted line The rest of the elements of the cut-set P_{i+1} are to be found either „parallel" to t_{i+1}, i e , joining the same parts, as it is, e.g , m, or „parallel" to l, as it is q. As it can be noticed in the figure, the elements of the first category can substitute t_{i+1}, resulting a new tree, while the elimination of t_{i+1} and the adding of an element of the q type results in the separation of T_3 and the appearance of a loop through l and q, But, let us still maintain t_{i+1}, substituting l by q in the figure We obtain a tree of the phase i to which, by hypothesis, corresponds a column in N_i This will have $i - 1$ elements identical to those of the column mentioned before, differing from one another by the presence of q, respective l. Obtaining through multiplication l, respective q, we have a pair of identical columns Naturally, we shall also obtain in the process of multiplication, columns in which l or q are repeated These are not acceptable be ause $n - 1$ elements cannot make up a tree So, we see that the appearen · of columns with repeated elements, as well as of pairs of identical columns a e criteria eliminating those combinations which do not lead to new trees These rules are included in the definition of the product of structural numbers

As it can be noticed in the same figure, branches of the s type, joining T_1 with T_i, can substitute t_{i+1}, resulting new trees As the s type branches do not belong to P_{i+1}, the trees of this kind are, apparently, lost But, let us still maintain t_{i+1}, substituting l by s We obtain a tree of the phase i to which, by hypothesis, corresponds a column in N_i Through multiplication by P_{i+1}, t_{i+1} is substituted by l, obtaining a tree of the mentioned kind

We can notice that none of the branches of the graph which are not of the m or s type can substitute t_{i+1}

3 If in a column of N_i there appear several elements l, l', $\in P_{i+1}$, excepting the necesity to figure several parts of the tree of the type T_i, the disscution of point 2 can be repeated for each of them, independently

So, the process of induction is complete, demonstrating the theorem

4 **Conclusions.** — In the case $k = n$ the theorem gives a procedure of generating all the trees of the linear graph

— From the development of the demonstration a certain generalization results So ,if, starting from a known tree, we want to obtain the set of all the trees which do not contain certain initial twigs, all we need is to represent the twigs in the product by structural numbers P'_i, which are obtained from P_i eliminating the respective twigs.

— As the demonstration can be applied to each connected part of an unconnected graph, independently, we can generalize the theorem to this case, replacing the term of tree by that of forest everywhere and considering n = nodes-p, where p is the number of connected parts

(Received April 3, 1982)

REFERENCES

1. S Bellert, J Franklin Inst, **274**, 425 (1962)
2 B R M Gandhi, V Purnachandra Rao, G S Raju, Int J Electronics, **32**, (6), 601 (1972)
3 V Militaru, *Lucrările Conferinței Naționale de Fizică*, București 21—23 oct 1982, p 532.
4 L Weinberg, *Progress in Radio Science 1960—1963*, Vol VI, Elsevier, Amsterdam, 1966
5. R E Kalman, N DeClaris, *Aspects of Network and System Theory*, Holt, Rinehart and Winston, Inc, New York, 1971
6 N Balabanian, T Bickart, *Teoria modernă a circuitelor*, Ed tehnică, București, 1974.
7 C Berge, *Théorie des Graphes et ses Applications*, Dunod, Paris, 1967
8 M Preda, P Cristea, I Dorobanțu, *Analiza topologică a circuitelor electrice*, Ed. tehnică, București, 1979

O PROCEDURĂ DE GENERARE TREPTATĂ A ARBORILOR UNUI GRAF LINIAR

(Rezumat)

Aplicarea formulelor topologice pentru funcțiile de circuit, elaborate de mulți autori, constituie baza unor metode de analiză, asistată de calculator, a circuitelor electrice, avantajoase datorită eliminării algoritmilor greoi de evaluare a determinanților. Cunoașterea tuturor arborilor grafului liniar asociat rețelei studiate este o condiție a aplicării acestor metode

Teorema demonstrată în această lucrare este o generalizare a altora, publicate anterior de alți autori, și permite elaborarea unui procedeu simplificat de generare a arborilor unui graf liniar. Evitînd utilizarea matricilor de rețea, metoda oferă avantaje în economisirea de timp de calcul și de spațiu de memorare

STUDIA UNIV BABEŞ-BOLYAI, PHYSICA, XXVIII, 1983

ESR AND MAGNETIC SUSCEPTIBILITY STUDIES OF SOME COPPER(II) p-CLORBENZOATES

O. COZAR, N GRECU*, I. BRATU**, M. COLDEA, V. GRECU***

1. **Introduction.** Recently, a vast amount of research has been devoted to the characterization of dimeric compounds, because these are excellent model systems for the study of magnetic interactions and for their biological and catalytic applications. A great number of complexes have been synthesized, the experimental and theoretical investigations concerning the temperature dependence of the magnetic susceptibility being reported by several authors [1—8].

Besides the magnetic susceptibility investigations which are fundamental to the determination of the singlet-triplet separation (2J) resulting from the izotopic exchange interaction, the ESR studies as in powders or solutions were also made [9—15] as in monocrystals [16—18], these giving the complementary information on their electronic structure and interactions inside of binuclear complexes

The electronic direct exchange interaction between the two copper ions with $s = \frac{1}{2}$ occurs in the case when the metallic ions are close enough together as in copper (II) acetat monohydrate ($R_{Cu-Cu} = 2\,64$ Å) [9,14]. In many other cases, the spin-spin coupling is achieved by a magnetic dipole-dipole interaction and by a superexchange interaction occuring through intermediate atoms or ions [14, 19]

These investigations are of considerable importance for their biological applications [20—23] Thus, the studies on the copper(II) complexes with amino-acids and peptides which serve as models of biological active systems, have been evidenced the presence of spin-spin interactions and the formation of dimeric states for $[Cu(DL\text{-}\alpha\text{-alanine})_2H_2O]_2$ [22] and tetrakis (L-tyrosinato) dicopper(II) [20] It was found that in metalloproteins which have more than one metallic ion, the copper tends to appear as even numbers, e.g cerebrocuprein contains $2Cu^{2+}$ and ceruloplasmin contains $8Cu^{2+}$ [24]

In the present work, the copper(II) p-clorbenzoates $[Cu_2R_4 \cdot CH_3OH \cdot 2H_2O]$ —(I) and $[Cu_2R_4 \cdot CH_3COCH_3 \cdot 2H_2O]$ — (II) where $R = (p\text{-}ClC_6H_4CO_2)$ as well as their monomeric species which occur at 77 K have been investigated using ESR and magnetic susceptibility measurements Both compounds have been synthesized after the method given by Lewis et al [1]

The ESR studies were performed at the 295 K and 77 K using a standard JEOL-JES-3B equipment in X band (~9 4 GHz) The magnetic susceptibility data were obtained using a Faraday type balance with 10^{-8}e m u /g sensitivity in the temperature range (80—293) K

2 **Results and Discussion** a) *ESR Investigations* The ESR spectra obtained at room temperature clearly show that both complexes contain coupled

* Institute of Physics and Technology of Materials, Bucharest.
** Institute of Isotopic and Molecular Technology, Cluj-Napoca
*** Faculty of Physics, Bucharest

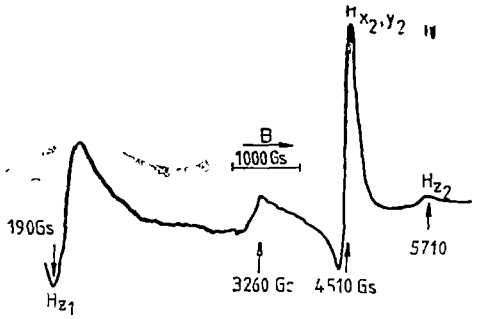

Fig 1 ESR spectrum of powdered $[Cu_2(p\text{-}ClC_6H_4CO_2)_4 \cdot CH_3OH \cdot 2H_2O]$ at room temperature

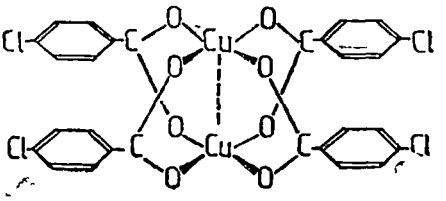

Fig 2 The $[Cu_2(p\text{-}ClC_6H_4CO_2)_4]$ structure

pairs of copper (II) ions The spectrum of the powdered $[Cu_2(p\text{-}ClC_6H_4CO_2)_4 \cdot CH_3OH \cdot 2H_2O]$ complex exhibits the absorption typical of a randomly oriented triplet state ($S = 1$) species having an axial symmetry (Fig 1) It is similar with the spectra obtained for other copper acetate like dimers [12, 13], which are characterized by a short Cu—Cu distance (~2 64 Å) Here the exchange interaction between the two copper ions (Fig. 2) appears as a superposition of the two $d_{x^2-y^2}$ atomic orbitals situated in parallel planes which form a δ type bond [1] At the same time, the formation of a σ bond along the Cu—Cu axis through the agency of the $d_{z^2}^2$ orbitals is also possible [25]

The absorption which is observed near 3200 Gs (Fig. 1) arises from monomeric impurities of spin $s = \frac{1}{2}$. The intensity of this absorption increases with the lowering of temperature. Thus the 77 K spectra (Fig 3) exhibit a very intense

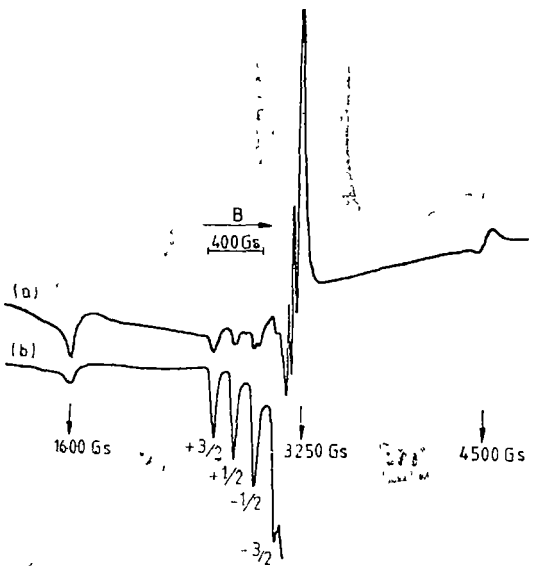

Fig 3 ESR spectra obtained at 77 K (a)-complex(I), b)-complex(II)

signal in the 3200 Gs region characteristic for izolated Cu^{2+} ions (monomeric species, $s = 1/2$) in the axial symmetry The hyperfine structure is well resolved in both parallel ($g_{\|}$) and perpendicular ($g_{\perp}$) bands The weak absorption from 4500 Gs (Fig. 3) indicates the presence of a little amount from initial dimeric species On the other hand the absorption from 1600 Gs is due to the forbidden $\Delta M_s = \pm 2$ transitions characteristic for dimeric species in which the copper-copper distance is $\simeq 4-5$ Å [14, 15, 26] This last type of dimeric species represents the majority from those existing at 77 K. However the spectra obtained at 77 K clearly show that the dimeric species are broken by freezing, this fact leading to the appearance of monomeric species. The appearance of monomeric species at low temperatures can be attributed to the water molecules contained in matrices of the studied complexes By freezing these lead to an increase of the Cu—Cu distance and thus to the breaking of the spin-spin coupling with their rearrangement in monomeric forms In this manner may also be explained the appearance of the second type of dimeric species at 77 K for which the copper-copper distance has been increased The presence of water molecules in matrices of studied complexes is explained by their chlatrate properties [27] Thus, the chlatrate molecules of CH_3OH and CH_3COCH_3 from complex (I) and respectively (II), may leave the matrix producing the active centers for the adsorption of water molecules Because the CH_3COCH_3 molecule has a greater volume than CH_3OH, a more pronounced hygroscopic character results for the complex (II) than the complex (I). This fact has been previously elucidated by us using the I R. and thermodiferential measurements [27]

The ESR spectra at 77 K (Fig 3) also show that the monomer/dimer ratio is greater for complex (II) than for complex (I) An estimation of this ratio was made from magnetic susceptibility data

b) *Magnetic susceptibility measurements* The magnetic susceptibility of both investigated complexes was measured in the temperature range 80—293 K It is noctied that the magnetic susceptibility obeys a Curie-Weiss low, $\chi = c/(T-\theta)$, with $\theta > 0$ (Fig 4)

The experimental magnetic moments per formula unit have the values $\mu_{exp}^{(I)} = 2\,675\ \mu_B$ for the complex (I) and respectively $\mu_{exp}^{(II)} = 2\,54\ \mu_B$ for the complex (II) The obtained magnetic moments are smaller than the theoretical value $\mu_s = 2\,82\ \mu_B$ calculated for the dimeric species ($S = 1$), when the two spins are coupled, and

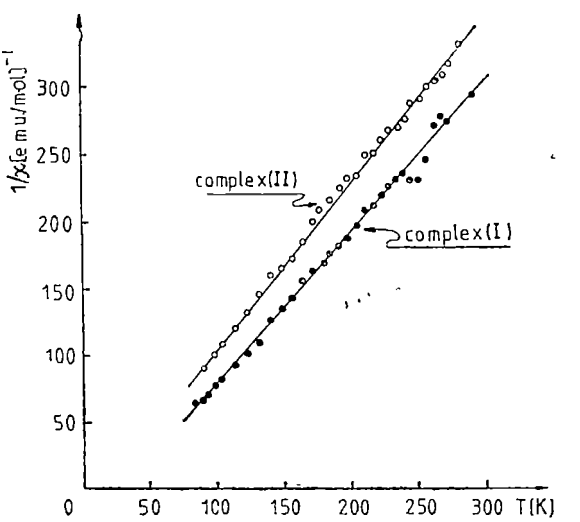

Fig 4 The temperature dependence of the reciprocal magnetic susceptibility

are larger than the value $\mu_m = 2.44\ \mu_B$ calculated for two $s = 1/2$ uncoupled spins, when the two monomeric species occur The difference between the experimental and calculated magnetic moments may be attributed to a mixture of dimeric and monomeric species If we denote with f_m and f_d the molar fractions of monomeric and respectively dimeric species in the sample, then the experimental magnetic moment value per formula unit is given by the expression [28]

$$\mu_{exp} = (f_m \mu_m^2 + f_d \mu_d^2)^{1/2} \tag{1}$$

with the condition $f_m + f_d = 1$, μ_m and μ_d being the two above mentioned magnetic moments for pure monomeric and respectively dimeric species

Replacing the experimental magnetic moment values in the equation (1), we have obtained

$$f_m = 40\% \text{ and } f_d = 60\% \text{ for complex(I)}$$

$$f_m = 75\% \text{ and } f_d = 25\% \text{ for complex(II)}$$

The difference between the number of monomeric species in the two complexes is due to the fact that the lattice of complex(II) contains more water molecules than complex(I) [27]

c) *Monomeric species* In figures 5 and 6 are shown the 77 K ESR spectra characteristic for monomeric species which occur in both studied complexes. A careful analysis of the hyperfine structure from the parallel band indicates the coexistence of two magnetic nonequivalent monomeric species in the case of complex(I), labelled by I′ and I″ (Fig 6)

The characteristic ESR parameters for monomeric species are given in Table 1 We notice that the values of parameters for I″ species are approximately equal to those obtained for monomeric species of the complex(II) This fact indicates that the two monomeric species are the same On the other hand, in the case of complex(II) only this type of monomeric species appears

A n t o s i k et al [29] have shown that chloroform forms the weak complexes with some copper (II) chelates in chloroform-toluene glasses at 77 K Taking into account these results, it may be considered that two monomeric species from complex(I) are due to the absence (I′) or the presence (I″) of axial perturbations, which arise from water molecules acting with the d_z^2 orbital of Cu^{2+} ions

We consider that the species (I′) has a square-planar symmetry (tetragonal D_{4h}), without axial perturbations.

In the case of I″ species a component of octahedral symmetry (Oh) arises because of two water molecules situated along of the Oz axis Thus the electronic distributions within the transition metal ion complex are sensible perturbed by interaction with the neighbouring water molecules This gives rise to the modifications in the values of g and hyperfine tensors (Table 1)

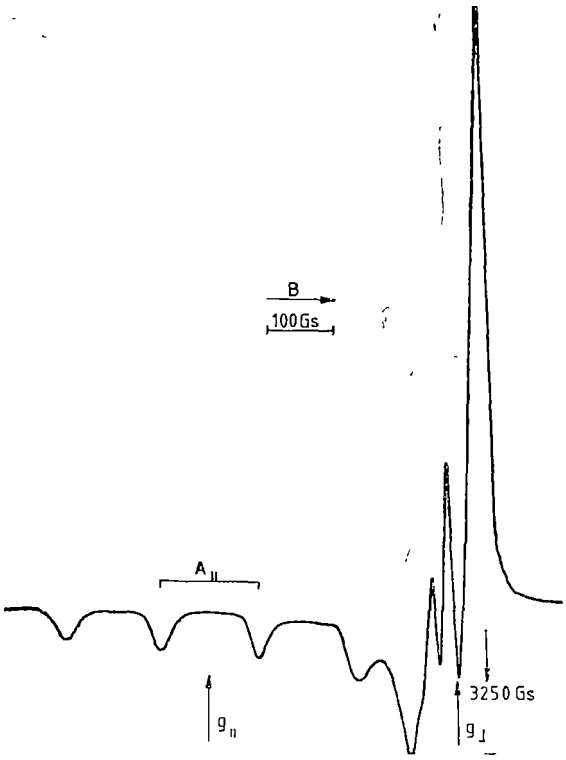

Fig 5 The 77 K ESR spectrum of the complex(II), in the 3200 Gs region

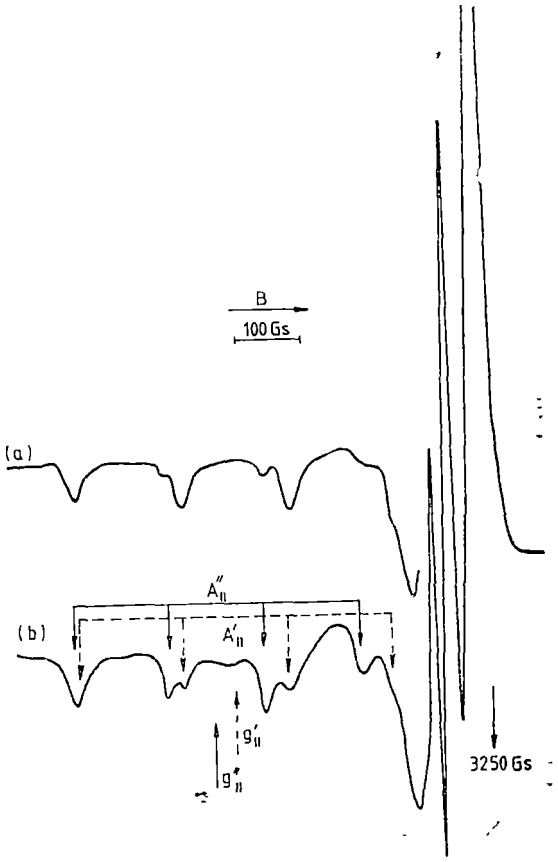

Fig 6 Modification in time of the 77 K ESR spectra for complex(I) in the 3200 Gs region

Table 1

Monomeric species	$g_{\|\|}$	$g_{\perp}$	$A_{\|\|}$ ($10^{-4}cm^{-1}$)	$A_{\perp}$ ($10^{-4}cm^{-1}$)	α^2
(I')	2 301	2 067	174	21 4	0 85
(I'')	2 327	2 046	162	43	0,83
(II)	2 324	2 044	165	43	0 84

The ratio of the two monomeric species (I''/I') from complex(I) changes in time due to the water molecules absorption ESR spectra recorded at a year interval show a modification of I''/I' ratio from 1/3 (Fig 6a) to 3/2 (Fig 6b) This fact indicates that a number of I' species become the I'' type species togheter with the increasing of the amount of adsorbed water This type of mono-

meric species which is characterized by the presence of two water molecules along Oz axis is the only present in the complex(II)

The ground state and the first excited states of the paramagnetic hole in the case of the square-planar complexes (I′ species) are described by the following antibonding orbitals [30, 31]:

$$|B_{1g}\rangle = \alpha d_{x^2-y^2} - \frac{\alpha'}{2}(-\sigma_x^{(1)} + \sigma_y^{(2)} + \sigma_x^{(3)} - \sigma_y^{(4)})$$

$$|B_{2g}\rangle = \beta d_{xy} - \frac{1}{2}(1-\beta^2)^{1/2}(p_y^{(1)} + p_x^{(2)} - p_y^{(3)} - p_x^{(4)})$$

$$|E_g\rangle = \begin{cases} \delta d_{xz} - \frac{1}{\sqrt{2}}(1-\delta^2)^{1/2}(p_z^{(1)} - p_z^{(3)}) \\ \delta d_{yz} - \frac{1}{\sqrt{2}}(1-\delta^2)^{1/2}(p_z^{(2)} - p_z^{(4)}) \end{cases} \tag{2}$$

The spin Hamiltonian parameters can be expressed as functions of the coefficients of the antibonding orbitals. These functions are [31]

$$g_{\parallel} = 2.0023 - \frac{8\lambda}{\Delta E_{xy}}[\alpha^2\beta^2 - f(\beta)] \tag{3}$$

$$g_{\perp} = 2.0023 - \frac{2\lambda}{\Delta E_{xz}}[\alpha^2\delta^2 - g(\beta)] \tag{4}$$

$$A_{\parallel} = P\left\{-\alpha^2\left(\frac{4}{7} + k\right) - 2\lambda\alpha^2\left[\frac{4\beta^2}{\Delta E_{xy}} + \frac{3\delta^2}{7\Delta E_{xz}}\right]\right\} \tag{5}$$

$$A_{\perp} = P\left\{\alpha^2\left(\frac{2}{7} - k\right) - \frac{22\lambda\alpha^2\delta^2}{14\Delta E_{xz}}\right\} \tag{6}$$

for which λ, P and k, and also the functions $f(\beta)$ and $g(\delta)$ have already been defined [31]. ΔE_{xy} and ΔE_{xz} are the energies of transitions $|B_{1g}\rangle - |B_{2g}\rangle$ and $|B_{1g}\rangle - |E_g\rangle$ respectively

Considering the two water molecules along Oz axis as two electric dipoles each of moment μ (= 1 84 10^{-18} e.s u) situated at a distance from Cu^{2+} ion, these alter the energy of a positive charge at (r, θ, φ) by an amount [29]

$$H' = e\mu a^{-2}[2 + 3r^2a^{-2}(3\cos^2\theta - 1)] \qquad (r < a) \tag{7}$$

and hence the molecular orbitals in the I″ monomeric species can be described in terms of the orbitals of I′ species perturbed by the axial interaction (7). The energies of orbitals (2) are altered by amounts given, to first order, by the appropriate diagonal elements of H' [29]

$$\begin{aligned} \langle B_{1g}|H'|B_{1g}\rangle &= \alpha^2(2e\mu a^{-2} - 216e\mu a^{-4}a_0^2Z_{\text{eff}}^{-2}) \\ \langle B_{2g}|H'B_{2g}\rangle &= \beta^2(2e\mu a^{-2} - 216e\mu a^{-4}a_0^2Z_{\text{eff}}^{-2}) \\ \langle E_g|H'|E_g\rangle &= \delta^2(2e\mu a^{-2} + 108e\mu a^{-4}a_0^2Z_{\text{eff}}^{-2}) \end{aligned} \tag{8}$$

where $a_0 = h^2(4\pi^2\mu e^2)^{-1}$ and $Z_{\text{eff}} = 11\,86$ is the effective core potential experienced by the $3d$ hole

These axial interactions lead to a decreasing of the separations ΔE_{xy} and ΔE_{xz} by the following amounts:

$$\Delta E'_{xy}\ [\text{cm}^{-1}] = (hc)^{-1}(\beta^2 - \alpha^2)(2e\mu a^{-2} - 216e\mu a^{-4}a_0^2 Z_{\text{eff}}^{-2}) \tag{9}$$

$$\Delta E'_{xz}\ [\text{cm}^{-1}] = (hc)^{-1}[(\delta^2 - \alpha^2)(2e\mu a^{-2}) - (\delta^2 + 2\alpha^2)(108e\mu a^{-4}a_0^2 Z_{\text{eff}}^{-2})] \tag{10}$$

and in agreement with relations (3)—(6) to a modification of $\tilde{g}$-tensor and $\tilde{A}$-tensor values The substitution of (9)—(10) into (3) and (5) yields the following express ons for the differences $\Delta g_{||}$ and $\Delta A_{||}$·

$$\Delta g_{||} = g_{||}(I'') - g_{||}(I') = \frac{g_{||}(I') - 2\,002}{\Delta E_{xy}}[(hc)^{-1}(\beta^2 - \alpha^2)(2e\mu a^{-2} - 216e\mu a^{-4}a_0^2 Z_{\text{eff}}^{-2})] \tag{11}$$

$$\Delta A_{||} = A_{||}(I'') - A_{||}(I') = -2\lambda P\alpha^2(hc)^{-1}\left\{\frac{4\beta^2}{(\Delta E_{xy})^2}(\beta^2 - \alpha^2)(2e\mu a^{-2} - 216e\mu a^{-4}a_0^2 Z_{\text{eff}}^{-2}) + \right. \tag{12}$$

$$\left. + \frac{3\delta^2}{7(\Delta E_{xz})^2}[(\delta^2 - \alpha^2)(2e\mu a^{-2}) - (\delta^2 + 2\alpha^2)(108e\mu a^{-4}a_0^2 Z_{\text{eff}}^{-2})]\right.$$

Equations (11) and (12) predict the following changes the parallel component of $\tilde{g}$-tensor for I'' monomeric species should be greater than the corresponding component for I′ species, and $A_{||}$ component of hyperfine tensor for I″ species should be numerically smaller than that for I′ species because λ and $A_{||}$ are both negative. The experimental results are in accord with this predic- ion (Table 1). It was obtained $\Delta g_{||} = 0\,026$ and $\Delta A_{||} = 12 \cdot 10^{-4}\text{cm}^{-1}$

Using the equations (11)—(12) and experimental values of $\Delta g_{||}$ and $\Delta A_{||}$, a distance of 2 6 Å between the Cu^{2+} ion and two water molecules situated along Oz axis from the I″ species has been obtained For this we have taken $\alpha^2 = 0.85$, $\beta^2 = \delta^2 = 0.95$ and $\Delta E_{xy} = \Delta E_{xz} \simeq 14700\,\text{cm}^{-1}$ as in the case of copper (II) chelates investigated by Antosik et al [29], which contain the oxygen atoms as ligands

3 **Conclusions.** ESR spectra obtained at room temperature show that in both studied Cu(II) p-clorbenzoates prevail the dimeric species ($S = 1$) characterized by a short Cu—Cu distance ($\sim 2\,64$ Å) as in the other copper acetate like dimers

At 77 K, the appearance of a great number of monomeric species $\left(s = \frac{1}{2}\right)$ is evidenced by ESR spectra This fact was attributed to the water molecules comprised in the matrices of studied complexes which lead by freezing to an increase of Cu—Cu distance and thus to the breaking of the spin-spin coupling with their rearrangement in monomeric species. The presence of ter molecules in matrices of the studied complexes is explained by their chlatrate properties The estimation of monomer/dimer ratio was made from magnetic sus-

ceptibility data Its values are 2/3 for complex with CH_3OH (I) and 3/1 for that with CH_3COCH_3(II) This difference occurs because the lattice of complex(II) contains more water molecules than complex(I)

On the other hand, in the case of the complex(I) the coexistence of two magnetic monoequivalent monomeric species has been evidenced The I′ species has a square-planar symmetry (D_{4h}) without axial perturbations In the case of I″ species a component of octahedral symmetry (*Oh*) arises from two water molecules acting with the d_z^2 orbital of Cu^{2+} ions This last type of monomeric species characterized by axial perturbations is the only present in complex(II)

Using the experimental differences $\Delta g_{||}$ and $\Delta A_{||}$ between the values of $g_{||}$ and $A_{||}$ parameters for the two types of monomeric species, we have obtained a distance of 2 6 Å between Cu^{2+} and apical water molecules

(Received June 15, 1982)

REFERENCES

1 J Lewis, Y C Linn, L K Royston, R C Thompson, J Chem Soc, 6464 (1965).
2 J Lewis, F E Mabbs, L K Royston, W R Small, J Chem Soc, **A**, 291(1969).
3 W E Hatfield, Inorg Chem, **11**, 2216 (1972)
4 W E Hatfield, in *Theory and Applications of Molecular Paramagnetism* (Edited by E A Boudreaux and L N Mulay), John Wiley & Sons, New York, 1976
5 M S Haddad, D N Hendrickson, Inorg Chem, **17**, 2622 (1978)
6 T R Felthouse, D N Hendrickson, Inorg Chem, **17**, 2636 (1978)
7 M S Haddad, E N Duesler, D N Hendrickson, **18**, 141 (1979)
8 J W Guthrie, R L Lintvedt, M D Glick, Inorg Chem, **19**, 2949 (1980)
9 B Bleaney, K P Bowers, Proc Roy Soc. London, **A214**, 451 (1952)
10 G F Kokoska, M Linzer, G Gordon, Inorg Chem, **7**, 1730 (1968)
11 D Chasteen, Inorg Chem, **10**, 2339 (1971)
12 J Doumit, G L McPherson, R L Belford, S B Lanoux, H B Jonassen, Inorg Chem, **16**, 565 (1977)
13 P Sharrock, C H Thibaudeau, A Caillé, Inorg Chem, **18**, 510 (1979)
14 J F Boas, R H Dunhill, J R Pilbrow, R C Srivastava, T D Smith, J Chem Soc, **A**, 94 (1969)
15 P D W Boyd, T D Smith, J H Price, J R Pilbrow, J Chem Phys, **56**, 1253 (1972)
16 G F Kokoszka, H C Allen, G Gordon, J Chem Phys, **46**, 3013 (1967)
17 C Chow, R D Willett, J Chem Phys, **59**, 5903 (1973)
18 K T McGregor, W E Hatfield, J Chem Phys, **65**, 4155 (1976)
19 M Kato, H B Jonassen, J C Fanning, Chem Rev, **64**, 99 (1964)
20 J F Villa, W E Hatfield, Inorg Chem, **11**, 1331 (1972)
21 J F Villa, Inorg Chem, **12**, 2054 (1973)
22 B Jezowska-Trzebiatowska, Pure Appl Chem, **38**, 367 (1974)
23 F X R Van Leeuwen, R Wever, B F Van Gelder, Biochimica et Biophysica Acta, **315**, 200 (1973)
24 D R Williams, Chem Revs, **72** (3), 203 (1972)
25 L S Forster, C J Ballhausen, Acta Chem Scand, **16**, 1385 (1962)
26 O Cozar, V Znamirovschi, M Gridan, Rev Roum Phys, **27** (4), 389 (1982)
27 O Cozar, I Bratu, R Semeniuc, I Ardelean, M Perici, Studia Univ Babeş-Bolyai, Physica, **27**, 29 (1982)
28 S V Vonsovskij, *Magnetizm*, Izd Nauka, Moskva, 1971

29 S Antosik, N M D Brown, A A McConnell, A L Porte, J Chem Soc, **A**, 545 (1969)
30 D Kivelson, R Neiman, J Chem Phys, **35**, 149 (1961)
31 H Yokoi, T Isobe, Bull Chem Soc Japan, **41**, 2835 (1968)

STUDII RES ŞI DE SUSCEPTIBILITATE MAGNETICĂ ASUPRA UNOR p-CLORBENZOAŢI DE CUPRU(II)

(Rezumat)

În lucrare sînt prezentate rezultatele structurale obţinute asupra unor p-clorbenzoaţi de cupru(II) prin măsurători RES şi de susceptibilitate magnetică La temperatura camerei predomină speciile dimere ($S = 1$) în timp ce la 77K apare un însemnat număr de specii monomere $\left(s = \frac{1}{2}\right)$ Estimarea raportului monomer/dimer s-a făcut din datele de susceptibilitate magnetică În cazul complexului (I) au fost evidenţiate două specii monomere magnetic neechivalente

STUDIA UNIV BABEŞ-BOLYAI, PHYSICA, XXVIII, 1983

THERMAL DIFFUSION COLUMNS THEORETICAL AND PRACTICAL ASPECTS

GHEORGHE VĂSARU*

The continuous development of the applications of stable and radioactive isotopes in various areas of research is due to the availability of a technology which makes it possible to enrich rare isotopes to the desired concentration at a reasonable expense. Thermal diffusion, (TD), particularly well adapted for laboratory scale production, belongs to the arsenal of isotope separation methods Recently the method has been used in chemical engineering and in petrochemical and other areas of industry to separate molecular solutions, dyestuff solutions, or petroleum product fractions The phenomenon is also of great theoretical interest for the study of intermolecular forces, transport phenomena, and certain aspects of statistical mechanics

TD consists in the fact that in the presence of a temperature gradient within binary or multicomponent mixtures, a transport of matter takes place, creating a concentration gradient In this the light component is concentrated in the higher temperature zone while the heavy component is enriched in the lower temperature zone

The existence of TD was first observed in liquid solutions, in 1856, by G. Ludwig. In the second decade of this century, D. Enskog and independently from him, S. Chapman developed the general kinetic theory of gases. This theory led to a conclusion which was unexpected at that time, namely, that the diffusion may appear in a gaseous mixture as a result not only of a concentration gradient (ordinary diffusion) but also of a temperature gradient (TD). The first experiments that confirmed the results of the theory were carried out in 1917 by S Chapman and F. W. Dootson.

Although as early as in 1919 S Chapman suggested the possibility of using it for the partial separation of isotopes on the basis of a small elementary effect, this phenomenon was not applied for that purpose until 1938 when K. Clusius and G. Dickel succeeded in combining this effect with a thermal convection current in a column, thus considerably enhancing the separation A TD column consists from a metal or glass cylinder kept at the temperature T_1; a concentric cylindrical heating element is placed inside this cylinder, kept at a higher temperature T_2, ($T_2 \gg T_1$) The fluid mixture is introduced and confined into annular space between two cylinders The horizontal temperature gradient between the two cylinders is responsable for two effects: first, a TD effect in the direction of the thermal gradient, and second, an effect involving natural thermal convection currents, the fluid being upward in the neighborhood of the hot wall and downward near the cold wall This countercurrent flow multiplies the single stage separation effect and after steady state has been reached, a maximum separation of the components is obtained The mixture

* Institute of Isotopic and Molecular Technology, R—3400 Cluj-Napoca, 5, P O Box 700, Romania

subjected to the separation process will be enriched in the light component (light isotope) at the top of TD column and in the heavier one at the bottom

The TD columns used frequently in practice are · a) hot wire type, with an electrical heated wire as hot wall and b) concentric tube type, with an electrical heated calrod The concentric tube type has the advantage of producing more separative work per unit length than hot wire type. The spacing between the hot and cold walls of this type of column is usually less than that in the hot wire column, being a fraction of a centimeter for gas-phase separations and only a fraction of a millimeter for liquid-phase separations

The invention of multistage TD column stimulated the interest in TD and transformed this laboratory phenomenon in a practical method for achieving dificult separations.

Since its discovery, the TD column has been used for separating components of both liquids and gaseous mixtures, and very often for the separation of isotopes The two TD columns, above mentioned, represents the standard equipment for the separations by TD, and in this context, TD is widely used for the separation of gaseous isotopic mixtures.

Some theoretical and experimental aspects of the TD columns will be examinated in this paper.

Thermal diffusion constant. The value of the elementary separation effect by TD for a given isotopic mixture is determined by the value of TD constant, α_T. This constant is very sensitive to the type of molecular interaction and if the molecular model are more complex, a temperature dependence must be taken in account.

Knowledge of the value of this parameter is especially important when attempting to select the most suitable process raw material for the separation of isotopes This fact has been responsable, especially during the recent years, for several studies on the development of a theory, of computing methods and of new experimental methods of determining this constant for a great number of isotopic mixtures

In the case of binary isotopic mixtures the expressions for the TD constant are greatly simplified compared with gaseous mixtures with different molecular components This simplification consists in the fact that the fields of force of all molecules are essentially identical If the quantum mechanical differences between identical and nonidentical particles are neglected, it may be possible to consider the isotopic mixture as a mixture of two species of particles which are identical, except that particles of the first species are somewhat heavier than those of the second This allows development of general expressions for α_T given by Chapman-Cowling method There are many theoretical expressions for this constant, for different molecular models (rigid elastic sphere model, inversion model, Sutherland model, Lennard-Jones model, modified Buckingham (exp-6) model, a s o) Its value is affected by the relative masses, sizes and shapes of the process gas mixture and is a function of the concentration of the components in the mixture

Generaly, the theory does not predict the TD constant as accurately as it does the other gas transport properties The accuracy of the theory in predicting TD constant for gases is greatest for the noble gases and tends to dimi-

nish with the complexity of molecule It is therefore desirable for many applications of TD to determine the α_T experimentally, and in this context, three methods are available a) the two-bulb method, b) the swing separator method and 3) the TD column method Each of these has inherent advantages and disadvantages The most precise results can be obtained using the method b) resulted from a considerable multiplication of the elementary separation effect. In addition, since only small temperature differences are needed between the hot and cold ends of the separation tubes in which take place the TD process, we can make precise measurements of α_T for small temperature intervals The operation time is less than in the case of method a) and no gas operation need to be carried out during the running of the apparatus There are advantages over the method a) However, the swing separator method shows more types of errors than the previous method

The method c) permits to obtain high separation factors with respect to the other two methods, reducing considerably the errors in measurement of α_T In contrast to the method b) this method makes possible to determine α_T at a single temperature, T_1, that of the cold wall This avoid the requirement of assigning an average temperature to the experimental data of α_T as is done in the previous two methods

Among the shortcomig of this method should be mentioned the need to know, with high precision, the other transport coefficients such as viscosity and diffusion Also, the present theory of the TD column being applicable only to monoatomic gases, and thus this method can give only qualitative values for α_T in the case of polyatomic gases

Extensive details on the theory of the elementary separation effect by TD, the relation of TD phenomenon with the molecular models, the experimental methods of determining α_T and theoretical and experimental values of this constant are given in [1—6] These problems are especially important when selecting the process gas mixture for the separation of a particular isotope

Thermal difusion column. A T h e o r e t i c a l a s p e c t s In order to increase the efficiency of TD process in columns, a column theory had to be developed, which would take into consideration both the geometry of the column and the kinetic properties of the gas mixture used as process gas Many theoretical and experimental studies has been undertaken for this purpose, leading to the development of a phenomenological theory of the column for predicting with more or less sucess the effects caused by the modification of the geometry of the column and of the operating conditions on the separation Among these theories, those of K Clusius, G Dickel, L Waldmann, J Bardeen, W van der Grinten, P Debye, H Jensen, W H Furry, R C Jones and L Onsager may be mentioned A more exact theory of more realistic columns, i e , of the cylindric and extreme cylindric columns, as an extension of the general theory for the plane case, has been developed by W H Furry and R C Jones. A study of great interest for the separation of isotopes by TD has been published by these authors in [1] It involved a broad exposition of the theory of TD columns together with their limitations and interpretation of certain experimental data After publication of this study, several investigators supplemented experimental data and improved the theory and today it is possible to make

a sufficiently precise evaluation of their performance The general form of the transport equation in a TD column is given by

$$\tau = Hc(1 - c) - K\frac{dc}{dz} \tag{1}$$

which is independent of time and where τ represents isotopic transport in the positive direction The quantities $H = H^0h$, $K = K_c + K_d$, $K_c = K_c^0k_c$; $K_d = K_d^0k_d$ are designated as column transport coefficients, h, k_c, k_d are shape factors which depend on the ratio of radii, the ratio of temperatures and the type of molecular interaction of the gas used as process gas, while H^0, K_c^0 and K_d^0 are coefficients which are not dependent on the type of molecular interaction; $\frac{dc}{dz}$ represents the isotopic concentration gradient and c — isotopic concentration, in molar fractions The coefficient H is proportional with TD constant and thus is a measure of the TD effect The others terms represents the remixing effect due to convection currents, (K_c), and ordinarydiffusion along the column, (K_d)

In the case of a binary mixture the exact solution of the equation (1) for the steady state condition, without extraction of enriched fraction, is given by the relation

$$Q_e = \exp\frac{HL}{K} = \frac{c_L(1 - c_0)}{c_0(1 - c_L)} \tag{2}$$

for the conditions $0 \leqslant z \leqslant L$ and $c_0 < c < c_L$, where L is the length of the TD column, c_0, c_L are the isotopic concentrations of one of the components at the ends of column, and Q_e is so called separation factor at total reflux. Since the transport coefficients H, K_c and K_d are proportional to p^2, p^4 and p^0, respectively, p being the operation pressure, the separation factor of the TD column depends on this pressure as follows

$$\ln Q = \frac{ap^2}{p^4 + b} \tag{3}$$

where

$$a = \frac{H'L}{K_c'}, \quad b = \frac{K_d'}{K_c'} \tag{4}$$

H'; K_c' and K_d' being the values of H, K_c and K_d, respectively, at 1 atm.

From these expressions it is obviously that the optimum operating pressure which allows obtaining a higher value for Q is

$$p_{\text{opt}} = b^{1/4} \tag{5}$$

for given values for a and b

The variation of separation factor Q with operating pressure represents a convenient means for checking the theory of TD column.

More details on the theory of TD column, shape factors for various molecular models and their effect on the transport coefficients of the column are

given in [1–2] [5—8] Shape factors has been calculated by R. C Jones and W H Furry [1] for Maxwellian model, S Raman and S C Saxena [9] for rigid elastic sphere model, G Reinhold and G. Vojta [10+], G Reinhold [11] and E Greene, R. L Hoglund and E. von Halle [12] for the inversion model, B B McInteer, M Reisfeld [13] for the Lennard-Jones (12,6) model J M. Saviron and coo [14] for Buckingham exp-6 model and A Youssef and M M Hanna [15] for polyatomic gases Knowledge of these shape factors is of interest for design of TD columns for separation of isotopic or gaseous mixtures

B Pratical aspects 1 *Structural details* A number of factors related to the optimal operation of a TD column (or a TD cascade) for long periods of time must be taken into consideration in the construction of this kind of plants, in order to maximize their efficiency In general, two material are used for the construction of TD columns glass and metal Glass TD columns are used expecially in the plants operated at pressures up to 1 atm They are fragile, but they have the advantage of being transparent, making it possible to see what is happening inside In this way it is possible to solve more easily the centering of the heating element in the column Because they break easily, this type of columns are not suitable when the operation must be carried out at pressures higher than atmospheric, in which case they are replaced with metallic columns

The geometry must be carefully considered for both glass and metallic TD columns in order to avoid parasitic phenomena which can affect in a negative form the separation process It is also essential that the system be completely leak-tight

As seen previously, the efficiency of a TD column depends on the ratio of radii and temperatures of the walls In the case of concentric TD column the ratio of radii, r_1/r_2, r_1 respectively r_2 being the radius of cold, respectively hot wall of the column, varied between 2—3, while those of hot-wire type, between 5—30 Most of concentric tube TD columns are made of metal The hot-wire TD column are much more widely used than the cercentric one and may be constructed from either glass or metal The hot-wire used as heating element plays the role of the hot wall The lengths of these columns ranging from 1 to 6 meters For the longer column, attempts are always made to use straight-line glass tube with a constant diameter

Glass TD columns (and metallic one) are described in gerat detail in literature [4—7] The difference in them consists in the design used at the both ends of the column for convenience in inserting, adjusting and changing the hot wall Standard ground-glass joints are often used in this purpose, especially for TD columns intended to be operated for short periods of time In the TD columns to be operated for longer times these ground-glass joints are used as little as possible, all parts of the column being welded instead When cascades are used, the TD columns could be similarly welded to each other

2 *Spacers* The coaxial placement of TD column within the cooling jacket and of the hot wall (hot-wire or calrod) inside of the column presents very important problems The first, and less difficult problem may be solved by attaching small glass rods, in the case of glass columns, or metalic rods, in the case of metallic columns, which are equal in length with the difference between the

inner radius of the outer wall of the cooling jacket and the outer radius of the cold wall of the column, in a perpendicular direction to the axis of the column. Sets of 3—4 such rods placed at a distance of about 1 m along the column, in the same plane, are sufficient to ensure good centering. The placing of the wire inside is a much difficult problem. At various times different types of spacers has been adopted and many experiments have been carried out to evaluate and explain their influence on the performance of the TD column. It is quite legitimate to devote so much attention to this problem, an off-center placement of the hot-wall results in lower or higher values of the azimuthal variation of the temperature, which will generate parasitic convection currents affecting the separation process in an undesirable manner.

The hot wall is kept in a coaxial position by means of spacers placed at various distances along the column. In the case of a—supplied hot wire columns these spacers also help to prevent wire vibration in the terrestrial magnetic field.

Quite often metallic TD columns are to be preferred because their good thermal conduction reduces the azimuthal temperature variation to a minimum. Their high polish surface has the additional advantage that radiative losses are reduced. They also can be constructed with greater precission than glass TD columns. In some cases, for concentric-tube columns heating by steam condensation or by rapid flow of liquids appear to be better than electrical heating. During the time, various type of spacers has been used: circular discs made from perforated aluminium plates attached to the hot platinum wire of the column by welding with gold, equilateral triangle plate made of Pt—Ir alloys and triangular disks, nickel wire attached perpendicularly to the hot tungstene wire, normal to each other, forming a cross. Small nickel wire were spotwelded to the tungstene wire of the column.

It has generally been observed that nearly all welding or melting methods may modify the structure of the wire at the place of the joint. For example, the material is easily overheated after a certain time of operation and may undergo fracture at the point of welding. In order to avoid this short coming self-supporting spacers has been used. They make it possible to slide the hot-wire freely along the axis of the TD column through a hole in the middle of the spacer. Two variants exists: the first consists of a cross-shaped brass plate with a hole in the middle to allows passage of the hot wire. One pair of the branches of the cross is bent upward and the other downward, and the two together act as an elastic double U which make it possible to attach the spacer at the desired level of the column. Since this type covers a large portion of the annular cross-section of the column, a second variant was developed, consisting of the winding of four pieces of an elastic wire around a cylindrical glass (or quartz) piece. The branches of the cross are also bent as in the previous model, creating a double elastic U. Because of the elasticity, the branches exert a pressure on the wall of the column, maintaining themselves at the desired height. The brass pieces around which the elastic wires are coiled have a diameter of 2—2.5 mm, while the guiding hole is of 0.3—0.8 mm. The whole spacer cover about 0.1—0.4 cm^2 [5—6].

Experimental studies on the effect of spacers on the separation found that introduction of various types of partial obstruction in the laminary gas flow, at regular intervals along a short TD column, could increase the separation effect

by creating vortexes in the gas confined into column. On the other hand, the spacers improve the centering, thus ensuring on increase of the average temperature of the gas inside of column and thereby increasing thermal diffusion effect

In spite of the interesting results obtained, there is still no theory of TD column available to take into consideration these facts in a quantitative manner Addition of a constant K_p to the sum of K_c and K_d which represent the parameter K from eq (1) is not sufficient to cover all deviations of the experimental results obtained with TD columns from the values predicted by the theory of R C Jones and W H Furry, carried out by exact calculation of the shape factors

3 *Hot wire and contact problem* In view of the long duration of the TD experiments, the problem of realiability of separation plant depends greatly on the quality of the material used for hot wire Pt—Ir alloys have a much higher mecanical strength than pure platinum, but its chemical stability, especially in an atmosphere containing oxygen, is not too good because iridium sublimes relatively rapidly on the cold wall of the TD column, resulting in a prematur destruction of the wire

If the process gases are not too agresive, either Cr—Ni or W or their alloys may be used as wires for long period experiments Good results we can obtain using Kanthal wires

Electrical supply of the wire is made at both ends of the column. Here we must to ensure a good electrical contact In this purpose many systems has been elaborated, especially for the end of the column which permits a safety termal elongation of the wire A simple solution involves the use of mercury as a contact liquid, immersing the lower end of tensioning weight of the wire in it In the case of concentric tube column, the system bellow is often used in this purpose

4 *Determination of the column walls temperature* This is an important operation, especially when experimental data are to be compared with theoretical ones As the temperature of the cold wall differs only slightly from that of the coolant, it is characterized, to a first approximation, by the temperature of the coolant at the point of entry into the cooling jacket This is true only if the coolant has a sufficiently high velocity and if the thermal conduction through the cold wall is high For more precise determinations, the thermal conductivity of the walls and the finite temperature difference between the inlet and outlet of the coolant must be taken into consideration, the latter by assuming that the coolant is subjected to laminar flow in the jacket and that the ideal transverse temperature distribution is determined only by conduction The most exact method, however, requires direct measurement of the temperature by thermoelectric methods

Similar difficulties are encountered in the determination of the hot-wall temperature The temperature of the calrod type heating element may be also determined by thermoelectric methods, by measuring the thermal elongation or by measuring the average temperature of the gas mixture, using a manometer The first two methods are more precise The third is easier to use

The methods used for measuring the temperature of the hot wire are also based on the measurements of thermal elongation and heat radiation The

latter can be used only for glass TD columns. If the wire has an electrical resistivity with a sufficiently high temperature coefficient, the temperature may be determined using the electrical resistivity

5 *Heat losses* The heat is transfered from the heating element of the TD column through the following four paths a) radiation of the heating element, b) convection currents in the gas, c) conduction through the gas and d) conduction through the spacers Convection and conduction by the gas are essential features in the operation of the TD column however, if heat losses by radiation or directly, by conduction through the spacers may be minimized, the whole separation operation can be made more economical Theoretical and experimental studies have been made on the heating element for this purpose, trying out different types of heat transfer toward the cold wall, in order to understand better the operation of the TD column and to increase the efficiency and economy of the separation of isotopes by TD

6 *Sampling for isotope analysis* Determination of the TD column constants by transient state experiments requires the withdrawal and analysis of samples at well-defined points along the column The withdrawal operation is also necessary when the TD column produces a certain enriched isotope fraction

Sampling may be made intermittently or continuously In the first case it is important to take into careful consideration the problem of the dead volumes, especially if the sample is withdrawn at the ends of the TD column or if several samples are withdrawn simultaneously at different points along the column. Each dead volume causes deviations in the temporary isotope concentration in transient-state experiments and therefore must be prevented as much as possible

7 *Interconnection of the TD columns* The interconnection of a certain number of TD columns, in order to be operated in a cascade, presents not only theoretical but also practical probems One of the most important of these is that of reducing to a minimum the volume of the connecting tubes between the individual TD columns and of the energy required to make an effective convection Under laboratory conditions, two systems of interconnection are used. They are based on the principle of the thermosyphon and of the gas pulser The first system is based on flow in a convective loop, which includes the ends of the interconnected TD columns The driving force of these convective flows is the density difference between two zones of the gas at different temperatures. In the second system, by some kind of pumping technique, a given volume of gas is sent slowly from the top of a TD column to the bottom of the next TD column, a s.o Thus we obtain ultimately a displacement of a given and constant volume of gas from the top of the first column of the cascade to the bottom of the last column of the cascade The pumping cycle is reversible, ensuring homogenization of the gas mixture from the top of one TD column with that of the bottom of the next, thereby ensuring that the whole gas mixture of the separation system will take active part in the separation process.

The most important advantage of gas pulsers are, first of all, their low energy consumption, which is smaller than that of the small mechanical pumps: secondly, it is possible to separate succesive TD columns conveniently, by stopping the pulsation when the operations are perturbed.

This system has also short-comings. First, the connection that it provides to the columns is discontinuous, which leads, in the case of continuous operation, to a reduction of its efficiency. Second, the effective pulsed volume decreases from column to column because the distance between the pulsing pump and the TD columns increases, and thus there is a minimum pulsed volume in the center of the cascade Third, the system is restricted to a series connection of TD columns. Serious difficulties arises if the TD columns are interconnected in parallel. Fourth, the effective length of the TD column decreases as a result of the back-and-forth movement of the gas in the column.

This comparative examination indicates that the principle of thermosyphon is to be preffered between the stages of a cascade which has a small relaxation time and a large transport, these essentialy determine the efficiency of the cascade On the other hand, the gas pulser is better to be used in the upper stages of the cascade Thus, a combination of these two systems seems to be an excellent compromise. Special attention must be given to the connection between the stages of the cascade with TD columns operated in parallel. If the bottoms and the tops, respectively, of the parallel columns are connected, parasitic circulation of the gas may appear in the loops created by the last two columns and the two connections between their ends, caused by a possible difference in the average temperature of the columns. This can affect seriously the separation capacity of the whole stage. This parasitic circulation may be substantialy reduced by using solenoid valves at the end of each TD column for blocking, this would allow only a single TD column, at a certain moment, in a given stage, to be opened toward the separation system. The valves are operated by a timer, which opens each TD column for several minutes in a cycle. Although this time is chosen somewhat arbitrarily, the duration of the cycle is so selected that it is short with respect to the equilibration time of the TD column

The circulation of the gas between the columns in a cascade may be provided also using gas pumps. The following essential features of gas pumps selected for this purpose must be pointed out. a) the gas losses must be smaller than 0 1 ml/day NTP at a pressure difference of 1 atm , b) the pump should be able to operate continuously for at least several months, without any control or intervention, c) the pumping rate should be in the range of 100—1000 ml/min. at a pressure difference of several Torr, d) it should have a small volume in order to reduce the holdup of the desired isotope to a minimum [6]

Final remarques. Isotope separation technology makes use of separation plants which generally are made up of TD columns of either hot-wire or concentric tube type. When high separation factors are desired, multistage ideal columns must be used In many cases this requires an excessively large number of TD columns connected in parallel or, additionally, a number of TD columns for the last stage which are supposed to be smaller than unity When concentric tube columns are considered as unit columns, the hot-wire columns make it possible to build such „fractions" of columns

Hot-wire columns make it possible to increase considerable the H^2/K ratio for a given energy consumption per unit of length, and thus, the separative capacity of the TD column.

In the first stages of a cascade it is often necessary to obtain high values

for H This may be obtained by means of concentric tube TD columns which permits to obtain several times H values as large as obtained in the hot wire TD columns, so that it can be substantially reduce the required number of TD columns to be used in parallel.

The concentric tube TD column make it possible to use other methods to heat the inner wall, e g , by condensed vapours or liquids passed through at high temperature For large scale plants, a design based on concentric tube TD columns makes it possible to use less expensive sources of energy TD, though its effect is small, has an area of application in the performance of such difficult separation as complex mixtures of close-boiling constituents, mixtures of thermaly stable isomeric compounds and mixtures of gases and isotopes Since the process is thermodynamically irreversible and the TD column throughput is small, it is unlikely that this phenomenon can be economically competitive with others feasible separation, methods, when large amounts of isotopic enriched product are desired However, since TD columns are simple and relatively inexpensive and can run for a long period of time without difficulties, this phenomenon can became competitive when small amounts of high enriched product are desired

(Received July 8, 1982)

REFERENCES

1 R C Jones, W H Furry, Rev Mod Phys , **18,** 151 (1946)
2 K E Grew, T L Ibbs, *Thermal Diffusion in Gases,* Cambridge Univ Press, 1952
3 G Vasaru, Fortschritte der Physik, **15,** 1 (1967)
4 G Vasaru, I , Rap, *Thermal Diffusion* A Bibliography, STI/PUB/21/28 IAEA, Vienna, 1968
5 G Vasaru, G Muller, G Reinhold, T Fodor, *Thermal Diffusion Column, Theory and Practice with Particular Emphasis on Isotope Separation,* VEB Deutscher Verlag der Wissenschaften, Berlin, 1969
6 G Vasaru, *Separation of Isotopes by Thermal Diffusion,* Translation Series ERDA-tr-32, Distribution Category UC-22, USERDA, Office of Public Affairs, Technical Information Center, Oak Ridge, Tenn July 1975
7 J E Power, *Thermal Diffusion,* in *New Chemical Engineering Separation Techniques,* H M Schoen, Ed , Interscience Publ , N Y 1962
9 S Raman, S C Saxena, J Chem Phys , **36,** 3345 (1962)
10 G Reinhold, G Vojta, Phys Letters, **2,** 230 (1962)
11 G Reinhold, Z phys Chem , **224,** 384 (1963)
12 E Greene, R L Hoglund, E von Halle, *AEC Research and Development Report K-1469,* Union Carbide Corp , 1966
13 B B McInteer, M Reisfeld, J Chem Phys , **33,** 570 (1960) , Report LAMS-2517, Los Alamos Sci Lab , 1961
14 J M Saviron, D Gonzales, M Quintanilla, J A Madariaga, Preprint, Zaragoza Univ , Spain, 1961
15 A Youssef, M M Hanna, Z phys Chem Neue Folge, **47,** 42 (1965)

COLOANE DE TERMODIFUZIE ASPECTE TEORETICE ŞI PRACTICE

(Rezumat)

Lucrarea conţine o analiză a principalelor aspecte legate de constanta de termodifuzie, factorii de formă, problemele constructive ale coloanelor, pereţii calzi, contactele electrice, determinarea temperaturii pereţilor coloanei, pierderile termice precum şi de interconectarea coloanelor de termodifuzie într-o cascadă de separare

Se indică şi căile de soluţionare a acestor probleme, facilitînd astfel operarea instalaţiilor de separare izotopică prin termodifuzie în condiţii de optim

STUDIA UNIV BABEŞ-BOLYAI, PHYSICA, XXVIII, 1983

A STUDY OF THE OPTICAL LINEAR DICHROISM OF PREFERENTIALLY ORIENTED SPECIMENS USING A CONVENTIONAL DOUBLE BEAM SPECTROPHOTOMETER

TUDOR PORUMB, RODICA SECARĂ, FLAVIA DOBOŞI, DAN STRUGAR

1 **Introduction.** The paper presents a method for the detection of the optical linear dichroism using a Spekord uv vis spectrophotometer, and illustrates the method with a study of the dependence of the linear dichroism on the internal order of uniaxial, preferentially oriented, specimens. Such specimens include polimeric fibres and stretched films, in which the direction of orientation („director") is parallel to the long axis of the specimen, and membranes of lyotropic liquid crystalline type, in which the director is perpendicular to the plane of the membrane

Among the various ways, listed in Table 1, of defining mathematically the linear dichroism, which, phenomenologically, arises from the dependence of the

Table 1

Mathematical ways of expressing linear dichroism*

1	Dichroic ratio	$R = A_{\|\|}/A_{\perp} = 1 + (3S\cos^2\omega)/(1 - S)$
2.	Dichroic difference	$D = (A_{\|\|} - A_{\perp})/A_r = 3S\cos^2\omega$
3	"Parallel" absorbance	$A_{\|\|}/A_r = 1 - S + 3S\cos^2\omega$
4	"Perpendicular" absorbance	$A_{\perp}/A_r = 1 - S$
5.	Incremental "parallel" absorbance	$(A_{\|\|} - A_r)/A_r = S(3\cos^2\omega - 1)$
6	Incremental "perpendicular" absorbance	$(A_{\perp} - A_r)/A_r = -S$

* Legend $A_{||}$, $A_{\perp}$ = Absorbance recorded at two mutually perpendicular polarization directions The uniaxial specimen is placed with its director in the plane defined by the direction of light propagation and the „parallel" direction

ω = Angle of tilt of the director relative to the „paralfiel" direction

A_r = Absorbance of an equivalent randomly disordered specimen (the $\omega = 0$ limit of $1/3\,A\,|| + 2/3A_{\perp}$)

S = Order parameter defined in text (equation 1)

absorption of plane polarized light on the orientation of the electric transition moment relative to the polarisation direction, the definition as dichroic ratio has the advantage of not requiring the knowledge of the absorbance of an equivalent completely disordered specimen. Any linear dichroism experiment determines uniquely a fundamental structural parameter of the axial specimen, the order parameter, which is defined as

$$S = (3 < \cos^2 \beta_i > -1)/2 \qquad (1)$$

where β_i are the angles between the individual transition dipole moments and the director of the specimen The mathematical relationships between dichroism and S can be deduced analytically [1] or numerically (see below) For generality, the formulae from Table 1 contain the angle ω of tilt of the specimen, measured between the director of the tilted specimen and the director of a

specimen placed in the classical position, i e with its director along the direction of the electric vector of the „parallel" polarized light The tilt is necessary in the case of lyotropic liquid crystal membranes, which cannot practically be placed tangentially to the incident beam, as required by the classical condition

In the experimental study reported below, one used specimens containing chromphores introduced by the experimentator as optical labels, the observation of dichroism being performed in the visible absorption band of the chromophore The aim of the investigation was to facilitate a discussion of the degree of internal order and the orientation of the chromophores within the specimens

2 **Theoretical computer aided simulation of a preferentially oriented specimen.** A preferentially oriented polimeric specimen, which can be pictorially compared to a „wheat field", may be described by a gaussian function centered along the director Such a specimen may be simulated by creating a population of the chemical groups of interest which obeys the gaussian model, as already described [2, 3] The simulation of an anizotropic property of the specimen, such as the order parameter or the absorption of plane polarized light, can be achieved by a summation of the effects over all the members of the population

For exemple, the calculation of the order parameter (S) for the electric transition moments of the chromophores in a specimen implies, according to definition (1), a summation of terms ot $\cos^2 \beta$, type The results obtained using this algorithm were plotted in Fig 1a as function of the angle between the

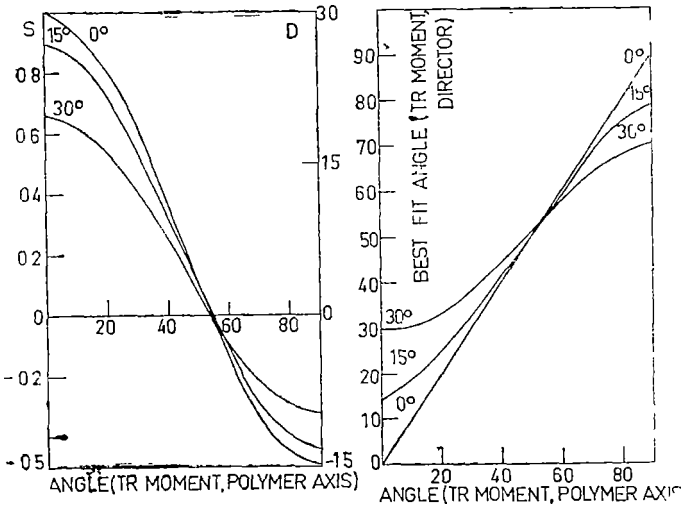

Fig 1 Computed (a) order parameters and reduced dichroic differences and (b) corresponding "best fit" angles between the transition moment and the director of the uniaxial system, as a function of the angle of the transition moment with the polymer axis, for different standard deviations of the gaussian distribution of the polymeric chains

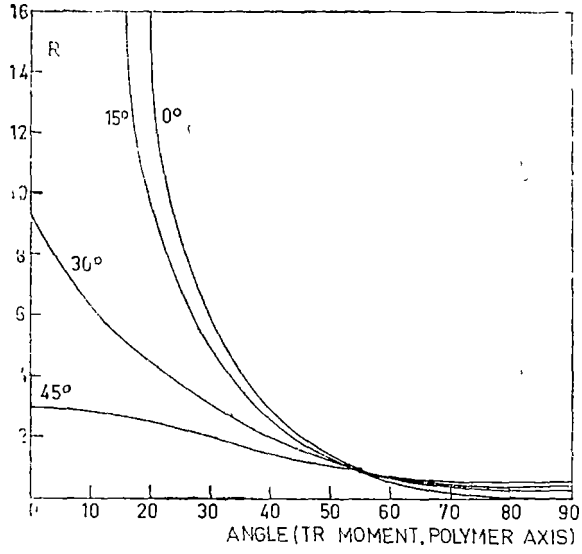

Fig 2 Computed dichroic ratios of preferentially ordered specimens (Legend as in Fig 1)

electric transition moment and the polymer axis, for various degrees of gaussian misalignment of the polymer chains in the preferentially oriented specimen. The formulation of linear duchroism as reduced dichroic difference (D) enjoyes popularity because of its simple relationship with S, namely $D = 3\ S$, as illustrated by Fig. 1a One notices that although the order parameter carries information on both orientation and degree of misalignment, the two cannot be separated without knowledge of one of the quantities from an independent experiment. Likewise, a vlue of zero for the order parameter may arise either from complete disorder or from the orientation of the electric transition moment at the,, magic angle'' of 54°44′ relative to the polymer axis, in any preferentially ordered specimen.

The angle β which can be calculated from S by eliminating the average symbols in equation (1) has the value of a ,,best fit'' angle of the transition moment relative to the director, and carries the same information as the order parameter (Fig. 1b). The dichroic ratio calculations are presented in Fig. 2

3. Linear Dichroism Studies of Stretched Polymer Films. *Experimental Procedure* The polyvinyl alcohol films were equilibrated with a high relative humidity atmosphere and then stretched, at room temperature. A 50% increase in length conferred the specimens positive birefringence, an indicator of preferential orientation

Results. The absorption spectra obtained from Methylene Blue and Chlorophyll a in PVA films are shown in Fig. 3. The dichroic ratio (R) spectra were calculated by dividing the points of the ''parallel'' and ,,perpendicular'' spectra in pairwise fashion, after the baselines (the spectra of the polarizer assembly alone) were translated so that they become tangent to the sample spectra in regions where the chromophores were known not to absorb The constant values for R throughout the respective bands (equal to about 1 86 and 0 9) correspond to order parameters equal to 0.222 and −0.035.

The molecule of Methylene Blue is known to orient itself parallel to the polymeric chains [1], because of its rod-like shape, and to have the transition moment responsible for the 650 nm band along its long axis (Fig. 3a). Therefore one may read off the misalignment parameter (the half width of the gaussian distribution) for abscisa 0 and R equal to 1.86 in Figure 2, as being greater than 45 degrees.

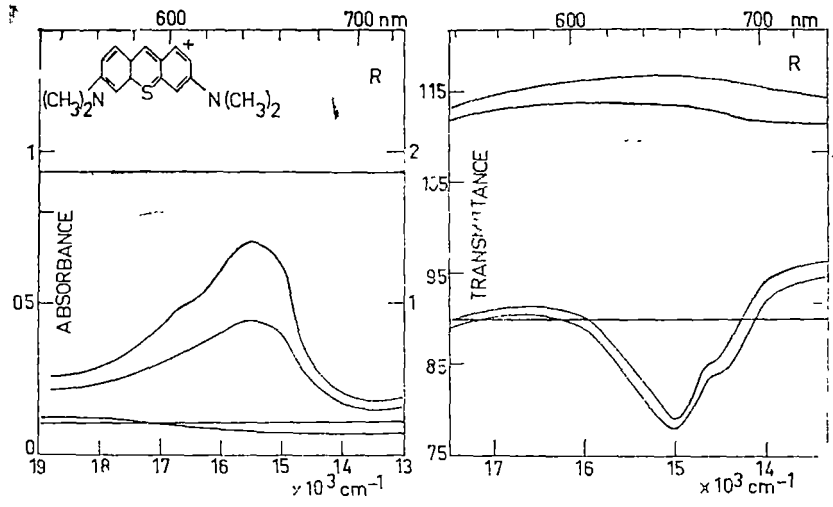

Fig 3 Absorption spectra obtained using plane polarized light from (a) Methylene Blue and (b) Chlorophyll a in stretched PVA films

The dichroic ratio for the Chlorophyll a sample falls in the region close to unity, which is, as a rule, uninformative

4. Linear Dichroism Studies of Lipid Multilayers — Models of Biological Membranes. *Linear Dichroism as Studied at Oblique Incidence.* As the aliphatic chains of the lipid molecules of the multilamellar structure are preferentially oriented along the normal to the membrane plane, the dichroism of such specimens cannot be studied but at oblique incidence One notices that the specimens would look isotropic at normal incidence.

The algorithm for the simulation of linear dichroism described under point 2 above was used to obtain a numerical proof, for a series of arbitrarily selected cases, of the theoretical relationship between the R, S and ω (optical, structural and experimental, respectively) parameters (Table 1). An example is given in Fig 4a. The linearity of the R vs $\cos^2\omega$ graph and the equality of the value of the order parameter calculated from the slope of the graph by virtue of the theoretical relationship (Table 1) to the value obtained from a separate simulation provide a confirmation of the analytically deduced formula.

A more general formula contains the reffractive index n (Snellius' reffraction law) ·

$$R = 1 + \frac{3S}{n^2(1 - S)} \cos^2\omega \qquad (2)$$

Experimental Procedure Lecithin/water multilayers were obtained by hydration of the lipid dried on microscope slides from chlorophorm solutions containing the largely liposoluble dye Acridine Orange as optical label. The slides were mounted in a special holder which allowed recording the absorption spectra at oblique incidence

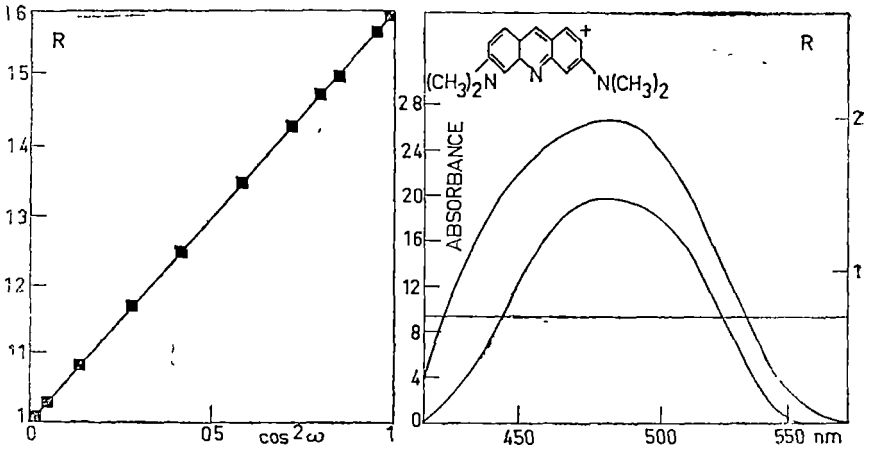

Fig 4 Linear dichroism recorded at oblique incidence (a) Simulation of the variation of the dichroic ratio of a hypothetical specimen with the angle of tilt ω defined in Table 1 (Transitionmoment coordinates in chromophore frame 1, 1, 0, Eulerian angles of attachement of chromophore to polymer 25, 0° [4], Gaussion standard deviation 10° [Chromophore population 864 members) (b) Processed absorption spectra obtained from Acridine Orange in lecithin/water multilayers, recorded at oblique incidence (text for details)

The processing of the experimental spectra required numerical subtraction of the contribution to the absorption due to the pure lipid, which was achieved by subtracting a library spectrum multiplied by a constant selected by trial so that features at two suitably chosen points of the absorption band became congruent with those in the known spectrum of the chrmophore

Results Fig 4b shows processed absorption spectra from Acridine Orange in lecithin multilayers tilted by an angle ω of 55°

The dichroic ratio for the band equals abont 0 7, which correspond, by formula (2), to an order parameter equal to −0 3

It is belived the techniques illustrated above may be useful in a variety of practical applications.

(Received July 8, 1982)

REFERENCES

1 B Norden, G Lindblom, I Jonas, J Phys Chem, **81**, 2086 (1977)
2. T Porumb, Studia Univ Babeş-Bolyai, Phys, **24** (2), 14 (1979)
3 T Porumb, H Porumb, Studia Univ Babeş-Bolyai, Phys, **25** (2), 34 (1980)
4 T Porumb, E F Slade, J Magnetic Reson, **22**, 219 (1976)

STUDIUL DICROISMULUI OPTIC LINIAR AL UNOR SPECIMENE PREFERENŢIAL ORIENTATE FOLOSIND UN SPECTROFOTOMETRU OBIŞNUIT

(Rezumat)

Se prezintă o metodă de detecţie a dicroismului optic liniar folosind un spectrofotometru Spekord UV VIS, ilustrîndu-se metoda cu studiul dependenţei dicroismului liniar de gradul de ordine internă din specimene uniaxiale preferenţial orientate (filme polimerice întinse, membrane de tip cristal lichid liotrop)

STUDIA UNIV BABEŞ-BOLYAI, PHYSICA, XXVIII, 1983

INFLUENCE DE LA PRESSION AMBIANTE SUR LES PROPRIÉTÉS THERMOÉLECTRIQUES DU RUTILE (TiO_2) REDUIT OU DOPÉ AVEC DU NIOBIUM

V. BABEŞ et V. CRISTEA

Comme on le précise dans les travaux récents étudiant les propriétés et les applications du rutile (TiO_2), l'intérêt pour ce matériau se manifeste constamment depuis presque 50 ans, soit à cause de la grande diversité de phénomènes mis en évidence [1, 2], soit, dans les dernières années, à cause de ses applications dans la photoélectrolyse de l'eau [3, 4]

Nos études de l'effet Seebeck sur le rutile réduit ou dopé avec du niobium [5, 6], nous ont révélé l'importance de la réalisation des conditions de vide identiques pour obtenir une bonne reproductibilité des résultats C'est ainsi qu'on a commencé l'étude systematique de la dépendance de la tension Seebeck, en fonction de la pression du gaz de l'enceinte et des autres facteurs qui déterminent les propriétés semiconductrices du rutile, c à d , le degré de réduction ou la concentration du dopant

On a mesuré la dépendance du pouvoir thermoélectrique (p t é) α en fonction de la pression de l'air préalablement séché, $\alpha = f(p)$, pour des échantillons monocristallins de rutile dopés avec du Nb en concentration allant de 0,005% à 1,0% , quelques résultats sont présentés dans la figure 1 Pour les échantillons réduits R (rutile monocristallin réduit sous vide à 1173°K), respectivement TF (couche mince de titane oxydée par chauffage à l'air à 773°K et après réduction sous vide à 500°K), la variation $\alpha = f(p)$ est de même type.

Le dispositif expérimental a été déjà décrit [7] On a réalisé une admission très lente du gaz dans l'enceinte de mesure afin d'éliminer l'influence de ce facteur sur l'équilibre thermique, et par la suite, la modification du gradient thermique

A partir des résultats ainsi obtenus, nous avons calculé la variation relative du p t é.

$$\frac{\Delta\alpha}{\alpha_v} = \frac{\alpha_{atm} - \alpha_v}{\alpha_v} \times 100\%$$

que nous avons représentée dans la figure 2 fonction de la concentration du niobium, C_{Nb} Pour comparaison, nous avons porté sur le même graphique les niveaux R et TF, correspondant aux échantillons réduits. La courbe ainsi obtenue peut être décrite par l'équation

$$-- = A - B \ln C_{Nb}$$

où A et B sont des coefficients distincts pour les deux régions caractéristiques, I ($A = -7{,}13$, $B = 5{,}12$) et respectivement II($A = 2{,}47$, $B = 1{,}06$) de la courbe (fig 2)

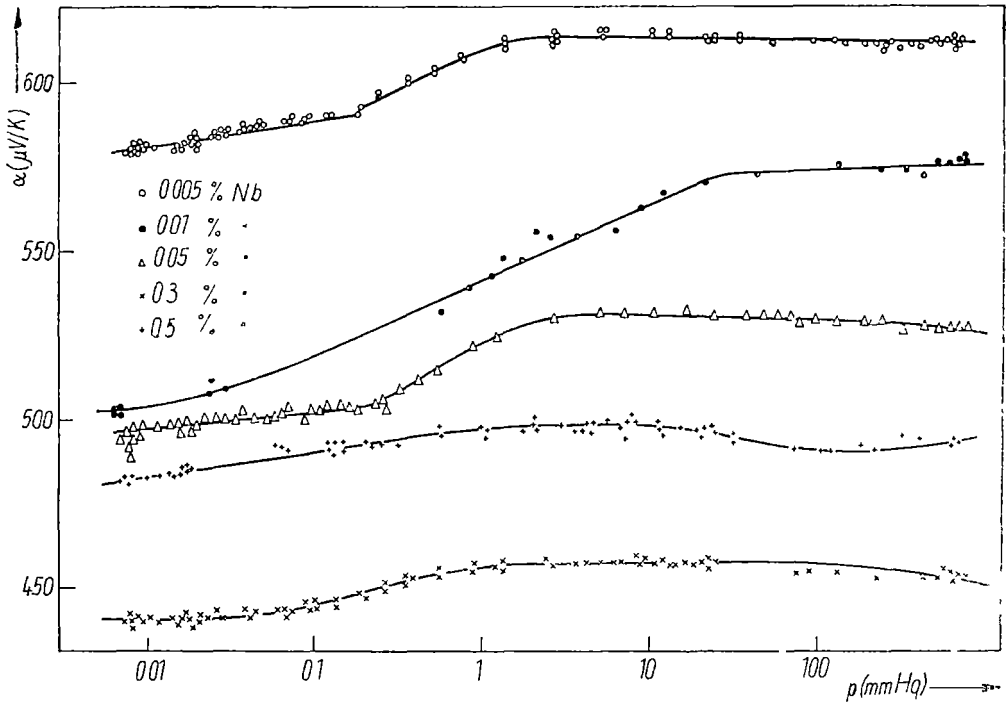

Fig. 1 Variation de $\alpha = f(p)$ pour quelques échantillons de rutile dopés avec du niobium.

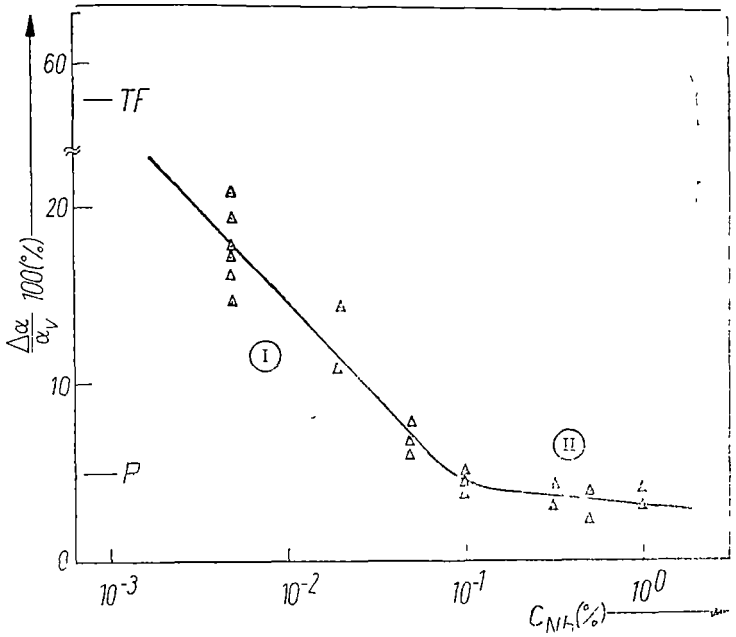

Fig 2 Dépendance de $\Delta\alpha/\alpha_v$ en fonction de la concentration du niobium.

L'analyse des résultats présentés auparavant, nous a suggéré les conclusions suivantes :

1. Si dans le cas des hautes températures de tels phénomènes de „saut" ont été observés pour plusieurs propriétés électriques du rutile (la résistivité [1], la tension Seebeck [8]) s'expliquent d'habitude par la perte de l'oxygène, génératrice de défauts de reseau agissant comme donneurs (vacances d'oxygène, ions de Ti interstitiels), nous n'avons pas trouvé de références concernant la dépendance du p.t.é du rutile avec la pression pour le cas des températures moyennes (environ 300°K).

2. L'abaissement de $\Delta\alpha/\alpha_0$ avec l'augmentation de la concentration de l'impureté, C_{Nb}, s'explique par le deplacement du niveau de Fermi vers le bas de la bande de conduction, le rôle du niveau de Fermi comme régulateur dans le processus de chemisorption de la surface étant bien connu [10].

3. L'étude de l'évolution du p.t.é. en fonction du temps permet de mettre en évidence l'existence des états lents de surface ($\tau \sim 10$ s), d'une manière analogue à la relaxation de la charge superficielle à l'adsorption du gaz sur le germanium [9].

4. Le changement du rapport $\alpha/\log p$ pendant l'augmentation de la pression dans l'intervalle allant d'environ 10^{-2}mm Hg, jusqu'à environ 10 mm Hg, peut être décrit par l'équation

$$\alpha = \alpha_1 + a \log p$$

où α_1 représente la valeur du p.t.é. pour $p = 1$ mm Hg et a est une constante dépendant de la concentration en Nb de l'échantillon. Cette observation conduit à la supposition d'un mécanisme d'adsorption de l'oxygène par „couches" successives, c.à.d. la modification de la pente de la courbe $\alpha = f(p)$ est due au passage d'une „couche" complète a une autre plus profonde avec l'augmentation de la pression. Ce mécanisme a été déjà proposé pour l'adsorption de l'oxygène sur le germanium [11].

(Manuscrit reçu le 8 juillet 1982

BIBLIOGRAPHIE

1 S N Subbarao, Y H. Yun, R Kershaw, K. Dwight et A Wold, Mat. Res. Bull, **13**, 1461 (1978).
2 E M Logothetis et R L Hetrick, Solid State Commun, **31**, 187 (1979)
3. D. Moraru, D. Teodoreanu et M. Teodoreanu, Electrotehnica, Electronica, Automatica, **27**, 1 (1979)
4 J. F. Houlihan, D. B. Armitage, T Hoovler, D. Bonaquist, D P. Madacsi et L N. Mulay, Mat. Res. Bull., **13**, 1205 (1978).
5 V. Cristea et V. Babeş, Phys. Stat Sol. (a), **45**, 617 (1978).
6. V. Cristea, Rev Roum. Phys, **23**, 587 (1978).
7. V. Cristea et V. Babeş, Studia Univ. Babeş-Bolyai, Phys. **24**, (2) 70 (1979).
8 J F Baumard et E. Tani, Phys. Stat Sol. (a), **39**, 373 (1977).
9 V V Kiselev, S N. Kozlov et Y A Zarifiancz, *Problemî fizicesko himii poverhnosti poluprovodnikov*, Izd Nauka, Novosibirsk, 1978, p 203

10. F F Volkenstein, *Fiziko-himia poverhnosti poluprovodnikov*, Izd Nauka, Moskva, 1973 p. 167
11. V G Litovtchenko, V I Liaschenko et D S Frolov, *Poverhnostnîe svoistva poluprovodnikov*, Izd Akad Nauk SSSR, Moskva, 1962, p 147

INFLUENŢA PRESIUNII AMBIANTE ASUPRA PROPRIETĂŢILOR TERMOELECTRICE ALE RUTILULUI (TiO_2) REDUS SAU DOPAT CU NIOBIU

(Rezumat)

Se pune în evidenţă experimental influenţa presiunii ambiante asupra tensiunii termoelectrice a rutilului redus sau dopat cu niobiu în diverse concentraţii, constatîndu-se apariţia unui „salt" în valoarea coeficientului Seebeck Se studiază dependenţa acestui coeficient de concentraţia de niobiu şi se propune o interpretare semicantitativă a fenomenelor evidenţiate

STUDIA UNIV BABEŞ-BOLYAI, PHYSICA, XXVIII, 1983

DOUBLE RESONANCE PARAMETRIC EXCITATION IN PLASMAS

C. BĂLEANU

As it is well known double resonance parametric excitation of waves in plasma occurs when two pumps are used for waves excitation This process is of interest in plasma heating and ionospheric applications and was at first studied in [4]. The papers [1], [4], [5], [6] and [9] concern the case of unmagnetized plasma and long wave length of pumps, whereas in [10] the double parametric excitation is investigated for finite wave length of pumps In the papers [7] and [8] the same process is discussed for an inhomogeneous magnetized plasma, while in [2] and [3] the authors investigate double resonance parametric excitation via turbulent unmagnetized plasma

The aim of our present paper is to investigate, using the method developed in [4], the parametric instabilities in a two component fully ionized unmagnetized plasma immersed in two elliptic polarized external electric fields We will assume that the pump frequencies are near the electron plasma frequency such that their difference is either approximately equal to the ion acoustic frequency Ω_0, or to the double $2\Omega_0$ of this last frequency

Accordingly, the applied electric field has the form·

$$\vec{E}_0(t) = 2\hat{e}_x E_{1x} \sin \omega_1 t + 2\hat{e}_y E_{1y} \cos \omega_1 t + \\ + 2\hat{e}_x E_{2x} \sin (\omega_2 t + \alpha) + 2\hat{e}_y E_{2y} \cos (\omega_2 t + \alpha) \tag{1}$$

where E_{1x}, E_{1y}, E_{2x}, ${}_{2y}E$ are time and space independent amplitudes, ω_1 and ω_2 the electric fields frequencies and α a constant phase difference

We start from the two Vlasov equations for electron and ion distribution functions respectively under the form they acquire after a Dawson transformation to a frame oscillating with the electrons was performed

$$\left(\frac{\partial}{\partial t} + \vec{u}\frac{\partial}{\partial \vec{\rho}} - \frac{e}{m}\vec{E}'(\rho, t)\frac{\partial}{\partial \vec{u}}\right)\tilde{F}_e(\vec{\rho}, \vec{u}, t) = 0 \tag{2}$$

$$\left(\frac{\partial}{\partial t} + \vec{V} - \frac{\partial}{\partial \vec{r}} + \frac{e}{M}\vec{E}'(\vec{r}, t)\frac{\partial}{\partial \vec{v}}\right)F_i(\vec{r}, \vec{v}, t) = 0 \tag{3}$$

together with Poisson equation

$$\operatorname{div} E = -4\pi e \int F_e d\vec{v} + 4\pi e \int F_i d\vec{v} = \vec{\operatorname{div}}\, \vec{E}' \tag{4}$$

Tilda denotes here quantities defined in the coordinates frame oscilating with electrons In the above equations $\vec{E}'(\vec{\rho}, t)$ is the fluctuation field

$$\vec{E}'(\vec{r}, t) = \vec{E}(\vec{\rho}, t) = \vec{E}(\vec{r}, t) - \vec{E}_0(t) \tag{5}$$

assumed to be of electrostatic origin, while $\vec{\rho}$ and $\vec{u}$ are given by

$$\vec{r} - \vec{r}_0(t) = \vec{\rho}, \quad \vec{v} - \vec{v}_0(t) = \vec{u} \tag{6}$$

$\vec{r}_0(t)$ and $\vec{v}_0(t)$ being here particular solutions of the equations of motion

$$\frac{d\vec{v}_0(t)}{dt} = -\frac{e}{m}\vec{E}_0(t), \quad \frac{d\vec{r}_0(t)}{dt} = \vec{v}_0(t) \tag{7}$$

Proceeding as in [4] we have obtained the following integral equation for the Fourier transform of ion density

$$n_i(\omega) = -\chi_i(\omega)\sum_{N,\,N'} \frac{\Delta_N \Delta_N^*}{\varepsilon_e(\omega - \omega_N)} n(\omega + \omega_N - \omega_{N'}) + \eta_0 \tag{8}$$

where

$$\eta_0 \equiv n_{i_0} + \chi_i \Delta_k^{-1}\left(\varepsilon_e^{-1}\Delta_i n_{e_0}\right) \tag{9}$$

$$\begin{aligned} \tilde{n}_{e_0}(\vec{k},\ \omega) &= i\int d\vec{u}\,\frac{F_e(\vec{k},\ \vec{u},\ t=0)}{\omega - \vec{k}\vec{u}} \\ n_{i_0}(\vec{k},\ \omega) &= i\int d\vec{u}\,\frac{F_i(\vec{k},\ \vec{u},\ t=0)}{\omega - \vec{k}\vec{u}} \end{aligned} \tag{9'}$$

The convolution operator Δ_i in this equation is defined by

$$\tilde{A}(\vec{k},\ \omega) = \Delta_i A(\vec{k},\ \omega) \equiv \int \frac{d\omega'}{2\pi}\Delta_i(\omega - \omega')\,A(\vec{k},\ \omega') \tag{10}$$

$$\Delta_i(\omega) = i\sum \Delta_N(\vec{k})\frac{1}{\omega + \omega_N} \tag{11}$$

In contrast with [4], where N stands for a pair of integers $(n_1,\ n_2)$ which may be thought of as occupation numbers for the pump modes, there appears in the case considered here four integers due to the elliptic pumps polarization, such that the frequencies are given by the following expression

$$\omega_N = (n_{1x} - n_{1y})\omega_1 + (n_{2x} - n_{2y})\omega_2 \tag{12}$$

Besides Δ_N is given in (8) and (11) by

$$\Delta_N(\vec{k}) = J_{n1x}(\mu_{1x})J_{n1y}(\mu_{1y})J_{n2x}(\mu_2)_x J_{n2y}(\mu_{2y})\ e^{i(n_{2x} - n_{2y})\alpha} e^{i(n_{1y} + n_{2y})\frac{\pi}{2}} \tag{13}$$

where $J_{nsx,\,y}(\mu_{sx,\,y})$ represents the $n_{sx\ y}$-th order Bessel function of the argument

$$\mu_{sx,\,y} = \frac{2e\vec{k}_{s,y}\vec{E}_{sx,\,y}}{m\omega_s^2} \qquad (s = 1,\ 2) \tag{14}$$

The inverse operator which allows us to pass from $\tilde{A}$ to A is:

$$\Delta_k^{-1}(\omega) = \Delta_{-k}(\omega) = i \sum_N \Delta_N^* \frac{1}{\omega - \omega_N} \tag{15}$$

while the expressions of the Fourier transforms of the partial dielectric function are:

$$\varepsilon_e(\vec{k}, \omega) = 1 + \chi_e(\vec{k}, \omega), \quad \varepsilon_i(\vec{k}, \omega) = 1 + \chi_i(\vec{k}, \omega) \tag{16}$$

Here $\chi_e(k, \omega)$ represents the electron susceptibility in the oscillating frame whereas $\chi_i(\vec{k}, \omega)$ the ion susceptibility in the rest frame. These two quantities are given by

$$\begin{aligned} \chi_e(\vec{k}, \omega) &= \frac{\omega_{pe}^2}{k^2} \int d\vec{u} \frac{1}{\omega - \vec{k}\vec{u}} \vec{k} \frac{\partial}{\partial u} \tilde{F}_{e0}(\vec{u}) \\ \chi_i(\vec{k}, \omega) &= \frac{\omega_{pi}^2}{k^2} \int d\vec{r} \frac{1}{\omega - k\vec{v}} \vec{k} \frac{\partial}{\partial v} \qquad F_{i0}(\vec{v}) \end{aligned} \tag{17}$$

In the above expressions $\vec{F}_{e0}(\vec{n})$ and $\vec{F}_{i0}(\vec{v})$ are the space — time average of the electron and ion distribution functions respectively Provided that the higher order termis than the second order anes are neglected in $\mu_{sx,y}$, the following selcetion rules establisched in [4] for the occupation numbers can be applied·

(a) $$n_{1x} - n_{1y} + n_{2x} - n_{2y} = n'_{1x} - n'_{1y} + n'_{2x} - n_{2y}$$

such that $(\omega + \omega_N - \omega_{N'})$ lies the ionic frequency range

(b) $$|n_{1x}| + |n_{1y}| + |n'_{1x}| + |n'_{1y}| + |n_{2x}| + |n_{2y}| + |n'_{2x}| + |n'_{2y}| = 2,$$

since only the second order terms in $\mu_{sx,y}$ are to be retained

(c) $n'_{1x} - n'_{1y} + n'_{2x} - n'_{2y} = \pm 1$; since $(\omega - \omega_{N'})$ must be close to the electron plasma frequency The table below lists for the case investigated in the present paper all the possible combinations of the occupation numbers which fulfil the three preceding conditions

n_{1x}	n_{1y}	n_{2x}	n_{2y}	n'_{1x}	n'_{1y}	n'_{2x}	n'_{2y}	$\omega_N - \omega_{N'}$	ω_N	$\omega_{N'}$
1	0	0	0	1	0	0	0	0	ω_1	ω_1
0	1	0	0	0	1	0	0	0	$-\omega_1$	$-\omega_1$
1	0	0	0	0	0	1	0	Δ	ω_1	ω_2
0	1	0	0	0	0	0	1	$-\Delta$	$-\omega_1$	$-\omega_2$
0	0	1	0	1	0	0	0	$-\Delta$	ω_2	ω_1
0	0	0	1	0	1	0	0	Δ	$-\omega_2$	$-\omega_1$
0	0	1	0	0	0	1	0	0	ω_2	ω_2
0	0	0	1	0	0	0	1	0	$-\omega_2$	$-\omega_2$
−1	0	0	0	−1	0	0	0	0	$-\omega_1$	$-\omega_1$
0	−1	0	0	0	−1	0	0	0	ω_1	ω_1
−1	0	0	0	0	0	−1	0	$-\Delta$	$-\omega_1$	$-\omega_2$
0	−1	0	0	0	0	0	−1	Δ	ω_1	ω_2

n_{1x}	n_{1y}	n_{2x}	n_{2y}	n'_{1x}	n'_{1y}	n'_{2x}	n'_{2y}	$\omega_N - \omega_{N'}$	ω_N	$\omega_{N'}$
0	0	−1	0	−1	0	0	0	Δ	$-\omega_2$	$-\omega_1$
0	0	0	−1	0	−1	0	0	$-\Delta$	ω_2	ω_1
−1	0	0	0	0	1	0	0	0	$-\omega_1$	$-\omega_1$
0	−1	0	0	1	0	0	0	0	ω_1	ω_1
−1	0	0	0	0	0	0	1	$-\Delta$	$-\omega_1$	$-\omega_2$
0	−1	0	0	0	0	1	0	Δ	ω_1	ω_2
0	0	−1	0	0	1	0	0	Δ	$-\omega_2$	$-\omega_1$
0	0	0	−1	1	0	0	0	$-\Delta$	ω_2	ω_1
0	0	−1	0	0	0	0	1	0	$-\omega_2$	$-\omega_2$
0	0	0	−1	0	0	1	0	0	ω_2	ω_2
1	0	0	0	0	−1	0	0	0	ω_1	ω_1
0	1	0	0	−1	0	0	0	0	$-\omega_1$	$-\omega_1$
1	0	0	0	0	0	0	−1	Δ	ω_1	ω_2
0	1	0	0	0	0	−1	0	$-\Delta$	$-\omega_1$	$-\omega_2$
0	0	1	0	0	−1	0	0	$-\Delta$	ω_2	ω_1
0	0	0	1	−1	0	0	0	Δ	$-\omega_2$	$-\omega_1$
0	0	1	0	0	0	0	−1	0	ω_2	ω_2
0	0	0	1	0	0	−1	0	0	$-\omega_2$	$-\omega_2$

Neglecting in (8) the inhomogeneous term it results:

$$X(\omega)n_i(\omega) = Y_+(\omega)\, n_i(\omega + \Delta + Y_-(\omega)n_i(\omega - \Delta) \tag{18}$$

where:

$$X(\omega) = \frac{\varepsilon(\omega)}{\varepsilon_e(\omega)} + \frac{1}{4}\,\chi_i(\omega) \sum_{s=1,2} |\,\mu_s\,|^2 \left\{ \frac{1}{\varepsilon_e(\omega + \omega_s)} + \frac{1}{\varepsilon_e(\omega - \omega_s)} \right\} \tag{19}$$

$$Y_{\pm}(\omega) = -\frac{1}{4}\,\chi_i(\omega) e^{\mp i\alpha} \mu_1^{(\pm)} \mu_2^{(\pm)} \left(\frac{1}{\varepsilon_e(\omega + \omega_1)} + \frac{1}{\varepsilon_e(\omega \pm \omega_2)} \right) \tag{20}$$

$$\mu_s^{(\pm)} = \mu_{sx} \pm i\mu_{sy} \tag{21}$$

$$\Delta = \omega_1 - \omega_2 \quad (22) \qquad (\omega) = 1 + \chi_e(\omega) + \chi_i(\omega) \tag{23}$$

We must observe here that the difference between our expression (18) and expression (25) given in [4], follows from the fact that in our above considerations the complex expresion (21) occur instead of the real ratio us of the excursion length in [4] From the developments of our present paper we may conclude that the parametric instabilities in a two component fully ionized unmagnetized plasma immersed in two elliptic polarized electric pump fields have the same qualitative behaviour as in a linear polarized pump fields Therefore, the results obtained in [4] for these linear polarized pump fields can consistently be extended to the case of elliptic polarized pump fields under the condition that the expression (41) from [4] for the ratio of the electrostatic field energy to the election thermal energy would be replaced by

$$\Lambda_s^2 = \frac{1}{4}\,|\,\mu_s\,|^2\,\varepsilon_e(\omega) \approx (E_{s0}^2/4\pi)\,(nT_e)^{-1} \cos^2\theta \left[\frac{\omega_{pe}^2}{\omega_s^4} \left(1 + \frac{k^2}{k_D^2} \right) \right] \tag{24}$$

where n is the electron density, T_e temperature, θ the angle between E_{s0} and k, E_{s0} being given by

$$E_{s0} = E_{sx}\hat{e}_x + E_{sy}\hat{e}_y \tag{25}$$

Similarly as in the case of two linear polarized pump fields, in the elliptic polarized pumps here studied, circumstances may occur such that the waves excitation in the considered plasma by two combined pump fields may have a lower threshold than by only one pump field.

Stimulating discussions with professor M. Drăganu are gratefully acknowledged.

(Received October 7, 1982)

REFERENCES

1 Y M. Aliev, O M Gradov, D Sunder, Beitr Plasma Phys, **15**, 345 (1975)
2. N E Andrejew, D Sunder, Beitr Plasma Phys, **17**, 273 (1977)
3 N. E Andrejew, D Sunder, Beitr Plasma Phys, **18**, 51 (1978)
4 D Arnush, K Nishikawa, B D Fried, C F Kennel, A Y Wong, Phys Fluids, **16**, 2270 (1973)
5 J A Fejer, B L Cragin, R L Showen, J Plasma Phys, **19**, 355 (1978)
6 B D Fried, A. Adler, R Bingham, J Plasma Phys, **24**, 315 (1980)
7. V. N. Radziewskii, Ukr Fiz Journal, **24**, 1545 (1979)
8 M S. Sodha, K P Maheshwari, R P Sharma, S C Kanshik, J Appl Phys, **50**, 1256 (1979)
9 D Sunder, D D Tshakaja, Fiz Plazmy, **3**, 865 (1978)
10 T Tanaka, J Phys Soc Japan, **42**, 670 (1977)

EXCITAȚIA DUBLEI REZONANȚE PARAMETRICE ÎN PLASME

(Rezumat)

Folosind metoda din [4] sînt studiate instabilitățile parametrice pentru o plasmă nemagnetizată situată în două cîmpuri electrice polarizate eliptic pentru cazul în care frecvențele celor două pompe sînt apropiate de frecvența oscilațiilor Langmuir, iar diferența lor este aproximativ egală cu o frecvență joasă de rezonanță

Pe baza studiului efectuat se poate trage concluzia că și în cazul polarizării eliptice apar situații în care excitația cu ajutorul a două cîmpuri pompă poate avea un prag mai scăzut decît în cazul folosirii unui singur cîmp pompă

STUDIA UNIV BABEŞ-BOLYAI, PHYSICA, XXVIII, 1983

THE SPIN-GLASS PHASE IN THE SPIN-DENSITY-WAVE MEDIUM

ZS. GULACSI, M. GULACSI and M. CRIŞAN

1. **Introduction.** The recent experimental data obtained by *Hedgcock* et al. [1], Strom-Olsen et al [2] Giurgiu et al [3] on the chromium alloys containing magnetic impurities suggested the coexistence between the spin-density-waves (SDW) and the spin-glass state. The interaction between the conduction electrons in the SDW state can generate an effective spin-spin interaction [3] In this paper we study the spin-glass phase which appears in a system of localized spins which interact by random exchange integral J_{ij} and at the same time the second order electron-spin interaction gives rise to another random spin-spin interaction

The Hamiltonian for such a model is

$$\mathcal{H} = -\sum_{i\neq j} J_{ij}\vec{S}_i\vec{S}_j - g\sum_{i\neq j} x_i x_j \tau_i \tau_j \vec{S}_i\vec{S}_j , \tag{1}$$

where $\tau_i = \pm 1$ indicates the two possible orientations of the SDW at the impurity site and x_i is a random variable which is given by the cos (QR) dependence of the SDW energy gap, $\Delta(R)$; g is an effective coupling constant given by $g = N(0)\ \Delta^2(J_1/v)^2$ In the definition of the effective coupling constant g, $N(0)$ is the density of states, Δ is the energy gap (the order parameter of the SDW), J_1 is the „$s - d$" (f) electron-spin integral and V is the electron-hole attractive interaction

In the sect 2 we will calculate the free energy, the magntization and the Edwards-Anderson order parameter in the approximation that the SDW state is not influenced by the spin-glass state The stability of the phase is discussed in sect 3 and in sect 4 we will present the conclusions which are obtained from this model

2 **The free energy, magnetization and the Edwards-Anderson parameter.** In the model described by the Hamiltonian (1) the exchange integral J_{ij} is a random variable with the Gaussian distribution

$$P_1(J)_{ij} = \frac{1}{\sqrt{2\pi}J}\exp\left[-\frac{(J_{ij}-J_0)^2}{2J^2}\right], \tag{2}$$

and x_i is a random variable distributed according to the cosinus distribution function

$$P_2(x_i) = \frac{1}{\sqrt{1-x_i^2}} , \tag{3}$$

The general formula for the free energy, in the replica-trick formalism will be written as

$$f = -T\lim_{N\to\infty}\lim_{n\to 0}\frac{1}{Nn}\left\{T_{r_n}\prod_{(i,j)}\int dx_i dx_j dJ_{ij}P_1(J_{ij})\times P_2(x_i)\ P_2(x_j)\exp\left(\beta\sum_{\alpha=1}^{n}\mathcal{H}^\alpha\right)-1\right\} , \tag{4}$$

where $\mathcal{H}^{\alpha}$ is given by (1) with the Zeeman term $\sum_i \vec{H}\ \vec{S}_i^{\alpha}$, $\vec{H}$ is the magnetic field, and α is the index of replica

In order to calculate (4) we have to evaluate the integral

$$\frac{1}{\pi^2}\sum_{\tau_i,\tau_j}\int_0^1\int_0^1 \frac{dx_i}{\sqrt{1-x_i^2}}\cdot\frac{dx_j}{\sqrt{1-x_j^2}}\ \exp\left[z\tau_i\tau_j x_i x_j\right] = F(z)\,, \tag{5}$$

For $i \neq j$, $F(z)$ can be expressed as

$$F(z) = \sum_{k=0}^{\infty}\frac{2K!}{(K!)^4}\left(\frac{Z}{4}\right)^{2k} \cong \exp\left[\frac{Z^2}{2^3} - \frac{Z^4}{2^9} + \quad\right] \tag{6}$$

but we will keep only the quadratic terms from (6) and the interactions of the spins from two replicas In this approximation (6) becomes

$$F\left[\frac{g}{T}\sum_{\alpha} S_i^{\alpha}S_j^{\alpha}\right] = \exp\left[\frac{g^2}{8T^2}\sum_{\alpha\beta} S_i^{\alpha}S_j^{\alpha}S_i^{\beta}S_j^{\beta}\right]; \tag{7}$$

and using (7) the free energy (4) becomes

$$f = -T\lim_{N\to\infty}\lim_{N\to 0}\frac{1}{Nn}\left\{Tr_n\exp\left[\sum_{i\neq j}\left(\sum_{\alpha=1}^{n}\frac{J_0}{T}\,S_i^{\alpha}S_j^{\alpha} + \sum_{\alpha\beta}\frac{1}{T^2}\,\bar{J}^2 S_i^{\alpha}S_j^{\alpha}S_i^{\beta}S_j^{\beta} + \frac{H}{T}\sum_{\alpha=1}^{n}S_i^{\alpha}\right] - 1\right\},$$

where $\bar{J}^2 = J_1^2 + (g/2)^2$, (8)

Following the usual way from the replica trick method [4] we get from (8)

$$f = T\left[\frac{\tilde{J}_0 m^2}{2T} - \frac{\tilde{\bar{J}}^2}{(2T)^2}(1-q)^2 - \int_{-\infty}^{+\infty}\frac{dr}{\sqrt{2\pi}}\,e^{-\frac{r^2}{2}}\ln(2\cosh\textstyle\sum)\right]; \tag{9}$$

where

$$\tilde{J}_0 = J_0 N\,,\quad \tilde{\bar{J}} = \bar{J}N^{1/2}\,,\qquad \sum = \frac{1}{T}\left[\tilde{J}_0 m + H + r\sqrt{q}\,\tilde{\bar{J}}\right],$$
$$\bar{J}_1 = J_1 N^{1/2}\,,\ \tilde{g} = gN^{1/2}\,,$$

and

$$q = \int\frac{dr}{\sqrt{2\pi}}\,e^{-\frac{r^2}{2}}\tanh\textstyle\sum;\ m = \int\frac{dr}{\sqrt{2\pi}}\,e^{-\frac{r^2}{2}}\tanh^2\textstyle\sum, \tag{10}$$

3 The astability of the spin-glass phase. From the free energy (9) we can calculate $f = f - f(q=0)$ and we get

$$\delta f = \frac{g^2}{4t_1}\left(\frac{\tilde{g}}{2T_N}\right)^2\left[\frac{1}{t_1^2}\left(\frac{\tilde{g}}{2T_N}\right)^2 - 1\right] > 0\,, \tag{11}$$

where $t_1 = T/T_N$ and T_N is the critical temperature for the SDW state. The result obtained from (11) shows that the spin glass state is unstable energe-

tically and the entropy per spin is negative at $T = 0$ If we neglect the direct spin-spin interaction $J = J_0 = 0$ the spin-glass phase appears only due to the effective spin-spin interaction. This phase appears at

$$T = \frac{1}{2}\tilde{g}(T,\ N,(0)V,\ \tilde{J}_1)\,, \tag{12}$$

The phase diagram in the variables $t_1 = T/T_N$, $j_1 = J_1/V$ can be obtained from (11—12) at a fixed $\theta = N(0)T_N$, and this phase diagram is given in fig 1 a.

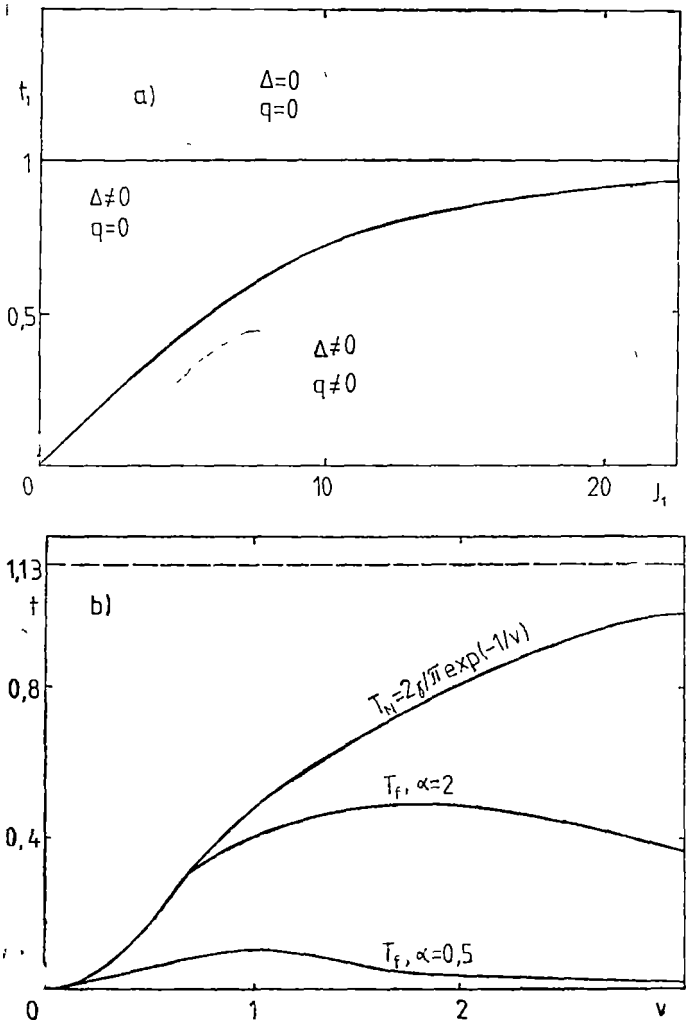

Fig. 1 Phase diagrams for $\tilde{J} = \tilde{J}_0 = 0$ for the variables
a) $t_1 = T/T_N$, $j_1 = \tilde{J}_1/V$ for $\theta = 0{,}01$;
b) $t = T/\Omega$, $v = N(0)V$ for $\alpha = 2$ and $\alpha = 0\,5$

The atractive electron-hole interaction is an important parameter of the model and from (12) we will study the phase diagram in the variables $t_1 = T/\Omega$, $v = N(0)V$ where Ω is the cut-off energy in the theory of the SDW state and $N(0)$ the constant density of states for the electrons For a fixed $\alpha = N(0)J_1\sqrt{N(0)\Omega}$ the phase diagram is given in fig 1 b and one can see that the maximum of the freezing temperature T_f defines a critical value $N(0)V_\alpha$ which separes the two different behaviours of T_N and T_f Concretely T_N is decreasing with T_N if $v < N(0)V_\alpha$, and T_N increases if T_f decreases for $v > N(0)V_\alpha$. For all values of α we have

$$N(0)V_\alpha > 1 \tag{13}$$

and this relation defines a critical interaction

$$v_c = N(0)V_c = 1 \tag{14}$$

with the properties·

1. For $v < v_c$ we have $T_N \simeq T_f$ for $V \to 0$ or $T_N > T_f$ if $v \to v_c$. The both temperature T_N and T_f are increasing (decreasing) with the variation of v, independent of α.
2. For $v > v_c$ the behaviour of T_N and T_f is determined by α For small α, $T_N \gg T_f$ and the changes in v give rise to the opposite variation in T_N and T_f.

The phase diagram for $\tilde{J} \neq 0$ in the variables, t, v, $\jmath = \tilde{J}/\Omega$ is given in fig. 2.

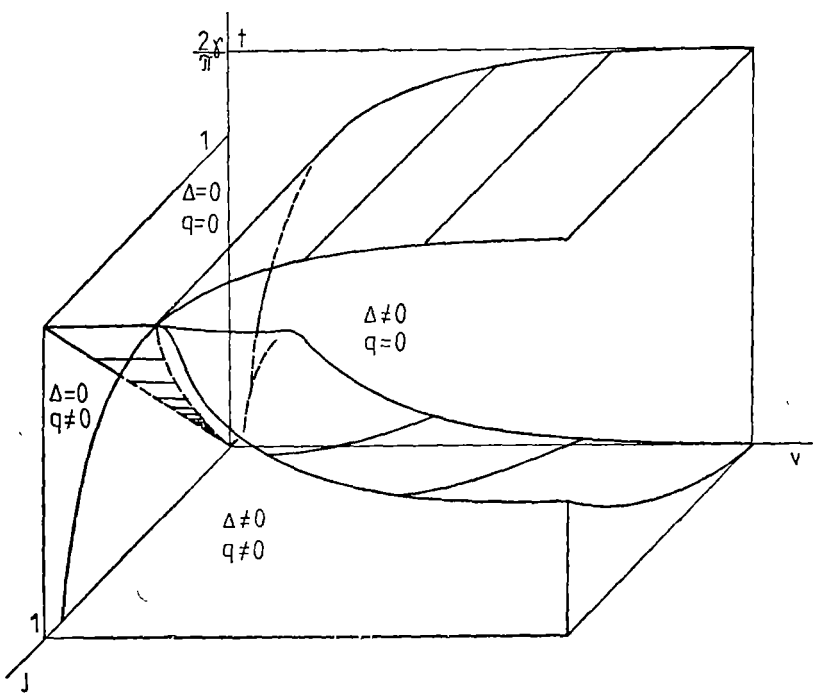

Fig 2 Phase diagram for $\tilde{J} \neq 0$, $\tilde{J}_0 = 0$ case in $t = T/\Omega$, $v = N(0)V$, $\jmath = \tilde{J}/\Omega$ variables, with $m = 0, \frac{\gamma}{\pi} = 0{,}57$.

The thermodynamic properties and T_f as function of concentration will be discussed in a future paper

4 **Discussions.** The model presented can be a resonable starting point in the explanation of the experimental results obtained by Giurgiu et al [3] for the chromium alloys with some rare earths impurities Our theoretical model considered a disorder of the impurities which is more realistic than the only disorder given by coupling between SDW and impurities However, the calculation of the phase diagram showed that the problem of the occurrence of the spin — glass in the SDW medium is dependent of some parameters which have been missed in [3] There is another problem which is still open. In [3] as in this paper the spin-spin interaction has been considered to be a long-range interaction. In this case we can perform easyly the average on the configurations, but if the nonmagnetic impurities or the thermal excitations change the spin-spin interaction in a schort-range interaction all our calculations are not correct and we have to look at the problem in the spirit of a recent model proposed by Abrikosov and Moukhin [5]

Finally we have to remark that the presence of the cusp in the magnetic susceptibility is not enough to decide about the neture of the nature of the spin-glass and the specific heat measurements will be necessary.

Acknowledgements One of the authors (M C) is grateful to Professor G Tolouse for useful discussions on the problem.

(Received October 19, 1982)

REFERENCES

1 F T Hedcock, J O Ström-Olsen, D F Wilford, J Phys F **7**, 855 (1977)
2 J O Strom-Olsen, D F Wilford, S K Burke and B D Rainford, J Phys F **9**, L 95 (1979)
3 A. Giurgiu, I Pop, M Popescu and Zs Gulacsi, Phys Rev B**24**, 1350 (1981)
4 S W Edwards and P W Anderson, J Phys F Met Phys, **5**, 965 (1975)
5 A A Abrikosov and S I Moukhin, J Low Temp Phys, **33**, 207 (1978)

FAZA STICLOASĂ DE SPIN ÎN MEDIU DE UNDE DE DENSITATE DE SPIN

(Rezumat)

Se analizează apariţia stării de sticlă de spin în prezenţa undelor de densitate de spin, folosind aproximaţia replicilor Diagrama de fază se obţine în aproximaţia că unda de densitate de spin nu este afectată de interacţia spin-spin

STUDIA UNIV BABEŞ-BOLYAI, PHYSICA, XXVIII, 1983

INSTABILITATEA MAGNETOHIDRODINAMICĂ DE TIP RAYLEIGH-TAYLOR A UNUI MODEL DE PLASMĂ COMPUSĂ ECUAŢIA DE DISPERSIE

MIRCEA VASIU

Introducere. În prezenta comunicare ne propunem să stabilim ecuaţia de dispersie pentru cazul unui model de plasmă în care se desfăşoară o instabilitate de tip Rayleigh-Taylor După cum se ştie o astfel de instabilitate apare, în cazul a două straturi de fluid suprapuse, la suprafaţa de separaţie a fluidelor, considerate ca avînd densităţi diferite. Fluidele se află sub acţiunea acceleraţiei gravitaţionale $\vec{g}$

Această problemă a constituit obiectul de studiu a numeroase lucrări consacrate atît comportării fluidelor obişnuite, cît şi celor ionizate, în prezenţa instabilităţii de tip Rayleigh-Taylor În acest sens menţionăm lucrările elaborate de: S Chandrasekhar [1], R Hide [2], S Talwar [3], S Maheshwari, P Bhatia [4], R. Sharma, K. Srivastava [5], P Ariel, B Aggarwala [6], M Vasiu [7]

Importanţa unor astfel de studii se explică prin interesul lor sub aspect aplicativ pentru plasma cosmică (în special pentru cazul unor modele de atmosfere stelare)

În lucrarea de faţă ne bazăm pe lucrarea noastră [7], în care s-a analizat problema stabilirii ecuaţiei de dispersie pentru un model de plasmă, în prezenţa instabilităţii Rayleigh-Taylor, care este constituită dintr-o singură componentă, ionizată, cu conductivitate electrică finită, supusă la acţiunea acceleraţiei gravitaţionale $\vec{g}$ $(0, 0, -g)$, şi la acţiunea unui cîmp magnetic $\vec{B}_0$ $(B_x, 0, B_z)$ uniform şi constant Modelul de plasmă pe care-l analizăm în prezenta comunicare este constituit din două componente: o componentă ionizată, cu conductivitate electrică finită şi o componentă neutră Atît componenta ionizată, cît şi componenta neutră se consideră incompresibile, nevîscoase. Densităţile componentelor respective ρ şi ρ_n se consideră funcţii de variabila z (utilizăm sistemul cartezian de axe $Oxyz$) Atît componenta ionizată, cît şi componenta neutră se află sub acţiunea acceleraţiei gravitaţionale $\vec{g}$ $(0, 0, -g)$ Componenta ionizată se află şi sub acţiunea unui cîmp magnetic uniform şi constant $\vec{B}_0$ $(B_x, 0, B_z)$. Între particulele ionizate şi cele neutre se exercită ciocniri caracterizate de frecvenţa de ciocnire ν_c

Sistemul de ecuaţii magnetohidrodinamice pentru micile perturbaţii. Scriind sistemul de ecuaţii magnetohidrodinamice pentru modelul de plasmă analizat, luînd în considerare cazul micilor perturbaţii (se neglijează din calcule pătratele şi produsele perturbaţiilor) se obţine următorul sistem de ecuaţii diferenţiale

$$\rho \frac{\partial \vec{v'}}{\partial t} = -\nabla p' + \frac{1}{\mu}(\vec{B}_0 \cdot \nabla)\vec{B'} - \nabla(\vec{B}_0 \cdot \vec{B'}) + \rho_n \nu_c (\vec{v_n'} - \vec{v'}) + g\vec{\rho'}, \qquad (1)$$

$$\rho_n \frac{\partial \vec{v}_n}{\partial t} = -\rho_n \nu_c (\vec{v}_n' - \vec{v}') + \vec{g}\rho_n', \tag{2}$$

$$\frac{\partial \rho'}{\partial t} = -(\vec{v}' \cdot \nabla)\rho, \tag{3}$$

$$\frac{\partial \rho_n'}{\partial t} = -(\vec{v}_n' \cdot \nabla)\rho_n, \tag{4}$$

$$\frac{\partial \vec{B}'}{\partial t} = (\vec{B}_0 \cdot \nabla)\vec{v}' + \nu_m \Delta \vec{B}', \tag{5}$$

$$\nabla \cdot \vec{B}' = 0, \ \nabla \cdot \vec{v}' = 0, \ \nabla \cdot \vec{v}_n' = 0, \tag{6}$$

unde $\vec{v}'$ este perturbaţia vitezei unui element de fluid ionizat, p' este perturbaţia presiunii fluidului ionizat, $\vec{B}'$ este perturbaţia cîmpului magnetic, $\nu_m = \frac{1}{\mu\sigma}$ este coeficientul de viscozitate magnetică (μ este permeabilitatea magnetică a mediului, σ este coeficientul de conductivitate electrică a mediului ionizat), ∇ este operatorul nabla, Δ este operatorul lui Laplace.

Precizăm că prin indicele n s-a notat apartenenţa mărimii respective la componenta neutră

Perburbaţiile se consideră de forma

$$\varphi'(x, y, z, t) = \varphi^*(z) \exp(\imath k_x x + \imath k_y y + \omega t), \tag{7}$$

unde $\varphi^*(z)$ este amplitudinea perturbaţiei (considerată ca funcţie de variabila z), k_x, k_y sînt componentele vectorului număr de undă, iar ω este pulsaţia.

Scriind sistemul de ecuaţii diferenţiale (1)—(6) în proiecţii pe axele de coordonate, înlocuind (7) în ecuaţiile respective, efectuînd calculele, se obţine sistemul de ecuaţii diferenţiale în amplitudinile perturbaţiilor.

$$\omega\rho u^* - \frac{B_z}{\mu}(DB_x^* - \imath k_x B_z^*) - \rho_n \nu_c (u_n^* - u^*) = -\imath k_x p^*, \tag{8}$$

$$\omega\rho v^* - \frac{B_z}{\mu}(DB_y^* - \imath k_x B_z^*) - \frac{B_x}{\mu}(\imath k_x B_y^* - \imath k_y B_x^*) -$$

$$- \rho_n \nu_c (v_n^* - v^*) = -\imath k_y p^*, \tag{9}$$

$$\omega\rho w^* - \frac{B_x}{\mu}(\imath k_x B_z^* - DB_x^*) - \rho_n \nu_c (w_n^* - w) = -Dp^* - g\rho^z, \tag{10}$$

$$\omega u_n^* + \nu_c (u_n^* - u^*) = -\imath k_x p_n^*, \tag{11}$$

$$\omega v_n^* + \nu_c (v_n^* - v^*) = -\imath k_y p_n^*, \tag{12}$$

$$\omega w_n^* + \nu_c (w_n^* - w^*) = -Dp_n^* - g\rho_n^* = -g\rho_n^*, \tag{13}$$

$$\omega\rho^* = -(D\rho)w^*, \tag{14}$$

$$\omega\rho_n^* = -(D\rho_n)w_n^*, \tag{15}$$

$$\omega B_x^* = (ik_xB_x + B_xD)u^* + \nu_m(D^2 - k^2)B_x^*, \tag{16}$$

$$\omega B_y^* = (ik_xB_x + B_xD)v^* + \nu_m(D^2 - k^2)B_y^*, \tag{17}$$

$$\omega B_z^* = (ik_xB_x + B_xD)w^* + \nu_m(D^2 - k^2)B_z^*, \tag{18}$$

$$ik_xB_x^* + ik_yB_y^* = -DB_z^*, \tag{19}$$

$$ik_xu^* + ik_yv^* = -Dw^*, \tag{20}$$

$$ik_xu_n^* + ik_yv_n^* = -Dw_n^*. \tag{21}$$

S-a admis că $D\rho_n = 0$ (presiunea componentei neutre este constantă) Componentele vectorilor viteză sînt $\vec{v}(u, v, w)$ și $\vec{v_n}(u_n, v_n, w_n)$.

Aplicînd un procedeu de calcul analog cu cel utilizat în lucrarea [7], se obține, în urma calculelor efectuate, pentru $\rho = \text{const}$, $\rho_n = \text{const}$. (la suprafața de separare $z = 0$), ecuația diferențială de forma

$$(D^2 - k^2)\left[D^2 + \frac{2ik_xB_x}{B_z}D - \left(\frac{\mu\Omega_m\Omega}{B_z^2} + \frac{k^2B_x^2}{B_z^2}\right)\right]w^* = 0. \tag{22}$$

Aceasta ne conduce la ecuațiile

$$D^2w^* - k^2w^* = 0 \tag{23}$$

și

$$D^2w^* + 2ik_x\beta\, Dw^* - \gamma w^* = 0, \tag{24}$$

unde

$$\beta = \frac{B_x}{B_z}, \quad \gamma = \frac{\mu\Omega_m\Omega}{B_z^2} + \frac{k^2B_x^2}{B_z^2}, \quad \Omega = \frac{\omega[\omega + \nu_c(1 + \alpha)]\rho}{\omega + \nu_c}. \tag{25}$$

Cazuri particulare. 1. În cazul în care se consideră plasma constituită dintr-o singură componentă (componenta neutră nu se ia în considerare) ($\nu_c = 0$), ecuația de dispersie (24), ținînd seama de (25) ($\Omega = \rho\omega$), se reduce la forma obținută în lucrarea noastră [7].

2. În cazul în care plasma se consideră constituită dintr-o singură componentă (componenta neutră nu se ia în considerare)($\nu_c = 0$) și componenta ionizată are o conductivitate electrică infinită ($\nu_m = 0$, $\Omega_m = \omega$) ecuația (24) se reduce la ecuația obținută în lucrarea [5]

Într-o altă lucrare ne vom ocupa de stabilirea criteriului de instabilitate magnetohidrodinamică pe baza ecuației (24)

(Intrat în redacție la 15 octombrie 1982)

BIBLIOGRAFIE

1 S Chandrasekhar, *Hydrodynamic and Hydromagnetic Stability*, Oxford, 1961, § 96—97.
2 R Hide, Proc Roy Soc A, 233, 376 (1955)
3 S Talwar, Zts f Astrophys, 47, 161 (1959)

4 S Maheshwari, P Bhatia, Beitr Plasma Phys, **17,** 41 (1977)
5 R Sharma, K Srivastava, Austr J Phys, **21,** 923 (1968)
6 P Ariel, B Aggarwala, Canad J Phys, **57,** 1094 (1979)
7 M Vasiu, Studia Univ Babeş-Bolyai, Phys, **26** (2), 67 (1981)

L'INSTABILITÉ MAGNÉTOHYDRODYNAMIQUE DE TYPE RAYLEIGH-TAYLOR D'UN PLASMA COMPOSÉ L'ÉQUATION DE DISPERSION

(Résumé)

Dans le présent article nous voulons déduire l'équation de dispersion pour le cas de l'instabilité magnétohydrodynamique de type Rayleigh-Taylor d'un plasma *composé*, incompressible, non visqueux, avec une *conductivité électrique finie*

Le plasma se trouve sous l'action d'un champ magnétique uniforme $\vec{B}_0(B_x, 0, B_z)$ et sous l'action de l'accélération gravitationnelle $\vec{g}(0, 0, -g)$

STUDIA UNIV BABEŞ-BOLYAI, PHYSICA, XXVIII, 1983

FAST NEUTRONS SPECTROSCOPY WITH ORGANIC SCINTILLATORS

L. DĂRĂBAN,* I. CHEREJI,* T. FIAT

1 **Introduction.** The best known methods for neutron spectroscopy are

a) the energy measurements of nuclear reaction products, i e the energy of α particle from ^6Li $(n, \alpha)T$ [1];

b) the time of flight measurements [2] and c) the energy measurements of the recoil protons [3—7].

The recoil protons can be detected by a proton recoils telescopic counter or by an organic scintillator in which the recoil protons are generated by neutrons scattering. The scintillator material can be stilbene and anthracene crystals, liquid or solid state plastic scientillators

In this paper the evaluation of the neutron spectrum with the ai dof NE—102 type of plastic scintillator is analysed and the problem of calibration in proton energy terms with the help of Compton electrons is discussed.

2 **Fast neutrons spectroscopy by recoil protons method.** Because the scattering of neutrons by protons is isotropic in the center of mass system up to 10 MeV incident energy (with 5% deviations up to 15 MeV [5]), the recoil proton spectrum for an incident group of monoenergetic neutrons will be rectangular shape, the recoil proton being equally likely to have any energy from that of the neutron downward:

$$E_p = E_n \quad \cos^2\theta \tag{1}$$

It follows, that the derivantive of the recoil protons rectangular shape spectrum will give the peak of monoenergetic neutrons spectrum [5, 6] But the recorded pulse height spectrum has not this ideal shape because the scintillation response of the counter to the protons energy is nonlinear

The distortions arise due to the finite size of the detector and to some of the multiple scattering effects [6, 7] as follows·

a) the proton escaping from the scintillator ends or walls causes the failing of all their energy deposition and consequently the neutronic peak will be decreased;

b) multiple scattering of neutrons by several protons provides a negative intensity peak in front of the actual neutronic peak so this later peal appeares slightly increased,

c) neutron-proton scattering after the neutron was elastically scattered by a carbon nucleus.

The net results of these distortions, wich are to some extent selfcompensatory is a decrease with 5% in the amplitude of the neutron peak at 2 6 MeV and with 25% at 14 MeV, respectively [7]. The recoil proton spectrum of 14 6 MeV neutrons is shown in Fig 1

* Institute of Isotopic and Molecular Technology, Cluj-Napoca

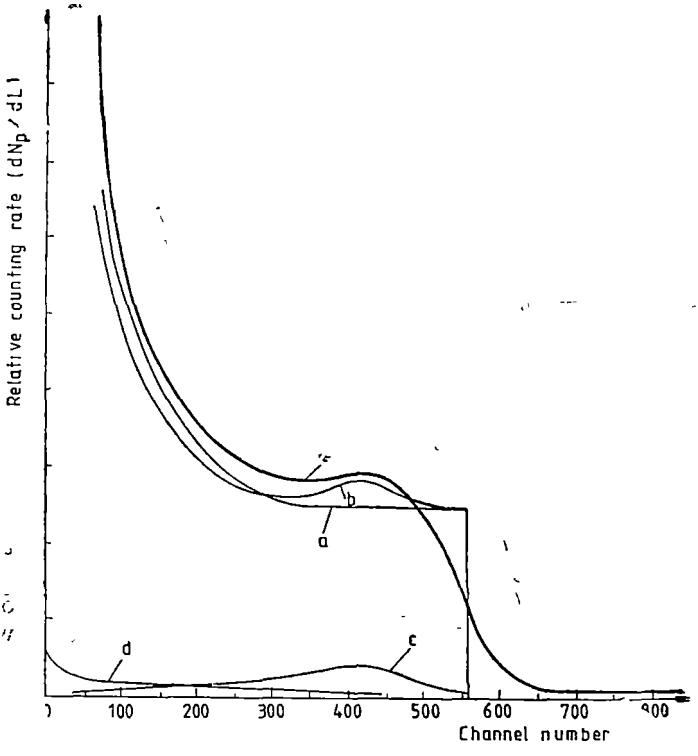

Fig 1 a prefect resolution b — singular and second $n-p$ scattering, c — second scattering from hydrogen, d — $n-p$ scattering after the neutron was elastically scattered by a carbon nucleus, e — actual spectrum line

The data were obtained with a plastic scintillator of NE-102 type in the range of 0—30 degree flight angle located at 5 cm from the tritium target bombarded by 65 KeV deuterons. The study of neutron energy from neutron generators in the cases of D—T and D—D reactions is discussed elsewhere [8].

The organic scintillators are known to be sensitive to gamma radiation. The neutron spectroscopy is difficult to perform when the gamma component is present In the above two cases the neutron component is pure The incident neutron spectrum can be unfolded from the observed recoil proton spectrum as in [6], using the relationship given bellow:

$$\frac{dN_n}{dE_n} = -\frac{E_n}{\varepsilon_n}\left[\frac{dL}{dE_p}\cdot\frac{d}{dL}\left(\frac{dL}{dE_n}\cdot\frac{dN_n}{dL}\right)\right]_{E_n=E_p} \tag{2}$$

where, dN_n/dE_n is the number of neutrons in an energy interval dE_n and ε_n is the neutron efficiency [9]·

$$\varepsilon_n = n_H \sigma_H d \frac{1-\exp(-a\cdot d)}{ad}$$

where d = the crystal length, $a = n_H \cdot \sigma_H + n_c\sigma_c$, n_H, n_c = number of hydrogen and carbon atoms per unit volume, respectively (atoms/cm^3) and σ_H, σ_c = total microscopic neutron cross section of hydrogen and carbon, respectively, for an neutron energy E_n (cm^2/atom).

The values of (3) function for stilbene crystal are given in ref. [9] Then

$$\frac{dL}{dE_p} = 0.191 \cdot E_p^{1.343} \tag{4}$$

which is the pulse height — energy relationship for different proton energies due to the non-linear response of the scintillation crystals to charged particles A detailed study of this so called „Birks function" is given by [10—14] for plastic scintillators and by [15, 16] for stilbene crystal. The observed recoil proton spectrum dN_p/dL can be converted in proton energy after a preliminary calibration of pulse height analizer channels with dL/dE_p values determined from Compton electrons energy. These values are fitted with the empirical relation (4) in the pulse height per channel terms and so we deduce dN_p/dE_p recoil proton spectrum. With the help of a computer program [8] this spectrum is derived and multiplied by dL/dE_p and $(-E_n)$ respectively, step by step in all neutron energy intervals as in (2)

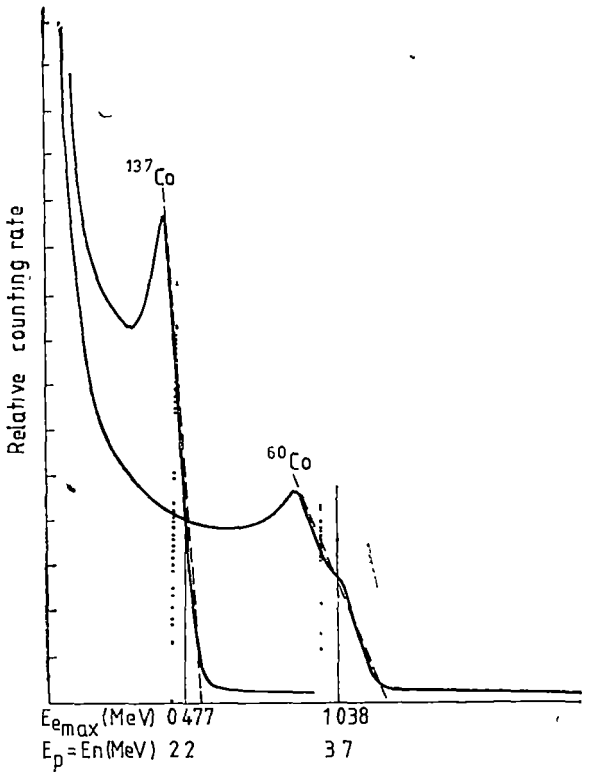

Fig 2 The calibration with Compton electrons energy

3. **Organic scientillators calibration with gamma radiation.** The absence of high atomic number materials in the scintillator results in a response to gamma rays which is completely due to Compton scattering The response of stilbene to gamma radiation is discussed in [5—7] and the plastic scintillators efficiency in [17—21] Therefore, using Comptons relationship we deduce for a ^{137}Cs gamma ray source that $E_{e_{max}} = 0\,479$ MeV and 1 038 MeV for ^{60}Co, respectively The Compton edge from these sources in the NE—102 plastic scintillator are shown in Fig 2 The intrinsic resolution of the spectrometer is estimated from the spread introduced into the Compton edge of gamma ray spectra observed. Due to statistical smearing processes one observes no definite high energy edge In [5]

the high energy side of Compton electron distribution is extrapolated to zero intensity, and this point is taken as the pulse height for $E_{e\max}$ electrons (dashed line in Fig. 2). There is also the possibility for using the 50% fractional peak height energy in a spectroscopic fashion as a measure of the Compton edge energy (solid line in Fig. 2) [6, 17—19]. In references [20, 21] this point is locatted at 2/3 and 80%, respectively from the drop off at the end of the Compton electron pulse spectrum (dotted line in Fig. 2). These Compton electron energies can be converted in equivalent proton energy which would produce an identically pulse height, described by the empirical relation [3]

$$E_p = \left(\frac{E_{e_{max}}}{0.15}\right)^{1/1.48} \tag{5}$$

or by experimental measurements given in [22] for stilbene crystals and by [23] for NE—102 type of plastic scintillator. Therefore the equivalent proton energies of ^{137}Cs and ^{60}Co source Compton electrons is $E_p = 2.2$ MeV and $E_p = 3.7$ MeV respectively.

To fit the (4) relation in pulse height analizer channels terms, we represented at different gain the spectra given in Fig. 2 and we reccalculated in fictive proton energy. The calibration curves of the three cases discussed above are given in Fig. 3.

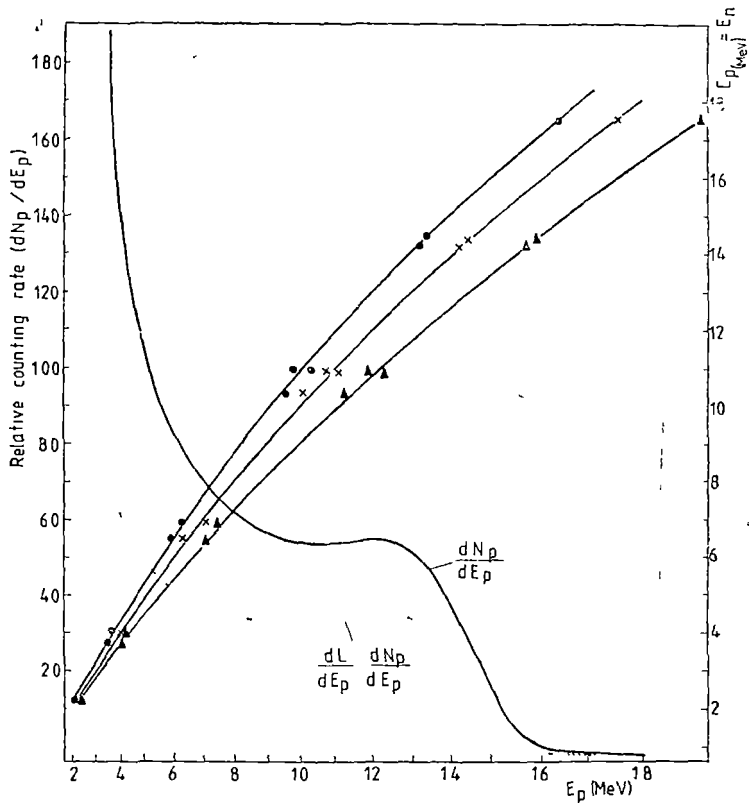

Fig. 3. Compton edge at mid-point (x) [6, 17, 19], or obtained by extrapolation to zero intensity (Δ) [5], or located at 80% from the dropoff at the end of the electron spectrum (0) [20, 21].

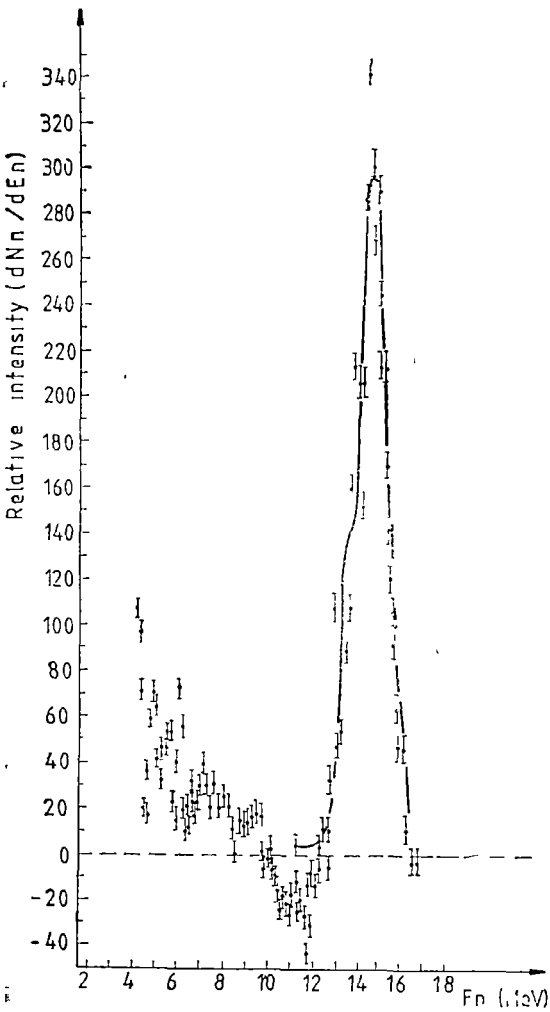

Fig 4 The fast neutrons from D—T reaction

Solid line spectrum is the recoil proton spectrum and dotted line spectrum is corrected recoil proton spectrum with the help of Birks function

4 **Results and discussion.** The best calibration is in the midpoint of the sudden dropoff case [6,17—19] Identical results have been obtained in D—D neutron spectrum calibration As an example, the neutron spectrum of the 14 6 MeV energy is represented in Fig 4 by solid line, after elimination of the distortion effects. The experimental points represent the uncorrectted neutron spectrum caused by the distortions effects The uncertainity in energy is about $\pm$ 0 5 MeV and is introduced by gamma calibration

A similar procedure was applied by using stilbene as a recoil protons detector

(Received December 2, 1982)

REFERENCES

1. I. E. Strain, W S Lyon, *Radiochem Methods Analysis*, vol II, p 254, IAEA, Vienna, 1965
2. I. E Lutkin, G W McBeth, Nucl Instr Meth, **107,** 165 (1973)
3. M N. Thompson, J. M Taylor, Nucl Instr Meth, **37,** 305 (1965)
4. R. G. Miller, R W Kavanagh, Nucl. Phys, **88,** 492 (1966)
5. C. M. Cialella, J. A. Devanney, Nucl Instr Meth, **60,** 269 (1968)
6 H. W. Broek, C. E Anderson, Rev Sci Instr, **31,** 1063 (1960)
7. M. Bormann et al, Nucl Instr Meth, **88,** 245 (1970)
8 L. Daraban, et al, *Proc Nat Conf Phys*, Bucharest, oct 1982, p 71
9. I B Marion, I L Fowler, *Fizika bistrih neitronov*, Gostatomizd, Moskva, (1963), p. 231.

10. H C Evans, E H Bellamy, Proc Phys Soc, **74,** 212 (1959).
11 I A Harvey, N W Hill, Nucl Instr Meth, **162,** 507 (1979).
12 G. D Badhwar et al, Nucl Instr Meth, **57,** 116 (1967)
13. D E Groom, M G Hauser, Nucl Instr Meth, **46,** 301 (1967).
14 D R Koehler, I T Grissom, Nucl Instr Meth, **40,** 235 (1966).
15 C. J Taylor et al, Phys Rev, **83,** 169 (1951)
16 J M Fowler, C E Roos, Phys Rev, **98,** 996 (1955)
17 I T Grissom, D R Koehler, Nucl Instr Meth, **37,** 336 (1965).
18 V V Verbinski et al, Nucl Instr Meth, **65,** 8 (1968)
19 K F Flynn et al, Nucl Instr Meth, **27,** 13 (1964)
20 J R Prescott, A S Rupaal, Canad J Phys, **39,** 221 (1961)
21 E Nardi, Nucl Instr Meth, **95,** 229 (1971)
22 B V Rîbacov, V A Sidonov, *Spectrometrija bîstrîh neitronov,* Ed. IGUIAESM SSSR, Moskva, 1958, p 97
23 J L Fowler et al, Nucl Instr Meth, **175,** 449 (1980)

SPECTROSCOPIA NEUTRONILOR RAPIZI CU SCINTILATORI ORGANICI

(Rezumat)

Este analizată metoda de determinare a energiei neutronilor rapizi pe baza prelucrării spectrelor protonilor de recul

Se discută metodele de etalonare a scintilatorilor organici în energii protonice, folosind energia electronilor Compton

Se stabileşte o cale de obţinere a spectrului neutronic în cazul piculu de 14,6 MeV ce rezultă pentru neutronii emişi din reacţia D–T.

Intreprinderea Poligrafică Cluj, Municipiul Cluj-Napoca cda. nr 3016/83

În cel de al XXVIII-lea an (1983) *Studia Universitatis Babeş-Bolyai* apare în specialităţile:

matematică

fizică

chimie

geologie-geografie

biologie

filozofie

ştiinţe economice

ştiinţe juridice

istorie

filologie

На XXVIII году издания (1983) *Studia Universitatis Babeş-Bolyai*, выходит по следующим специальностям:

математика

физика

химия

геология-география

биология

философия

экономические науки

юридические науки

история

филология

Dans sa XXVIII-e année (1983) *Studia Universitatis Babeş-Bolyai* paraît dans les spécialités:

mathématiques

physique

chimie

géologie-géographie

biologie

philosophie

sciences économiques

sciences juridiques

histoire

philologie

Abonamentele se fac la oficiile poştale, prin factorii poştali şi prin difuzorii de presă, iar pentru străinătate prin ILEXIM, Departamentul export-import presă, P.O. Box 136-137, telex 11226, Bucureşti, str. 13 Decembrie nr. 3.

Lei 35